AFFDL-TR-71-91

CYCLIC PITCH CONTROL ON A V/STOL TILT WING AIRCRAFT

C.E.Kolesar
The Boeing Company, Vertol Division

TECHNICAL REPORT AFFDL-TR-71-91

October 1971

Approved for public release; distribution unlimited

Air Force Flight Dynamics Laboratory
Air Force Systems Command
Wright-Patterson Air Force Base, Ohio

UNCLASSIFIED
Security Classification

DOCUMENT CONTROL DATA - R & D

(Security classification of title, body of abstract and indexing annotation must be entered when the overall report is classified)

1. ORIGINATING ACTIVITY (Corporate author)	2a. REPORT SECURITY CLASSIFICATION
Vertol Division The Boeing Company P. O. Box 16858 Philadelphia, PA 19142	Unclassified 2b. GROUP N/A

3. REPORT TITLE

CYCLIC PITCH CONTROL ON A V/STOL TILT WING AIRCRAFT

4. DESCRIPTIVE NOTES (Type of report and inclusive dates)
Final Report (March 1970 - May 1971)

5. AUTHOR(S) (First name, middle initial, last name)

Charles E. Kolesar

6. REPORT DATE	7a. TOTAL NO. OF PAGES	7b. NO. OF REFS
October 1971	112	5

8a. CONTRACT OR GRANT NO.	9a. ORIGINATOR'S REPORT NUMBER(S)
F33615-70-C-1000 b. PROJECT NO. 698BT c. Task Area Number: 02 d. Work Unit Number: 005	D210-10353-1 9b. OTHER REPORT NO(S) (Any other numbers that may be assigned this report) AFFDL-TR-71-91

10. DISTRIBUTION STATEMENT

Approved for public release; distribution unlimited.

11. SUPPLEMENTARY NOTES	12. SPONSORING MILITARY ACTIVITY
Copies of the referenced contractor test reports are also available from DDC.	Air Force Flight Dynamics Laboratory Wright-Patterson AFB, Ohio 45433

13. ABSTRACT

This report presents the key results of a model wind tunnel test program that was directed towards investigating the use of cyclic pitch propellers as the low speed longitudinal control system of a four propeller V/STOL tilt wing transport-type aircraft. The almost linear pitch control effectiveness of this system through transitional flight and in-ground effect along with the correlation with theory is discussed, and the moderate power increase associated with its use is shown. Data is presented to illustrate the small influence that cyclic pitch inputs have on longitudinal stability and lateral/directional stability. Cyclic pitch control coupled with stabilizer control is discussed along with cross-coupling of cyclic pitch with the wing surface controls utilized for roll/yaw control. A comparison of 1/12th scale isolated prop data with 1/3rd scale isolated prop data is shown that validates the use of small scale cyclic propellers for definitive test results.

DD FORM 1 NOV 68 1473

UNCLASSIFIED
Security Classification

Security Classification

14. KEY WORDS	LINK A		LINK B		LINK C	
	ROLE	WT	ROLE	WT	ROLE	WT
1. Cyclic Pitch Control 2. Cyclic Pitch Propellers 3. Tilt Wing V/STOL Aircraft 4. V/STOL Propellers 5. V/STOL Wind Tunnel Models						

UNCLASSIFIED

Security Classification

AFFDL-TR-71-91

CYCLIC PITCH CONTROL ON A V/STOL TILT WING AIRCRAFT

C. E. Kolesar

D210-10353-1

FOREWORD

This report is the final report of the work accomplished on Contract F33615-70-C-1000-Project No. 698BT, V/STOL Cyclic Pitch Propeller Wind Tunnel Program by the Vertol Division of The Boeing Company at Philadelphia, Pennsylvania. The contract work was performed over a 12-month period from March 1970 to April 1971 under the sponsorship of the Air Force Flight Dynamics Laboratory, Air Force Systems Command, Wright-Patterson Air Force Base, Ohio. Project Engineer for the Air Force was Lt. F. S. Stoddard (FDV). Work at the Vertol Division was under the overall technical direction of K. B. Gillmore, V/STOL Technology Manager.

Acknowledgement is made to the following major contributors for program management, technical direction, test data analysis, model design, and wind tunnel testing aspects; plus, those personnel that made valuable technical contributions through consultation.

Program Managers	P. Prager/W. Lapinski
V/STOL Aerodynamics (1/12th scale models)	C. Kolesar
V/STOL Structures (1/3rd scale prop model)	E. Widmayer
Wind Tunnel Manager	F. Harris
Wing Tunnel Project Engineers	M. Drozda, D. Joyce
Model Design	C. Albrecht
	H. Parkinson
	F. McArdle
	P. Dixon
	E. Kulesa
Wind Tunnel Operations and Test	K. Farrance
	I. Walton
	D. Ekquist

This report was submitted in May 1971.

This technical report has been reviewed and is approved.

Richard E. Colclough
Acting Chief
V/STOL Technology Division

ABSTRACT

This report presents the key results of a model wind tunnel test program that was directed towards investigating the use of cyclic pitch propellers as the low speed longitudinal control system of a four propeller V/STOL tilt wing transport-type aircraft. The almost linear pitch control effectiveness of this system through transitional flight and in-ground effect along with the correlation with theory is discussed, and the moderate power increase associated with its use is shown. Data is presented to illustrate the small influence that cyclic pitch inputs have on longitudinal stability and lateral/directional stability. Cyclic pitch control coupled with stabilizer control is discussed along with cross-coupling of cyclic pitch with the wing surface controls utilized for roll/yaw control. A comparison of 1/12th scale isolated prop data with 1/3rd scale isolated prop data is shown that validates the use of small scale cyclic propellers for definitive test results.

This page intentionally left blank.

TABLE OF CONTENTS

TABLE OF CONTENTS (Cont.)

LIST OF ILLUSTRATIONS

LIST OF ILLUSTRATIONS (Cont.)

LIST OF ILLUSTRATIONS (Cont.)

LIST OF ILLUSTRATIONS (Cont.)

LIST OF TABLES

LIST OF ABBREVIATIONS AND SYMBOLS

Symbol	
A_p	Propeller disc area, ft^2
b	Wing span, ft.
c	Mean aerodynamic chord, MAC, ft.
C_{ℓ_s}	Slipstream rolling moment coefficient, R.M./q_sSb (positive, right wing down)
$C_{\ell_{s_\beta}}$	Rolling moment derivative (slipstream notation)
C_{L_s}	Slipstream lift coefficient, L/q_sS
C_{M_p}	Propeller moment coefficient, $\frac{\text{Hub Pitching Moment}}{\rho n^2 D^5}$
C_{M_s}	Slipstream moment coefficient, M/q_sSc (positive, nose up)
C_{n_s}	Slipstream yawing moment coefficient, Y.M./q_sSb (positive, nose to the right)
$C_{n_{s_\beta}}$	Yawing moment derivative (slipstream notation)
C_{NF_p}	Prop normal force coefficient, Normal Force/$\rho n^2 D^4$
C_p	Propeller power coefficient, Shaft Power/$\rho n^3 D^5$
C_T	Thrust coefficient, $T/\rho n^2 D^4$
C_{T_s}	Slipstream thrust coefficient, $T/q_sA_p = \frac{T/A_p}{T/A_p + q}$
C_{X_s}	Slipstream longitudinal force coefficient, X/q_sS (positive, forward)
C_{Y_s}	Slipstream side force coefficient, Side Force/q_sS (positive, to the right)
$C_{Y_{s_\beta}}$	Side force derivative (slipstream notation)
D	Propeller diameter, ft.
h/D	Ground height ratio (outboard prop plane height to propeller diameter)
i_w	Wing tilt angle, deg.

LIST OF ABBREVIATIONS AND SYMBOLS (Cont.)

Symbol	
I.G.E.	In-ground effect
J	Propeller advance ratio, V/nD
L	Aircraft lift, lb.
M	Aircraft moment, ft.lb.
n	Propeller rotational speed, rps
O.G.E.	Out-of-Ground effect
q	Dynamic pressure, lb/ft^2
q_s	Slipstream dynamic pressure, $q+T/A_p$, lb/ft^2
$\mathcal{A}$	Horizontal stabilizer angle, deg.
S	Wing area, $ft.^2$
T	Propeller thrust, lb.
TAF	Total propeller activity factor
V	Velocity, fps or knots
V_F	Full scale flight path velocity, knots
X	Aircraft longitudinal force, lb.
α_p	Propeller shaft angle, deg.
β	Aircraft sideslip angle, deg. (positive, nose left)
γ	Cyclic pitch angle, deg. (positive angle, nose down moment)
δ_F	Flap angle, deg.
δ_s	Spoiler angle, deg.
$\theta_{.75}$	Collective or propeller blade angle at 3/4 radius, deg.
ρ	Density, $slugs/ft^3$

SECTION I

INTRODUCTION

In the period from March 1970 to April 1971, the Vertol Division of the Boeing Company performed, under contract to the U. S. Air Force[1], a wind tunnel test program on a cyclic pitch longitudinal control system as applied to a four prop V/STOL tilt wing transport-type aircraft. The 87,000 lb. "V" gross weight aircraft represented in the model program utilized 26ft. diameter propellers and had a wing loading of 73 lb/ft^2. Figure 1 is an artist's rendering of a typical configuration studied over the past three years at Boeing-Vertol.

In this V/STOL concept, the propeller is a vital part of the flight control system in the low speed regime, contributing to control about all axis: roll and yaw control through differential collective settings, with the axis phasing dependent upon the wing tilt angle, and longitudinal control via the cyclic pitch system. This incorporation of low speed longitudinal control into the primary propulsive/lifting system eliminates the need for a separate system such as a tail rotor, to provide the pitch control function. The cyclic pitch control system studied was monocyclic in the sense that cyclic blade motion was generated only by about one axis - the pitching axis of the aircraft - and developed control by effectively off-setting the resultant propeller thrust vector - above or aft of the normal propeller thrustline in the case of nose down cyclic and below or forward of the thrustline for nose up cyclic.

The test program consisted of five tests conducted during 1970 of four separate models. The overall objectives of the program were to: (1) determine the effectiveness of cyclic pitch for longitudinal control in hover and through transition, (2) determine the interactions between the wing/flap lifting system and cyclic pitch, (3) establish the influence of cyclic inputs on low speed descent performance, (4) establish the effect of the utilization of cyclic pitch on aircraft static stability and aircraft surface control power - stabilizer for longitudinal trim and differential flaps/spoilers for yaw and roll control with axis phasing dependent upon the wing tilt angle, and (5) determine the effects of cyclic pitch on blade loads and moments. One important element of the program was determining the change in power required for cyclic pitch control.

---

[1]Air Force Flight Dynamics Laboratory, Wright-Patterson Air Force Base, Ohio

Figure 1. V/STOL TILT WING AIRCRAFT WITH FOUR CYCLIC PITCH PROPELLERS

In the initial portion of the report, a rather detailed description of the models is presented. This description gives a general idea of the scope of model hardware development and auxiliary test equipment required for the program.

Tne four models used for the program were: (1) a 1/12th scale full span tilt wing model with 2.14 ft. diameter propellers, (2) an isolated prop model utilizing one of the propeller/nacelle assemblies from the full span model, (3) a 1/3rd scale prop model having an 8.8 ft. diameter, and (4) a 1/12th scale semispan tilt wing model with leading edge boundary layer control. The full span model was tested both out-of-ground effect and in-ground effect, with a moving ground plane being used for the in-ground effect testing.

Data and results from the various tests of these models are documented in the individual test reports listed in the References. The data included in this final report summarizes the key findings noted in these test reports (References 1 thru 5).

SECTION II

TEST PROGRAM

1. DESCRIPTION OF TEST PROGRAM MODELS

Figures 2 through 5 are photographs of the various models as installed for testing in the 20 ft. by 20 ft. test section of the Boeing-Vertol V/STOL wind tunnel.

The 1/12th scale 2.14 ft. diameter three way isolated propeller was pedestal mounted on the tunnel yaw table as depicted in Figure 2. This pneumatically powered model incorporated an instrumented shaft for torque measurements and a six component strain gage internal balance that was located between the cyclic pitch mechanism and the 50 HP air motor. A flexible bellows joint in the drive shaft isolated the propeller forces and moments. Compressed air for the motor was delivered up the hollow pedestal, through the opening between the aft nacelle fiberglass fairing and the air motor exhaust tube, and was then routed into the front face of the motor.

Cyclic pitch action was imparted to the blades through a set of pitch links attached to a swashplate driven by scissors mounted on the rear face of the hub. Elastomeric bearings were used in the hub to support the blade retention housing and thus permit angle motion. Collective and cyclic pitch angles were manually set on each blade individually.

Figure 3 shows the 1/3rd scale 8.8 ft. diameter four way isolated propeller mounted on the 10,000 lb. Boeing-Vertol Test Stand (DRTS), with the main body of the test stand attached to the main tunnel hydraulic powered sting/strut support system. This vertically traversing strut is used to adjust the height of the model in the test section. The propeller/hub, cyclic pitch mechanism, stack assembly, and five component strain gage balance were fixed to the end of the DRTS four ft. long pitch cone which is in turn trunnion mounted at the butt end of the main body. An angular pitch range from 0° to 105° was provided by this arrangement.

The four bladed model propeller with one blade instrumented for loads, was Froude scaled from a design suitable for full scale tilt wing application. This design represents a compromise to achieve required hover figure of merit and good cruise efficiency and is a design that evolved through many iterations. Model blade construction featured a fiberglass spar, compressed balsa core, woven glass skins, and a titanium root end.

The cyclic pitch system utilized elastomeric bearings, rotating scissors, swashplate, and pitch arms. Collective and cyclic pitch blade angles were remotely adjustable through the use of three hydraulic actuators . These actuators translated

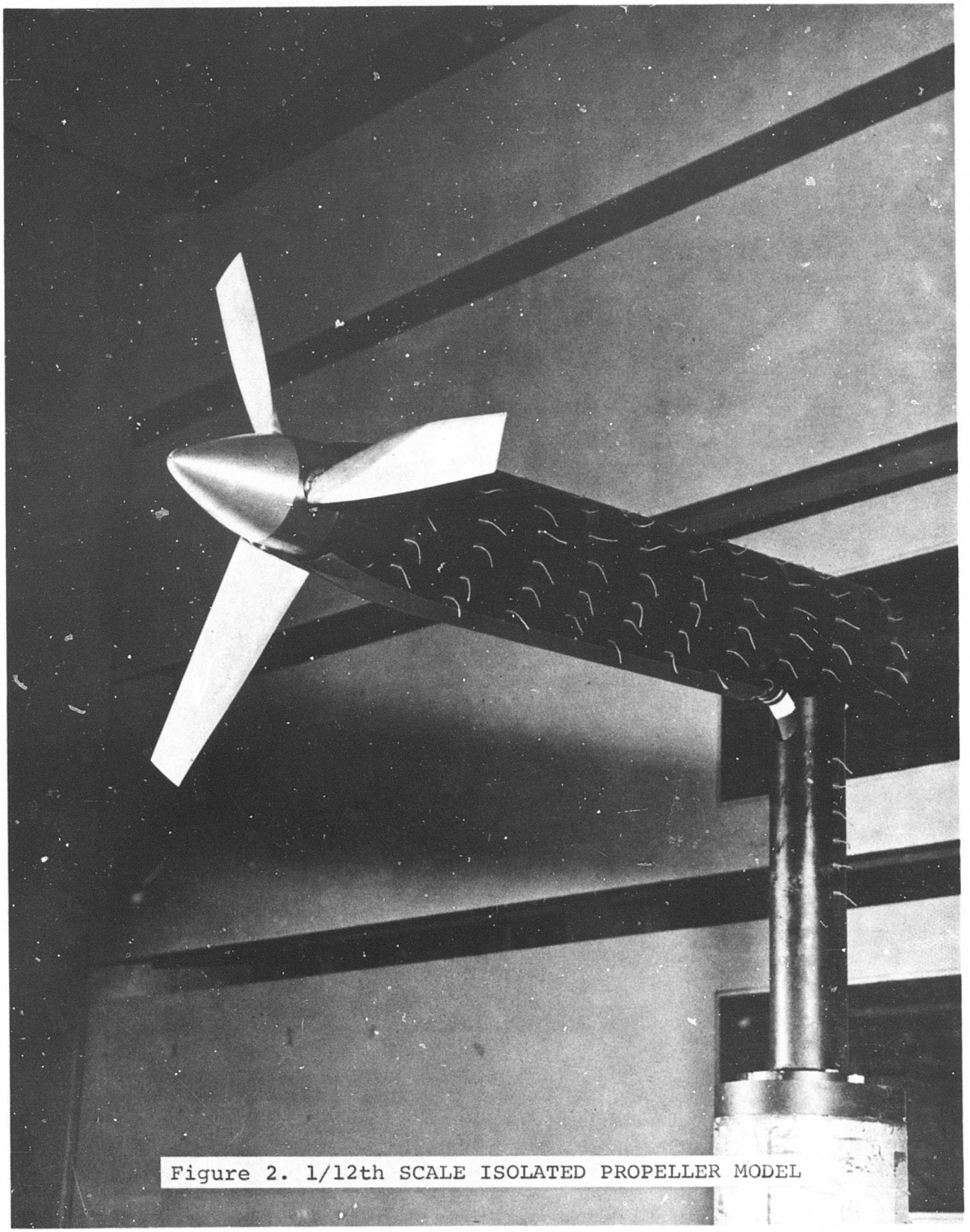

Figure 2. 1/12th SCALE ISOLATED PROPELLER MODEL

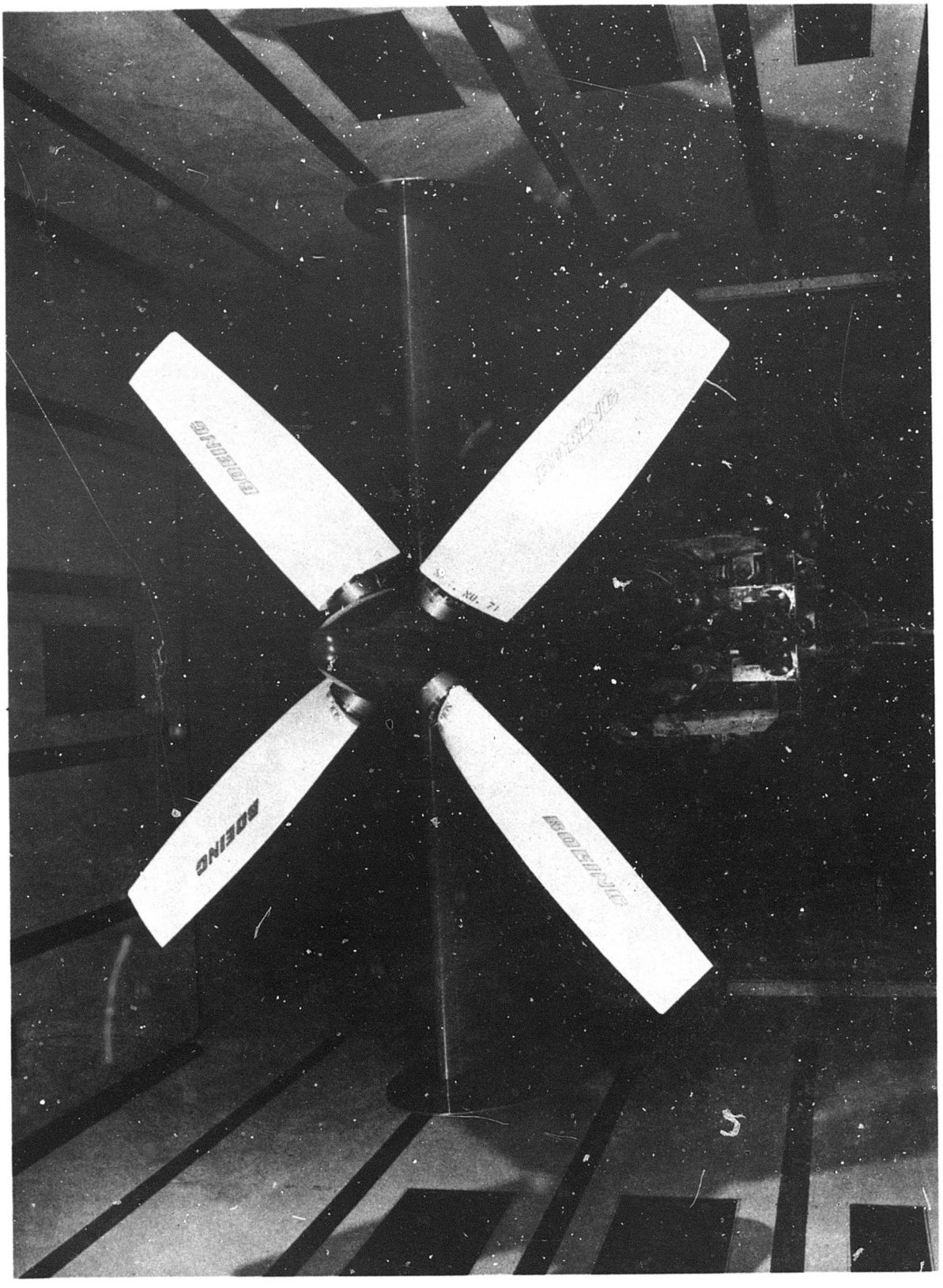

Figure 3. 1/3rd SCALE PROPELLER MODEL

the swashplate to set the desired blade collective angle. One of the three actuators was used for tilting the swashplate to set the desired cyclic pitch angle.

The 1/12th scale full span tilt wing model with overlapped propellers (7% diameter) and tapered wing, having an average wing chord to prop diameter ratio of 0.44, is illustrated in Figure 4. This sting mounted model, which featured full span slats and full span large chord double slotted flaps with movable fore flap plus Fowler action, used four of the same type of nacelle assembly (propeller/cyclic hub/internal balance/air motor) that was tested in the 1/12th scale isolated prop test.

The main tunnel sting support system was selected for mounting the model so that both variable ground height hover data and moving ground plane data could be obtained along with pitch and yaw data. The 16 ft. long sting pivots, for model angle of attack motion, about its attachment point on the vertical moving main strut. This enables the model to be retained near the center of the test section as the model is pitched. A "yaw adapter" that provides pure yawing motion for selected angles of attack was attached to the forward end of the main sting. The model itself was attached to the "yaw adapter" via a hollow sting extension that passed through the aft end of the fuselage and was bolted onto the aft end of the internal six component strain gage balance. This balance was located with its center immediately below the wing pivot.

High pressure air entered the model through the hollow sting extension. Interactions of the model air supply system on the fuselage balance measurements were minimized by ducting the air symmetrically past the balance from the forward section of the sting via dual ducts (one per fuselage side) and thence into a plenum chamber located forward of the balance in the frontal portion of the fuselage. A set of internal flexible bellows were used to connect the dual ducts to the plenum chamber structure. Air for each air motor was individually ducted forward from the front wall of the plenum chamber, aft over the top of the plenum chamber through four pipes which were connected to a hollow segmented air pivot joint. Four internal wing spanwise air ducts (one per motor) were used to direct the air outboard from the wing root into the forward portion of the air motors bolted directly to the wing. Mass flow into each motor was remotely controlled by the four individual motor control valves used in conjunction with the main tunnel compressor system controls.

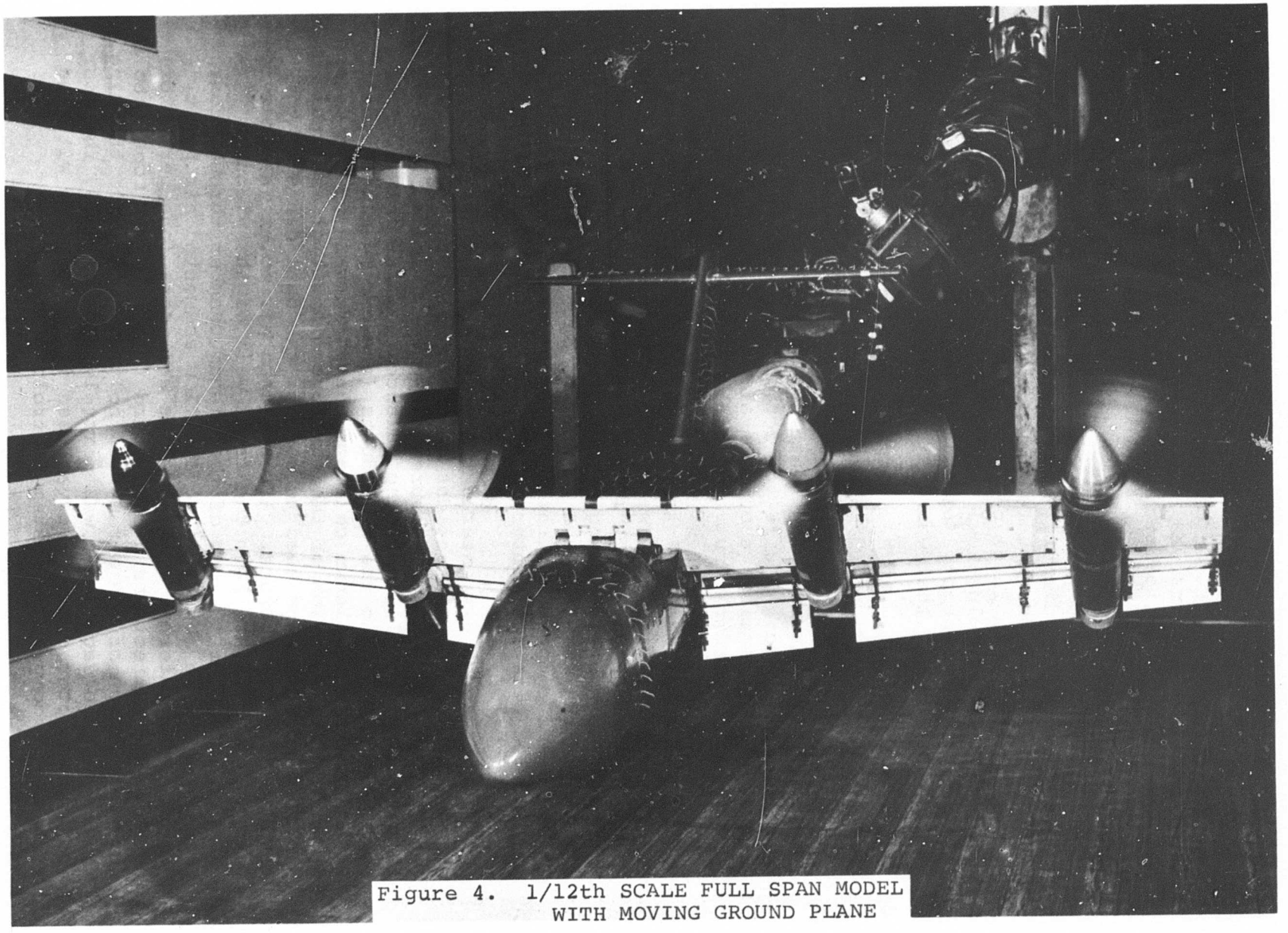

Figure 4. 1/12th SCALE FULL SPAN MODEL WITH MOVING GROUND PLANE

The 1/12th scale electric powered semispan tilt wing model, used to study leading edge boundary layer control (BLC) for low speed descent performance improvement, is shown in Figure 5. This model utilized a rectangular wing with a wing chord to prop diameter ratio of 0.56 and 2.14 ft. diameter three way non-overlapped propellers, but with a lower activity factor (57%) than the propellers used on the full span model. The high lift system comprised full span slats used in conjunction with the leading edge BLC and full span large chord double slotted flaps featuring 22% chord Fowler action plus an extending fore flap.

Model instrumentation consisted, in addition to the BLC system pressure and temperature instrumentation, of propeller thrust and torque flexures in each nacelle and a four component strain gage balance located at the wing root, but below the platform or ground board serving as a plane of symmetry. A cylindrical tube extension was used to attach the four component balance and thereby, the wing itself to the tunnel yaw table located in the test section floor. In this set-up, the balance rotated with the wing.

Tubing used to transmit blowing air to the wing was "looped around" the wing root balance in a manner which virtually eliminated any balance interactions. Three spanwise tunnels were cut in the wing for directing the blowing air to the leading BLC slot. This slot was divided into three separate spanwise segments. The pressure ratio applied to each of these segments could be adjusted separately by three individual control valves or the flow to a particular segment could be completely shut-off.

Cyclic hubs used during the semispan model test were similar in design and construction to those utilized in the full span model test.

Table I summarizes the primary characteristics of the various models used in the test program.

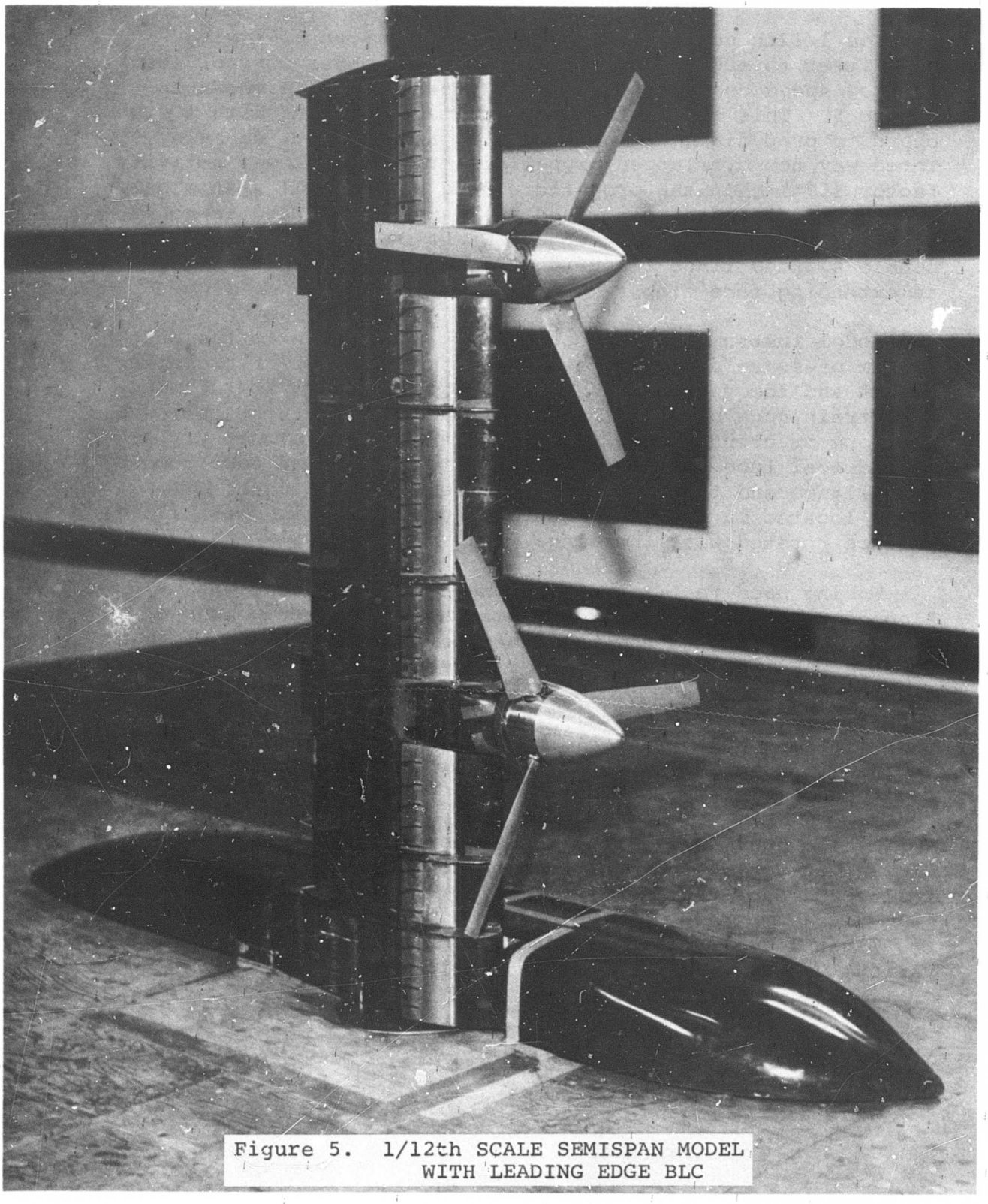

Figure 5. 1/12th SCALE SEMISPAN MODEL WITH LEADING EDGE BLC

Table I. PRIMARY CHARACTERISTICS OF TEST PROGRAM MODELS

MODEL	FEATURES
o 1/12th Scale Isolated Propeller	2.14ft. dia. three way prop. 480 total activity factor. 8° cyclic at 5000 RPM. 50 HP air motor.
o 1/3rd Scale Dynamic Propeller with Nacelle and wing	8.8ft. dia. four way prop. 640 total activity factor. 12° cyclic at 1100 RPM. 0° to 60° of collective. DRTS (Dynamic Rotor Test Stand). 400 HP electric motor.
o 1/12th Scale Full Span Model	Four 1/12th scale isolated prop nacelle assemblies. 7% dia. overlapped props. 0.55 tapered wing. 9.2 aspect ratio. 0.44 average chord/diameter. 0.61 wing area/ prop area. 15% chord full span slats. 49% chord(extended) double slotted flaps. Spoilers. 0.083 vertical tail volume. 1.33 horizontal tail volume. High tail position.
o 1/12th Scale Semi-span BLC Model	Two 2.14 ft. dia. three way non-overlapped props. 273 total activity factor. 8° cyclic at 5000 RPM. 8 HP electric motors. Rectangular wing. 7.8 aspect ratio. 0.56 chord/diameter. 0.79 wing area/prop area. 15% chord full span slats. 44% chord(extended) double slotted flaps. Leading edge BLC. Adjustable slot (3 segments).

2. MODEL TEST PROGRAM OBJECTIVES

Table II lists the test objectives pertinent to each model. As mentioned previously in the Introduction, the overall objectives were to determine the effectiveness of cyclic pitch for longitudinal control in hover and throughout transitional flight, establish the influence that the wing/flap lifting system exerts on cyclic pitch effectiveness, measure the low speed descent capability with cyclic inputs, determine the effect of cyclic pitch control on aircraft stability about the longitudinal, lateral, and directional axes, investigate the influence of cyclic pitch on the aircraft surface controls, acquire blade load data throughout the transitional flight regime, and of especial concern, determine the increase in power required due to cyclic pitch.

Early in the formulation of the test program, it was recognized that these objectives could be most rigorously attained by testing both the full span model and one of its four propeller/cyclic hub/nacelle assemblies as an isolated propeller. This approach provides a direct comparison of the test data. Unfortunately the test results from these models are compromised to some degree, since model scaling considerations of the four prop full span model limited the propeller diameter to a size in the order of 2 plus ft. Test results of particular concern were the absolute value of the cyclic pitch control effectiveness and power measurements indicated by a propeller operating with a relatively low three-quarter radial station Reynolds number of 620,000 at the 5000 RPM cyclic hub operating speed (2.78 in. blade chord @ 3/4 R).

As a consequence of these factors, the 1/3rd scale 8.8 ft. diameter propeller was an important element in the test program. The 8.8 ft. propeller developed a Reynolds number at the 3/4 radial station (0.95 ft. chord) of 2.2 million when operating at its design speed of 1100 RPM. This model was also of sufficient size for blade load and pitch link load instrumentation, thereby enabling the effect of cyclic pitch on propeller design loads to be established.

One of the design problems of a tilt wing aircraft is stall of the wing center section over the top of the fuselage. Separation of this area can be tolerated at forward flight speeds in the order of 40 kts, due to the low dynamic pressure (6 lb/ft^2) prevailing on this "unbathed" portion of the wing. At higher speeds, in the order of 60 kts, wing center section stall can have an adverse effect on aircraft characteristics such as directional stability due to vertical tail "blanketing" and can result in horizontal tail buffeting at positive fuselage angles when the tail becomes immersed in the wake emanating from the center section. In the 1/12th scale semi-span test, leading edge boundary layer control was applied to

Table II. TEST PROGRAM OBJECTIVES

MODEL	ITEM
o 1/12th Scale Isolated Propeller	o Cyclic pitch control effectiveness in hover and through transition. o Power required for cyclic pitch control. o Effect of cyclic on thrust, normal force, side force, and hub yawing moment.
o 1/3rd Scale Dynamic Propeller with Nacelle and Wing	o Same as 1/12th scale propeller model plus o Effect of cyclic on blade loads and control loads. o Wing-propeller interference.
o 1/12th Scale Full Span Model (Two Tests)	o Cyclic pitch control effectiveness in hover and through transition. o Power required for cyclic pitch control. o Hover yaw control and effect of cyclic pitch. o Effect of cyclic pitch on descent performance. o Longitudinal stability and effect of cyclic pitch. o Effect of cyclic pitch on horizontal tail effectiveness. o Lateral/directional stability and effect of cyclic pitch. o Cross-coupling of cyclic pitch and roll/yaw wing surface controls. o Cyclic pitch control effectiveness in ground effect. o Effect of cyclic pitch on lateral/directional stability in ground effect.
o 1/12th Scale Semi-span BLC Model	o Investigation of leading edge BLC (various spanwise extents) as a means of improving descent performance. o Effect of cyclic pitch on descent performance with leading edge BLC. o Improvement in wing center section stall with leading edge BLC.

the wing/body center section to improve the noted situation by increasing the stall angle and was also applied to other portions of the wing for the purpose of improving the descent performance.

The full span model was tested through transition from hover to the conventional aircraft flight mode configuration of wing down and flaps retracted. Since the data in the report is presented as a function of slipstream thrust coefficient, the relationship between this parameter and full scale flight speed is desired. This relationship is shown in Figure 6. The speeds along the flight path were calculated for the representative four prop tilt wing aircraft having a 73 lb/ft^2 wing loading (tunnel test section ambient conditions). This wing loading would decrease to 66 lb/ft^2 for typical atmospheric design conditions of 2500 ft/93°F. It can be seen from this figure that the transition speed range varied from 21 kts to 113 kts. Note that for C_{T_s} values greater than 0.70 (roughly 52 kts), the speed variation with C_{T_s} is basically the same for the three flight conditions shown: 10° climb angle, level flight and 10° descent angle.

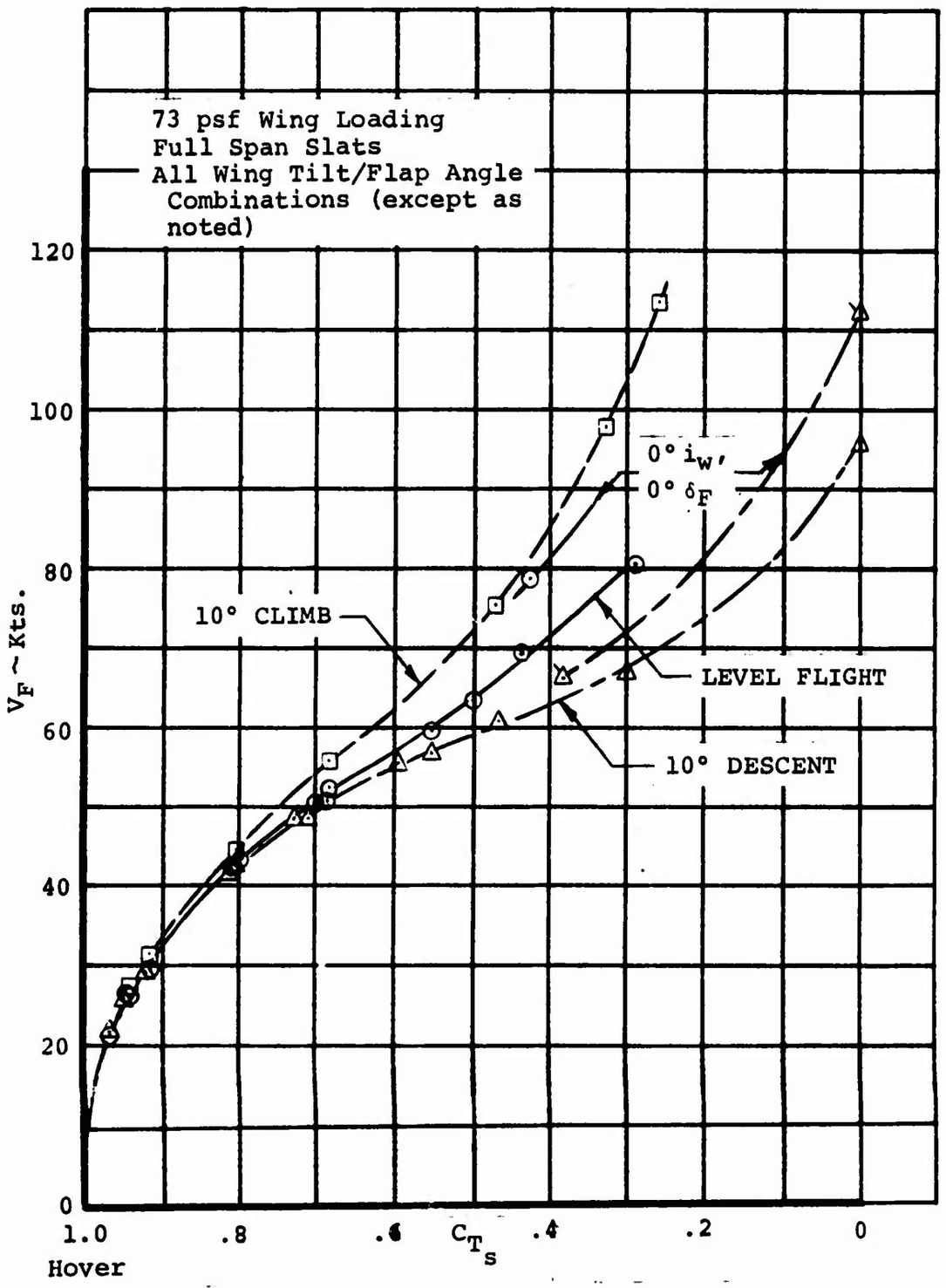

Figure 6. FULL SCALE FLIGHT SPEED AS A FUNCTION OF C_{T_s}

SECTION III

CYCLIC PITCH CONTROL CAPABILITY

1. CYCLIC PITCH EFFECTIVENESS AND POWER REQUIRED IN HOVER

The effectiveness of the propellers in producing aircraft pitching moment when cyclic pitch control is applied was investigated in the hover mode on the full span model with the wing tilted to 90° and in a clean configuration: flaps retracted, representing a zero yaw control input condition, and slats retracted. Data was acquired with cyclic inputs ranging from +8° (nose down moment) to -8° (nose up moment) at preselected ground heights which varied from an h/D of 4.0 to an h/D of 1.10. Ratios of h/D's from 4.0 to 2.0 represent an out-of-ground effect (O.G.E.) condition and an h/D of 1.2 represents hovering at a 2 ft. wheel height.

Figure 7 compares the cyclic pitching moment generated out-of-ground effect on the full span model as measured by the fuselage balance (moments transferred about the wing pivot) with that measured by the nacelle balances (hub moments). The non-dimensional moment C_{M_p}/C_T used in the plot is the ratio of moment coefficient to thrust coefficient in propeller terminology which enables the aircraft moments to be directly compared with the propeller hub moments.

The variation in moment with cyclic pitch angle was found to be linear over the range of angles evaluated, -8° to +8°. Not presented in Figure 7 are the test data that shows the moment to be essentially invariant with ground height down to the lowest height tested, an h/D of 1.0. The positive aircraft pitching moment measured with zero cyclic angle was produced by the propeller thrustlines being located below the wing pivot.

It can be noted in Figure 7 that the aircraft pitching moment produced by cyclic is 27% greater than that contributed by the four propeller hub moments. This positive difference is attributed to a change in prop normal force. An examination of the prop normal force data from the nacelle balances, an example of which is shown in Figure 8, established that the change in normal force with cyclic is in the correct direction. With positive cyclic a negative increment in prop normal force is produced (a forward acting force at the propeller hub with the wing tilted 90°) that in turn produces a negative pitching moment (nose down) about the wing pivot.

Figure 9 compares the hub pitching moment measured on the full span model with that measured on the 1/12th scale isolated prop model, and thus directly shows the effect of the wing on cyclic pitch effectiveness in an O.G.E. hover condition.

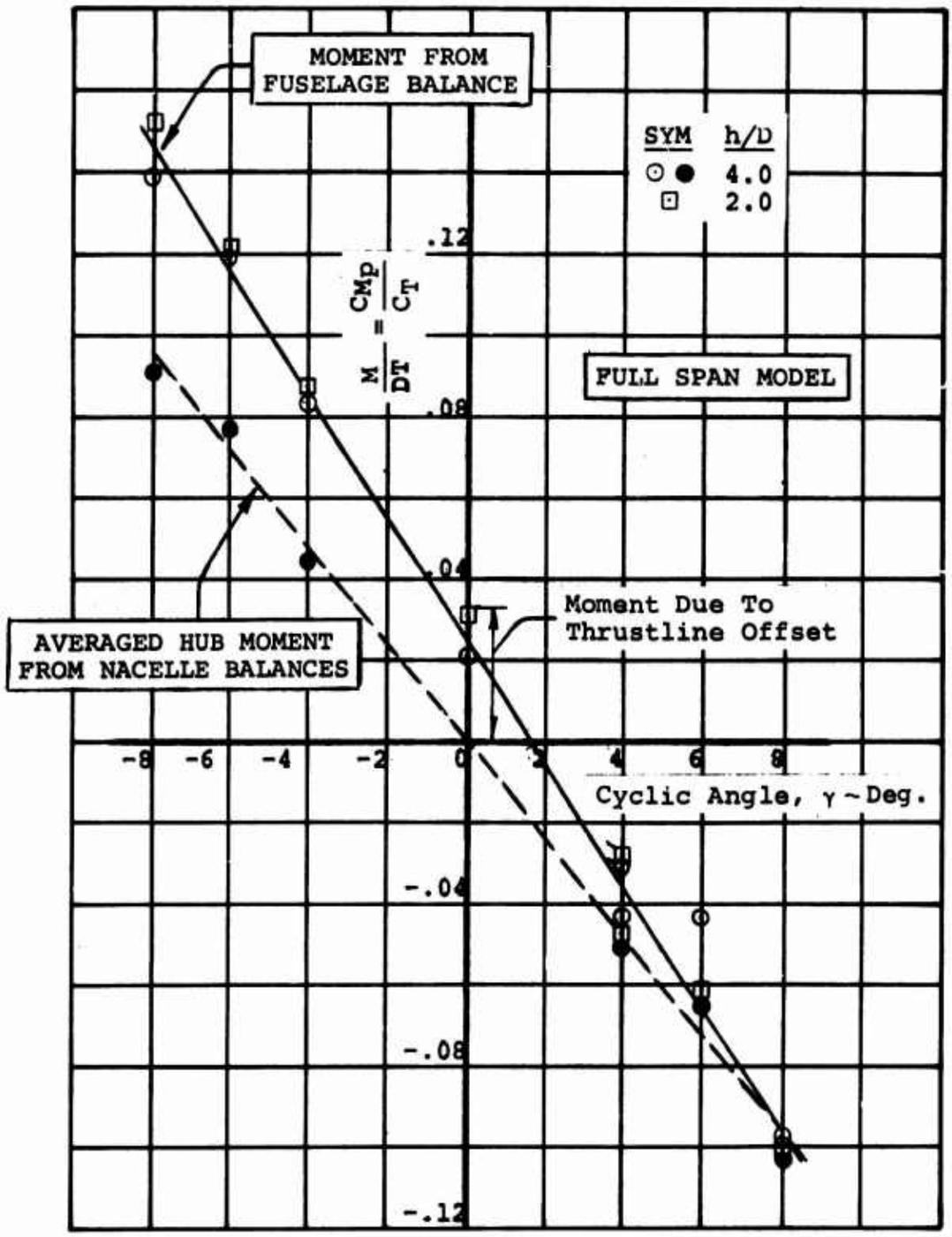

Figure 7. COMPARISON OF A/C PITCHING MOMENT DUE TO CYCLIC WITH HUB PITCHING MOMENT/O.G.E. HOVER

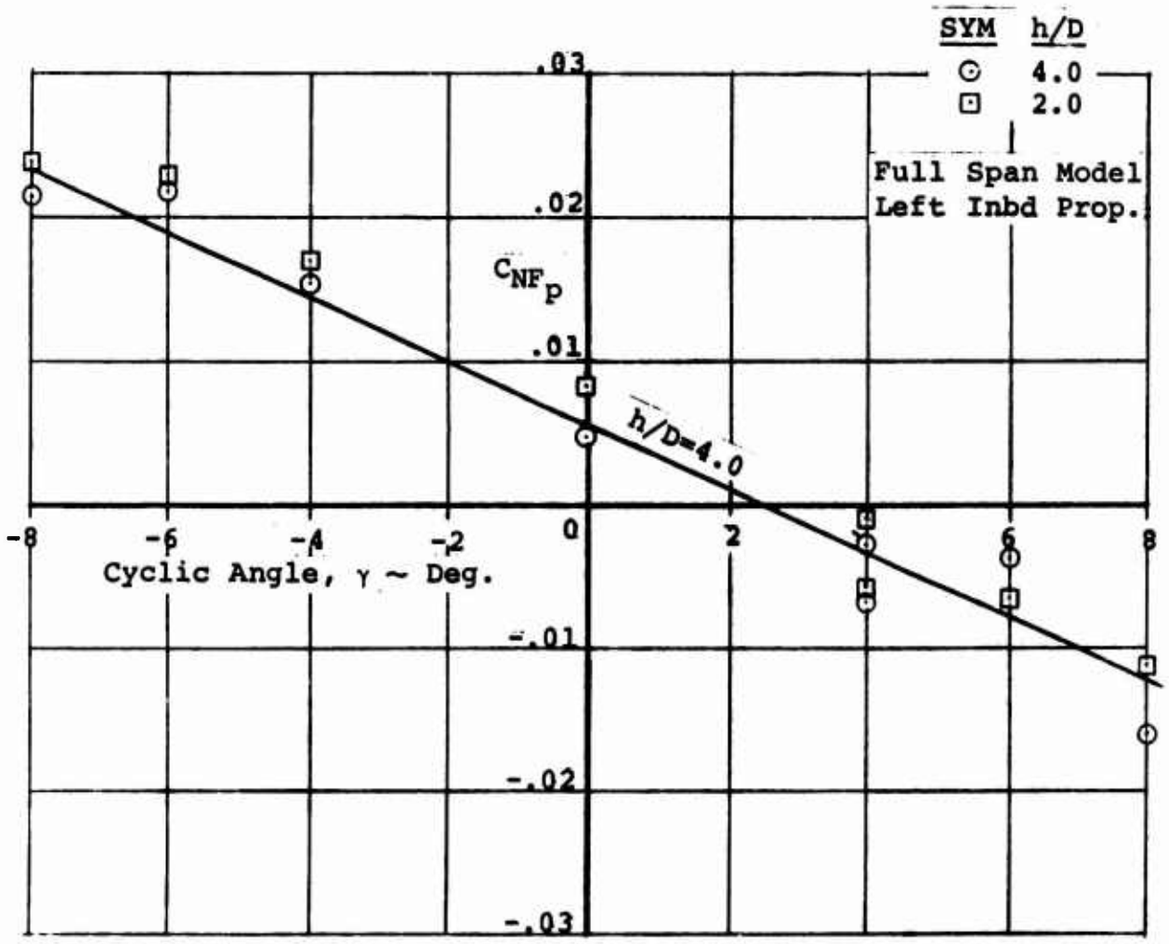

Figure 8. CHANGE IN PROP NORMAL FORCE WITH CYCLIC/O.G.E.HOVER

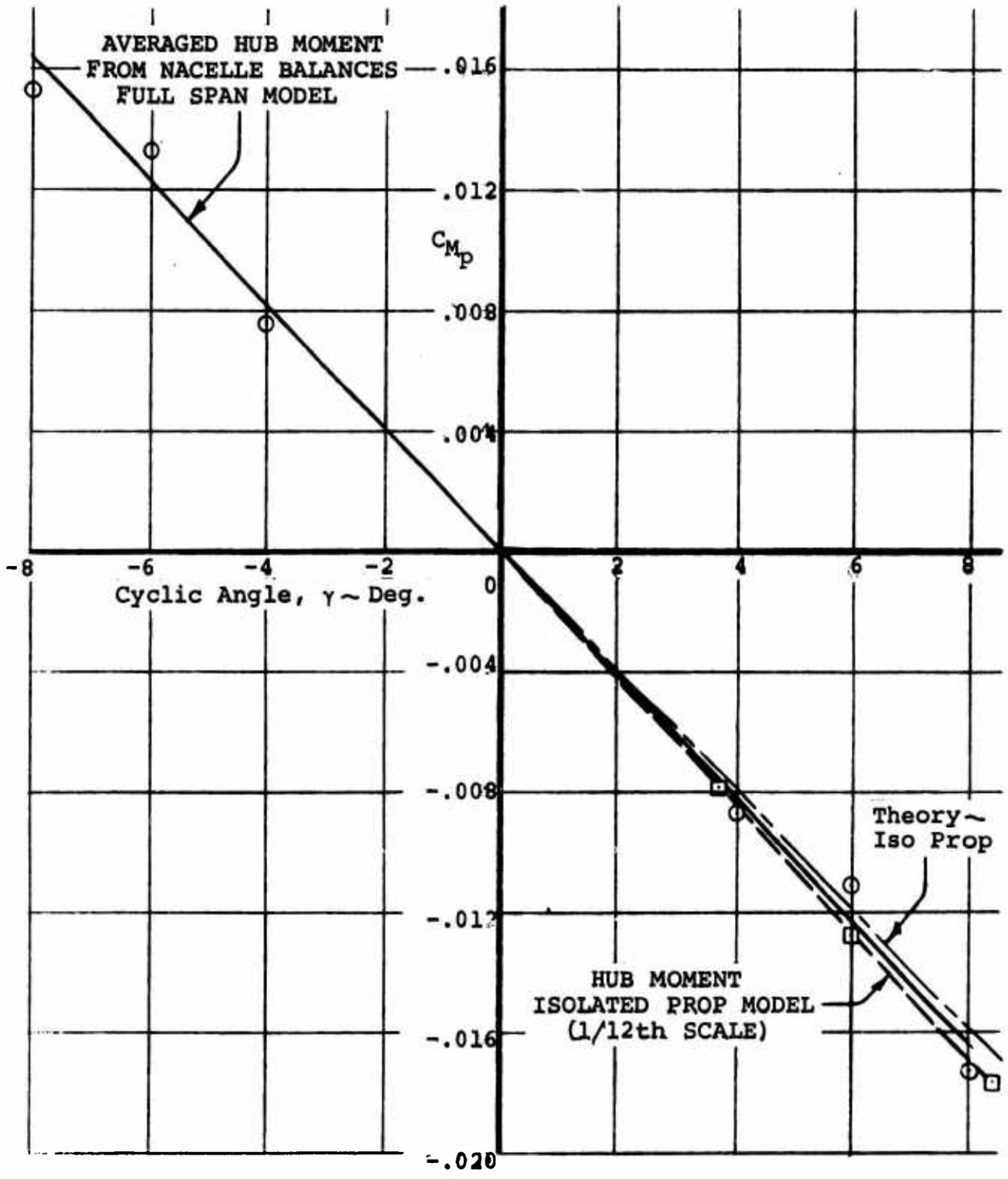

Figure 9. EFFECT OF WING ON PITCHING MOMENT DUE TO CYCLIC/O.G.E. HOVER

Since the curves are only 3% apart, it can be concluded that the wing has no significant influence on the effectiveness. In addition, Figure 9 shows the close agreement between the isolated prop data and theory based on blade element considerations.

As a consequence of the 1/12th scale propeller having a total activity factor of 480 and the 1/3rd scale propeller model being designed with a TAF of 640 it would be expected that a direct comparison of the respective cyclic pitching moment data (Figure 10) will show a substantial increase in cyclic pitching moment capability for the 1/3rd scale prop. An adjustment of the 1/12th scale data by the ratio of activity factors increases the measured cyclic effectiveness from .00212 $\Delta C_{M_p}/\Delta\gamma$ to .00282 $\Delta C_{M_p}/\Delta\gamma$, a value that compares favorably with the .00289 $\Delta C_{M_p}/\Delta\gamma$ value measured for the similar blade planform 1/3rd scale model. In addition, the 1/3rd scale prop data could be adjusted slightly downward (4% per 1/3rd scale data) to correct for the effect of the higher thrust coefficient (C_T) at which the 1/3rd scale test data was obtained. This close agreement in the two sets of data indicates that the cyclic pitch control capability of a relatively low Reynolds number 2 ft. diameter propeller model is not degraded when moderate collective pitch and cyclic pitch angles are used. Higher settings would probably show a difference between 1/12th scale and 1/3rd scale data.

The data presented in Figure 10 is also interesting in that the cyclic pitch capability measured on the 1/3rd scale model is linear over the range from -10° to +10° of cyclic pitch. Even with 12° of cyclic, only a 6% fall-off from linearity was experienced.

Noted on Figure 10 is the total cyclic angle required for the representative tilt wing aircraft hovering with a gross weight of 87,000 lb. at 2500 ft/93° atmospheric conditions. A total angle of 8.7° is shown, divided into 1.7° for c.g. trim and 7° for meeting a pitch acceleration value of 0.6 radian/sec^2. This angular value of 8.7° is conservative from two aspects: an option exists to trim out approximately 60% of the c.g. travel in hover with flap deflection, and second, the 27% favorable change in aircraft pitching moment due to the effect of cyclic on prop normal force as shown in Figure 7 is not included. As a consequence of these two factors and in addition, since the full cyclic pitch capability of the full scale 26.4 ft. diameter / 640 TAF propeller would not be utilized, the activity factor and/or the propeller diameter could be reduced.

Figure 11 evaluates the wing effect on the shaft power increase due to cyclic at the O.G.E. hover condition where the power requirements of a V/STOL vehicle are maximum. The shaft power increase with cyclic as measured during the 1/12th scale

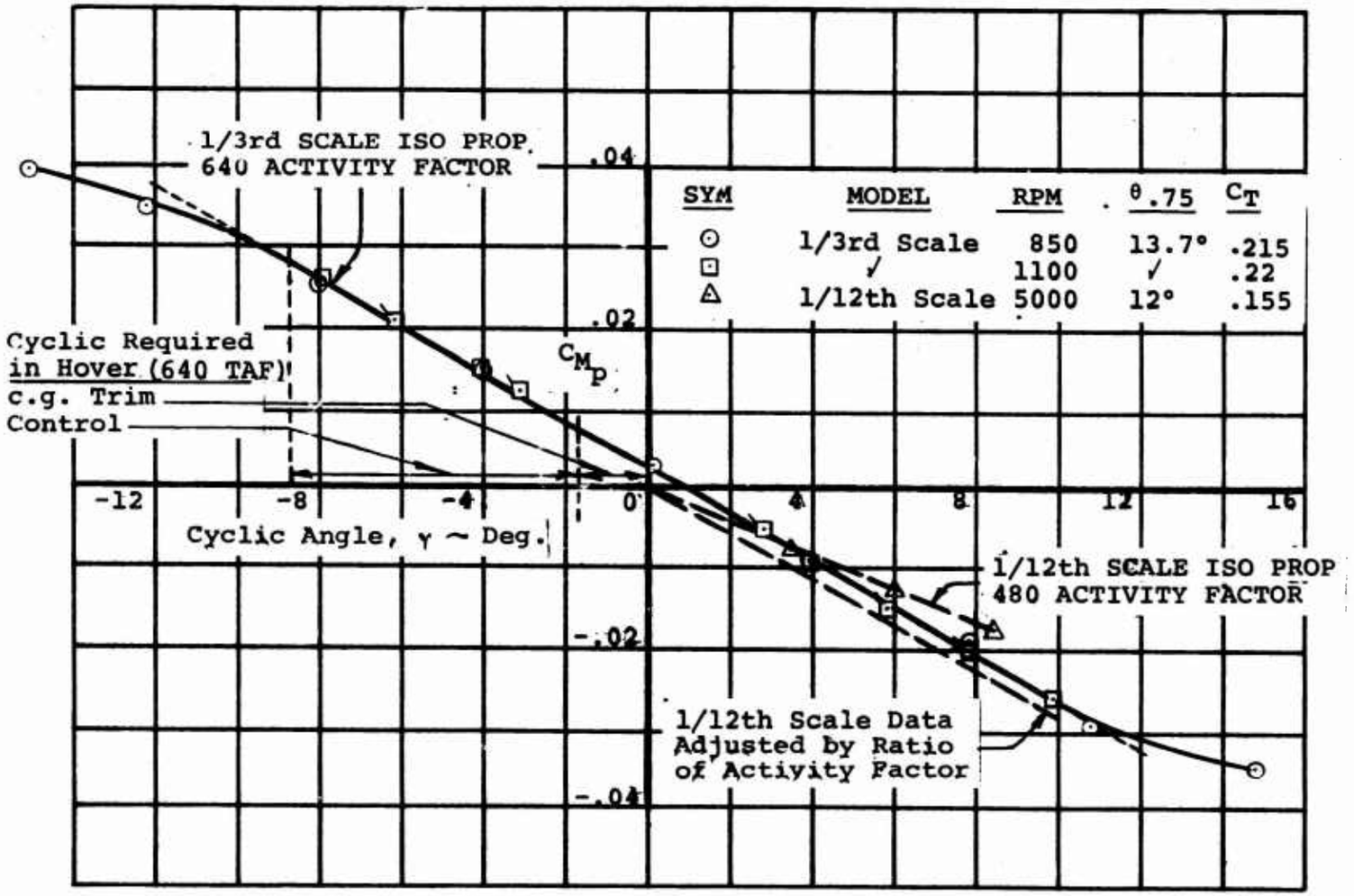

Figure 10. COMPARISON OF HUB PITCHING MOMENT DUE TO CYCLIC--1/12th & 1/3rd SCALE MODELS O.G.E. HOVER

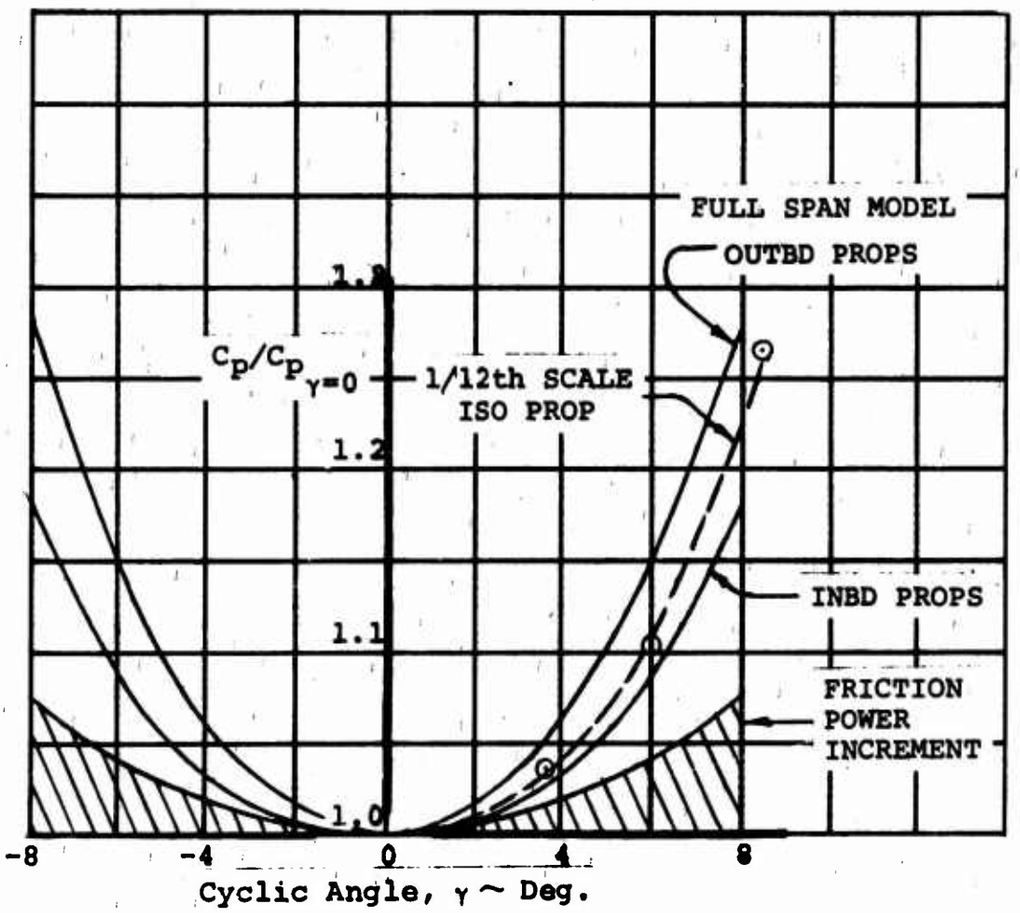

Figure 11. EFFECT OF WING ON POWER REQUIRED DUE TO CYCLIC/O.G.E. HOVER

isolated propeller test is seen to be essentially an average of that measured on the outboard and inboard props of the full span model indicting that the wing has only a small influence. The outboard props exhibited higher power requirements than the inboard props. This is probably a result of the overlapping, whereby the outboard props have been placed in the direct influence of the inboard props; however, the difference appears to be excessive for the amount of the overlap used, 7%D.

As a result of the power being measured via strain gaged shafts, the data represents shaft power requirements, and thereby includes the friction losses in the cyclic hub assemblies. The friction losses in the 1/12th scale models will be large as a result of operating these hubs at 5000 RPM. An indication of the magnitude of the friction power requirements for the 1/12th scale hub was provided by the rolling moment component of the six component nacelle balance. This data is also presented in Figure 11. The difference between the shaft power curve and the friction power curve represents the aerodynamic power required by the cyclic pitch action, which is seen to be 15% with 8° of cyclic.

Measurements of the power increase due to cyclic from the 1/12th scale model were anticipated to be high at moderate cyclic angles as a result of bearing friction, and excessively high at the larger cyclic angles due to the additional factor of a low blade Reynolds number prevailing at a condition where relatively high blade angles are required. This assumption is substantiated in Figure 12, which compares the power measurements from both the 1/12th scale and 1/3rd scale isolated prop models. In this figure, the friction power measurements from the 1/12th scale model are shown along with the plotted shaft power data. This data indicates that cyclic power increments from a 1/12th scale model are reasonable if friction power is accounted for and the cyclic angle does not exceed about 6°, whereas with the 1/3rd scale model power measurements exhibited a normal variation up to 12° of cyclic. The 14.6% power increment produced by the 1/3rd scale model with the 8.7° cyclic pitch control requirement includes the bearing friction power.

Associated with the power required due to cyclic is the effect of cyclic inputs on propeller thrust. A loss in thrust when cyclic is applied would decrease the hover capability or increase the power required to hover at a given gross weight. The 1/3rd scale data presented in Figure 13 shows that this is not the case. No change in thrust occurred with cyclic angular inputs up to 15°. A possible explanation for the invariable thrust up to large cyclic angular inputs would be the favorable influence of dynamic stall on the blade element lifting capability.

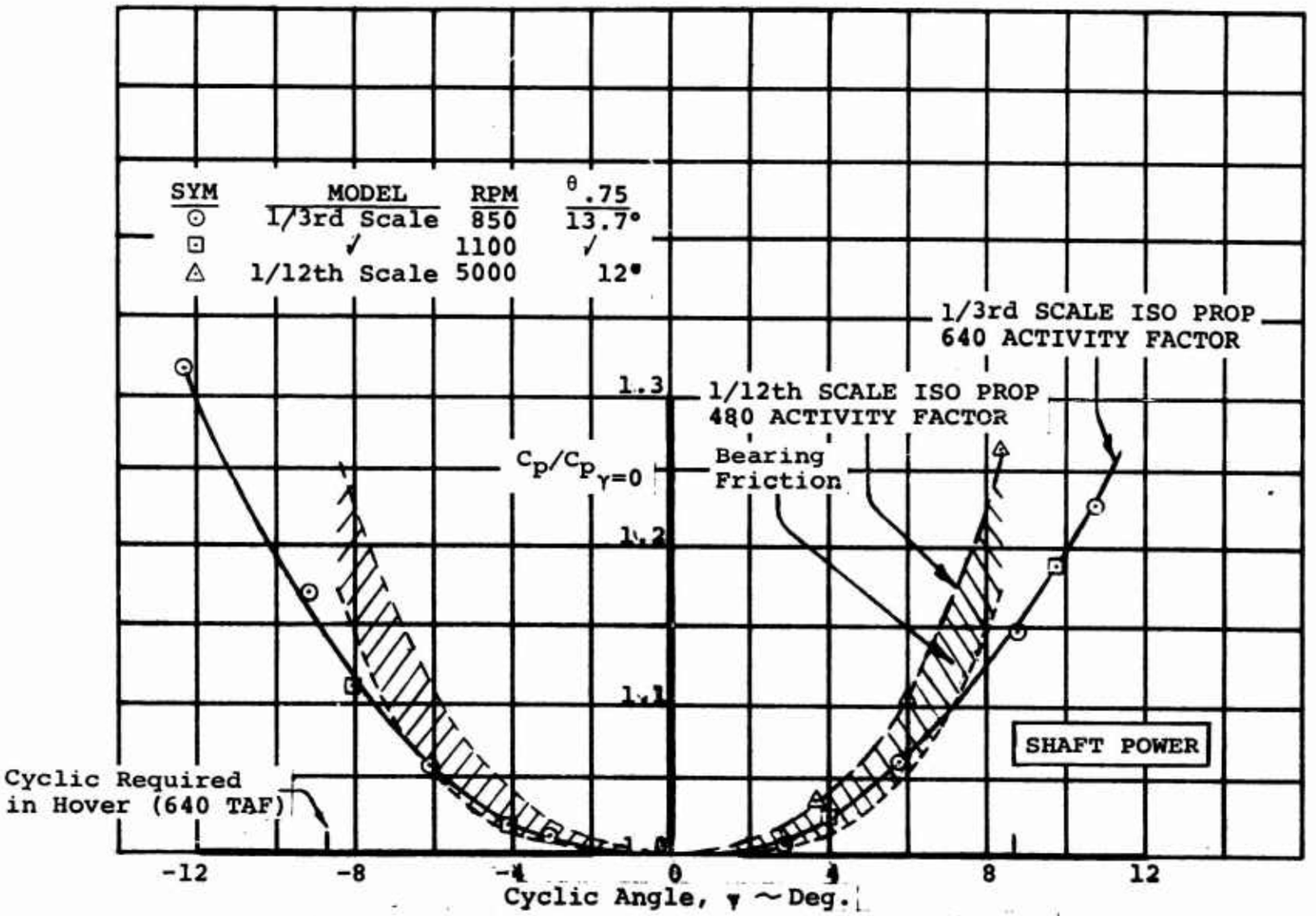

Figure 12. COMPARISON OF INCREASE IN POWER DUE TO CYCLIC-1/12th & 1/3rd SCALE MODELS O.G.E. HOVER

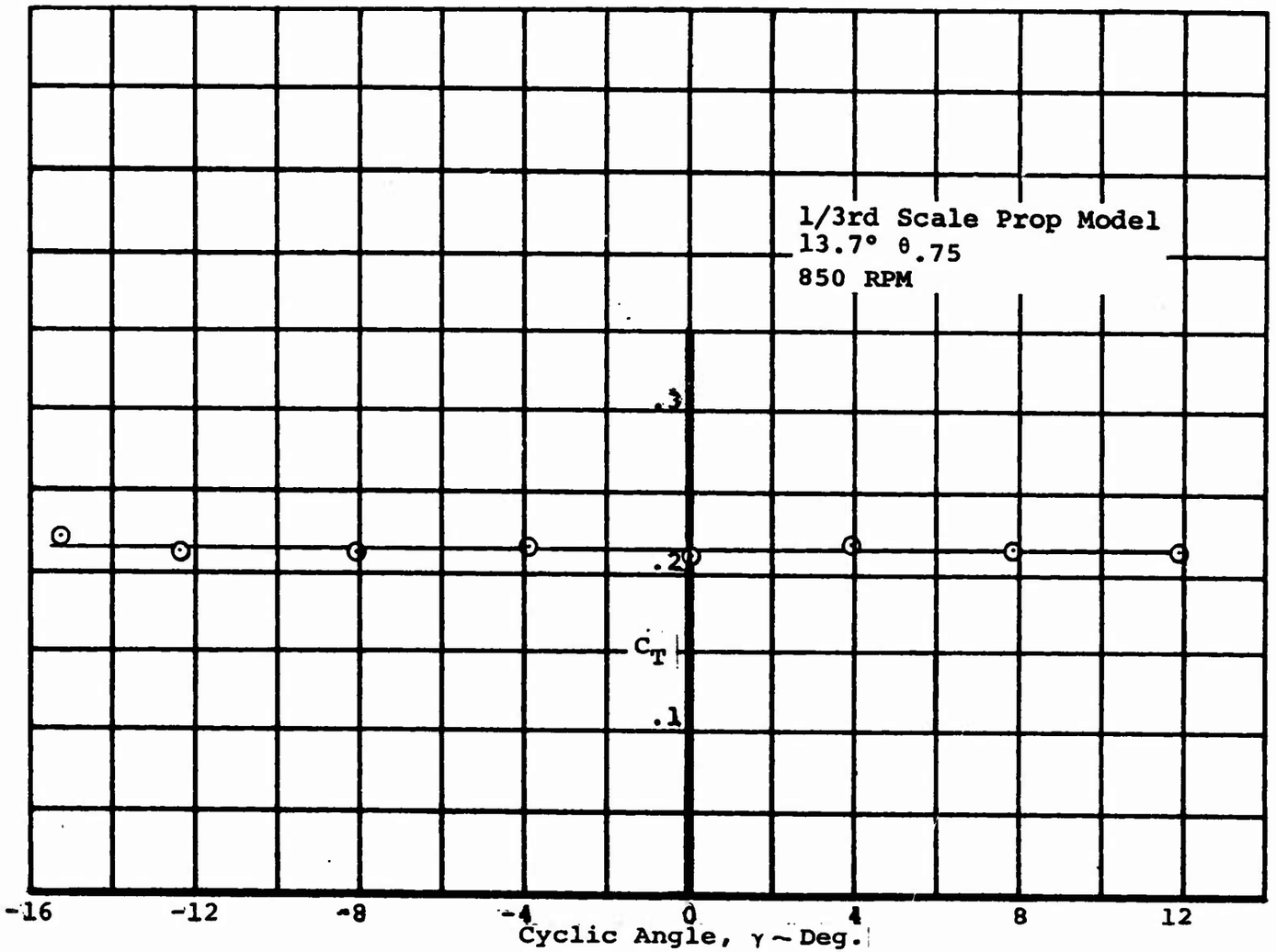

Figure 13. EFFECT OF CYCLIC ON THRUST IN O.G.E. HOVER

2. CYCLIC PITCH EFFECTIVENESS IN TRANSITION

Both 1/12th scale and 1/3rd scale isolated propellers when tested over a wide range of shaft angles and advance ratios representative of transitional flight, exhibited the same small variation in cyclic pitch effectiveness with advance ratio, J. The hub pitching moment developed per degree of cyclic proved to be constant from hover up to an advance ratio of 0.3 with a gradual increase in effectiveness of a 10% magnitude being experienced at 0.5 J. Figure 14 provides the comparison. The incremental difference in effectiveness between the 1/12th scale and 1/3rd scale model, as recorded in the hover condition and noted to largely result from the difference in activity factors, is maintained over the transition range evaluated.

Data obtained on both 1/12th scale and 1/3rd scale prop models showed that the incremental hub pitching moment due to cyclic pitch is virtually independent of shaft angle up to angles in the order of 90°. For example, in the 1/12th scale test, ΔC_{M_p} varied by an average of only 4% from zero shaft angle up to 60° of shaft angle over the speed range tested. Figure 15 illustrates the insensitivity of cyclic moment to large changes in shaft angle. The similarity between the 1/12th scale and 1/3rd scale test results in both hover and transition, validates the use of a relatively low Reynolds number 2 ft. diameter propeller model for investigating cyclic pitch control capability and characteristics other than power changes.

Of concern in the investigation of the control capability of installed cyclic propellers was the large increase in basic hub pitching moment and prop normal force produced at high propeller shaft angles or wing tilt angles with the high lift system extended, a condition experienced in descent. Figure 16 shows that the initial rate of build-up of hub pitching moment on the installed propeller is about three times that of the isolated propeller for the various advance ratios (J) tested. The curves for the outboard props appear to be bending over (decrease in $\Delta C_{M_p}/\Delta\alpha_p$) at much lower angles of attack than the isolated prop. Companion prop normal force data presented in Figure 17, shows a definite "peaking" of the installed propeller data at substantially lower angles of attack than for the isolated prop, following an increase in the normal force to a magnitude approximate 2.5 times larger than measured on the isolated prop at the same geometric propeller angle of attack. This "peaking" was also evident in the total aircraft moment measurements from the full span model at high C_{T_s} or low speed conditions where high wing tilt angles are required, as shown in the following Figure 18.

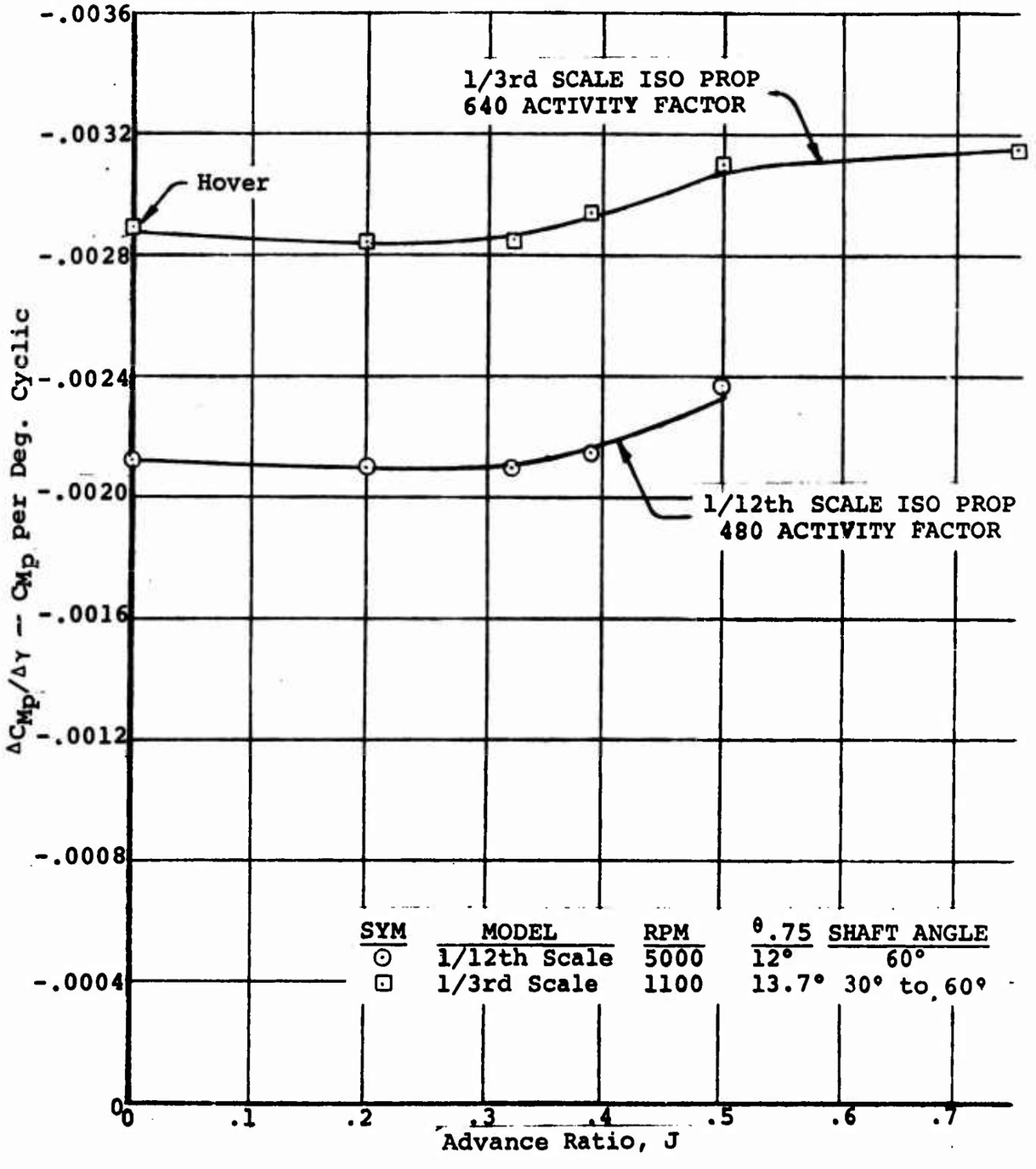

Figure 14. CYCLIC PITCH EFFECTIVENESS IN TRANSITION
1/12th & 1/3rd SCALE ISO PROP MODELS

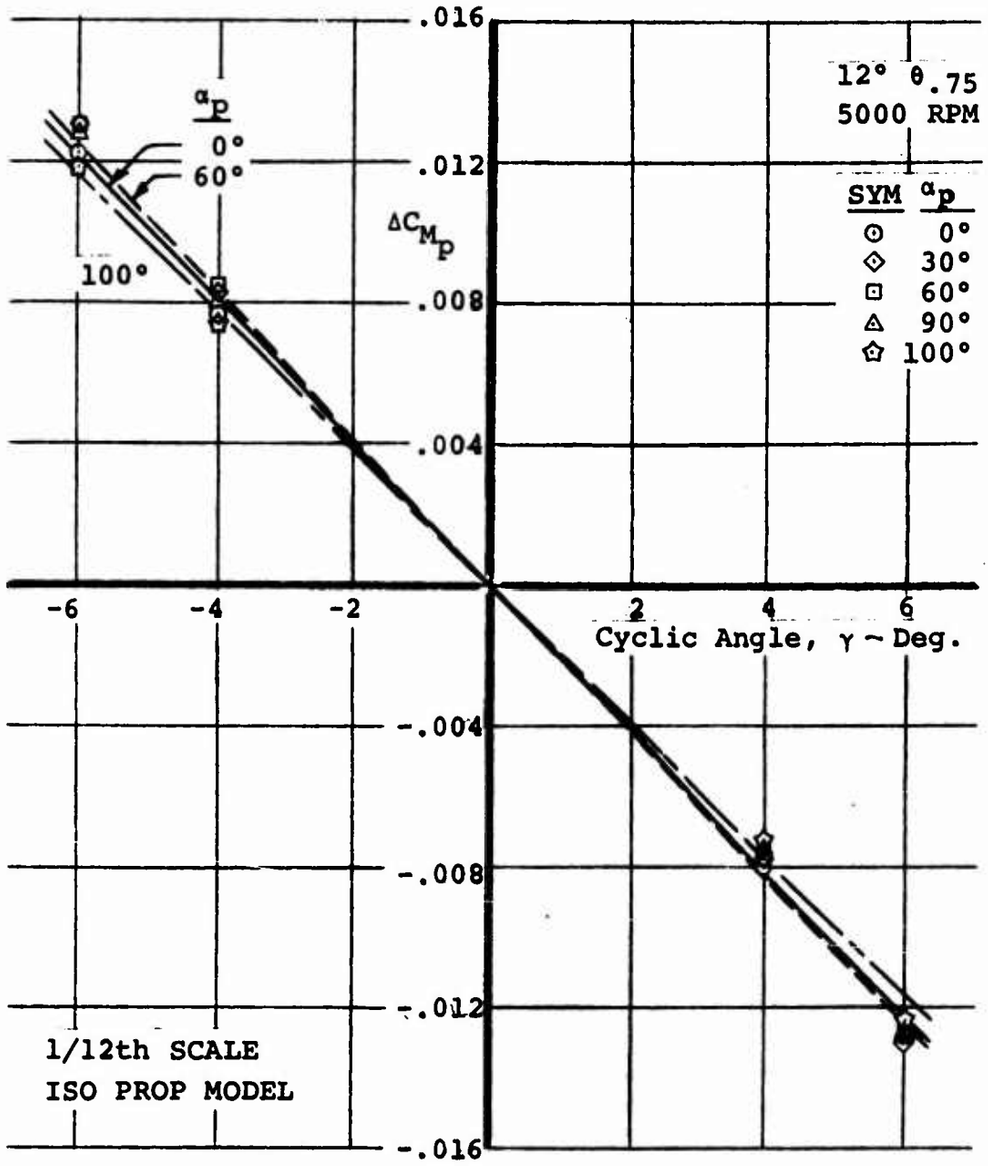

Figure 15. INSENSITIVITY OF CYCLIC MOMENT TO SHAFT ANGLE/J=.32

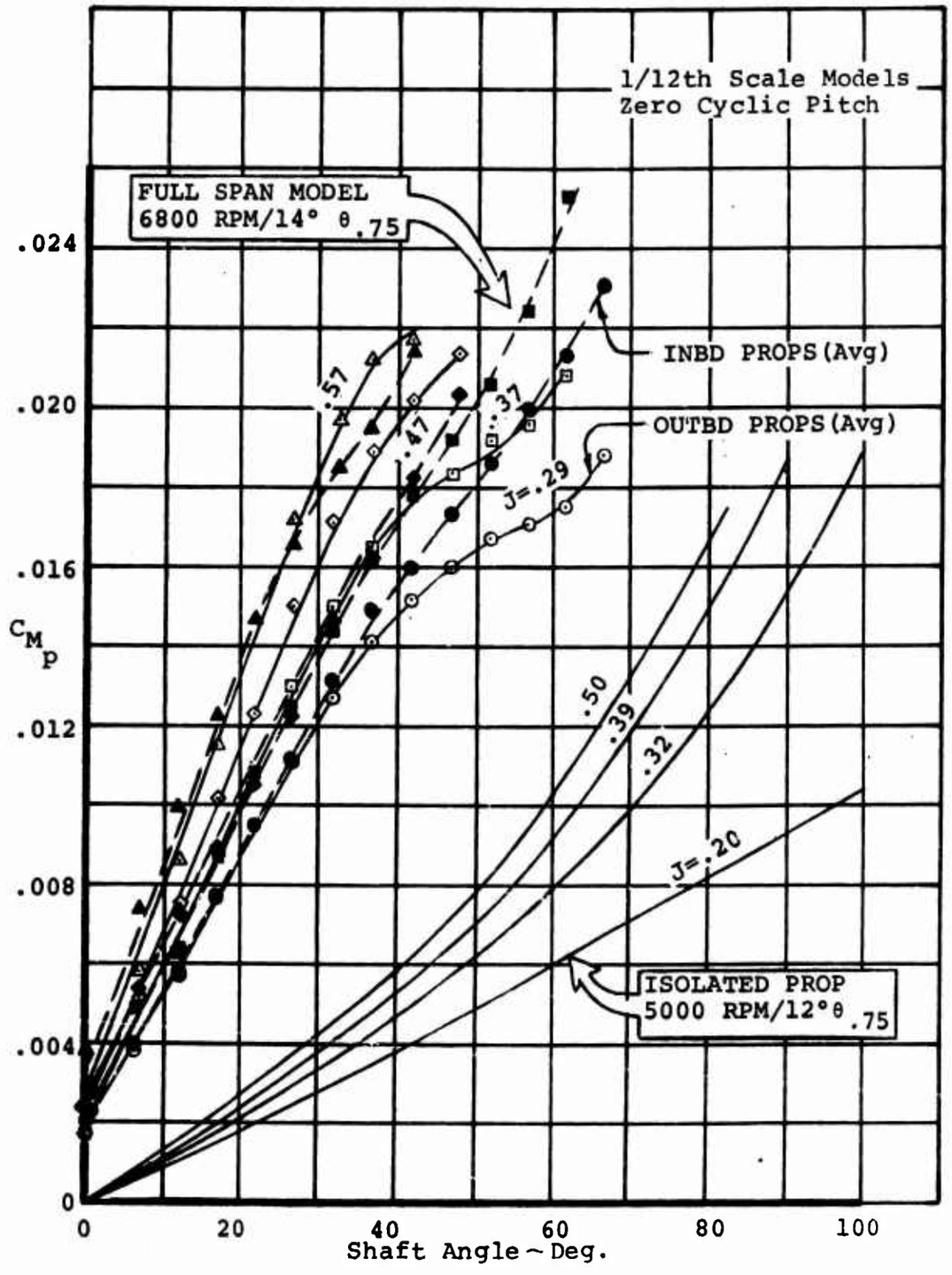

Figure 16. EFFECT OF WING/SLATS & 60° FLAPS ON BASIC HUB PITCHING MOMENT

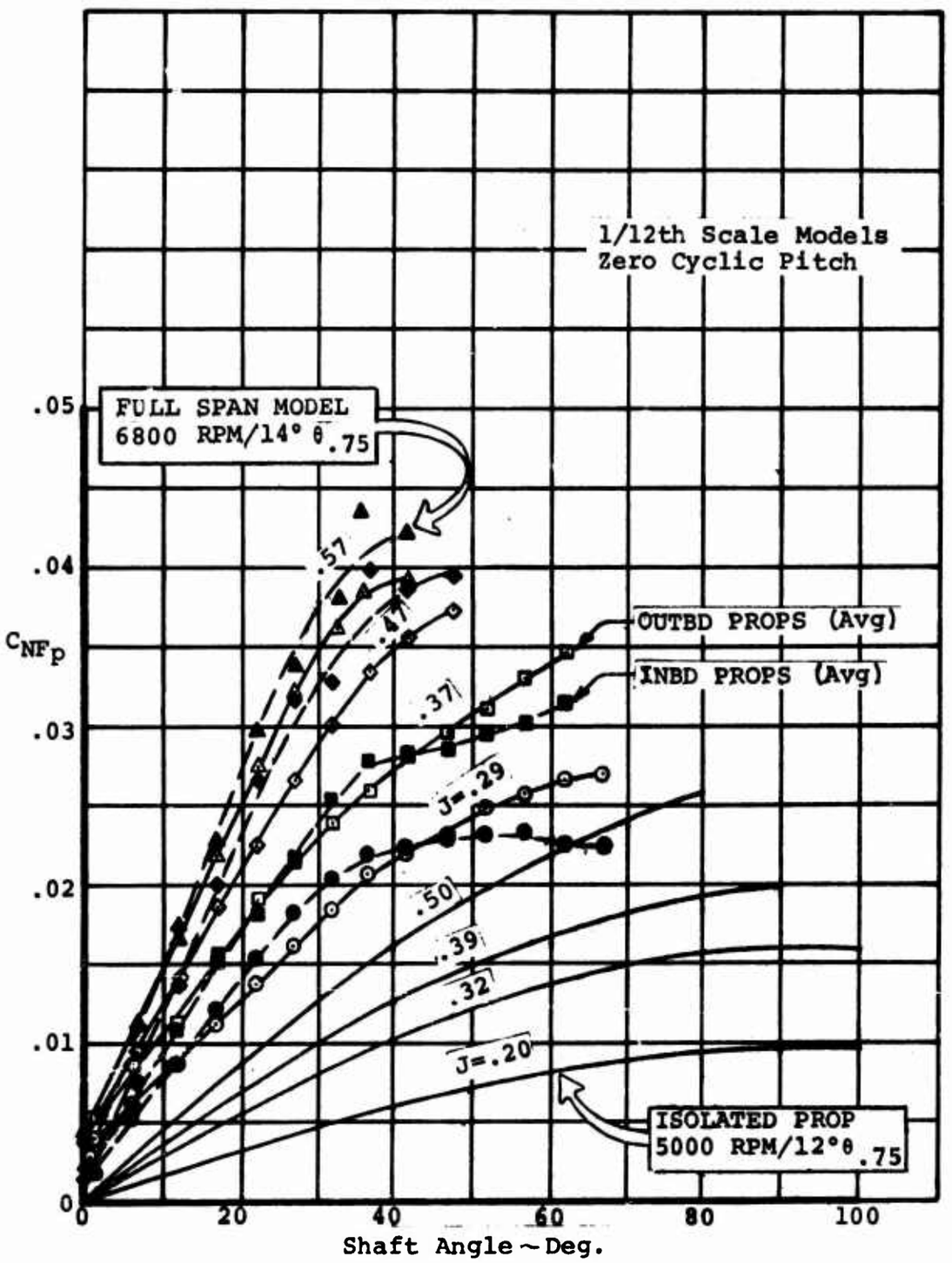

Figure 17. EFFECT OF WING/SLATS & 60° FLAPS ON PROP NORMAL FORCE

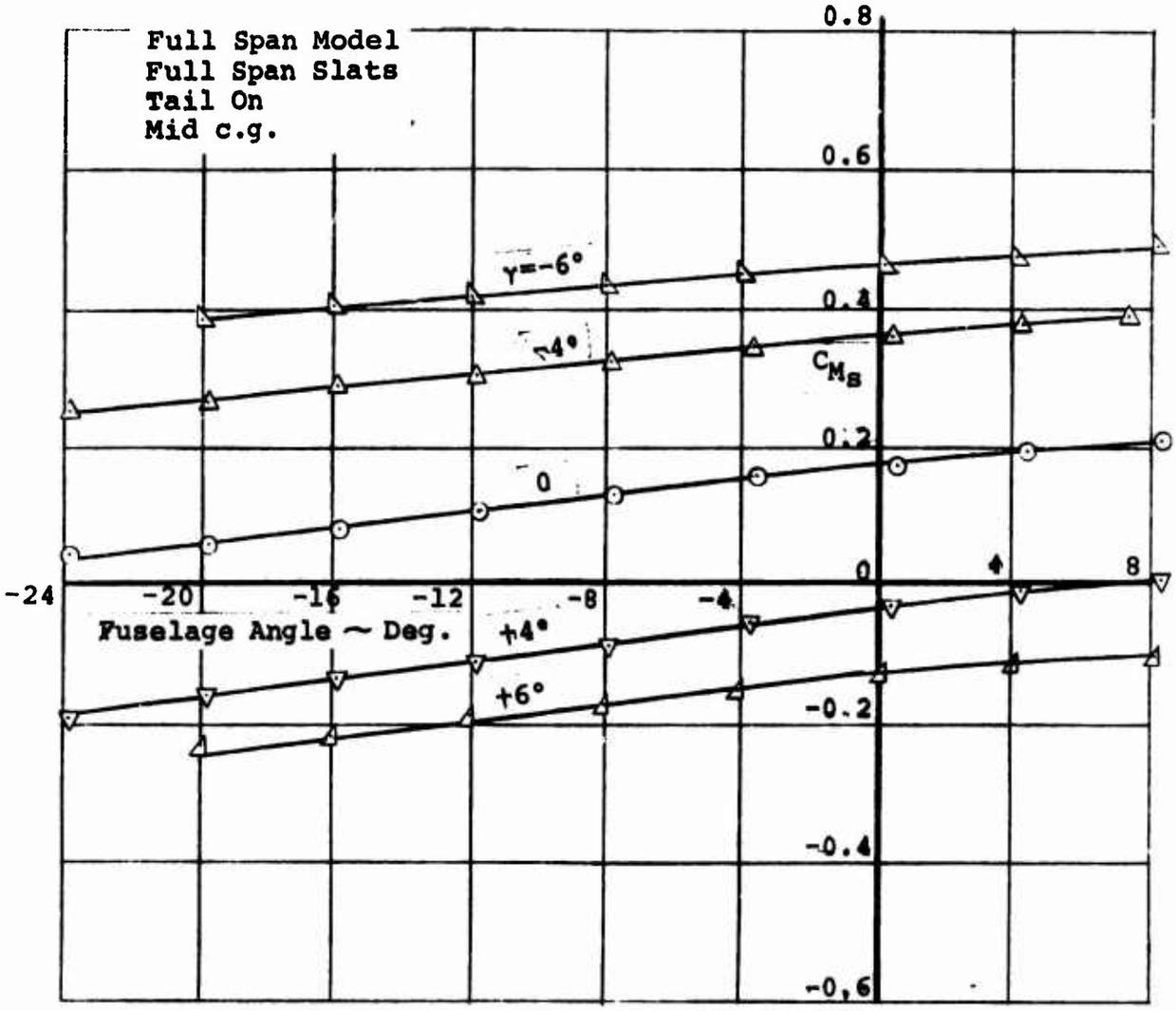

Figure 18. CYCLIC PITCH CONTROL
55° WING TILT/60° FLAPS
C_T = .93

Data for determining possible wing/flap effects on cyclic pitching moment characteristics was obtained through testing of the full span model at selected combinations of wing tilt, flap angle, and slipstream thrust coefficient representative of points in the transition regime. This testing of the full span model followed a more detailed investigation of the tail-on and tail-off longitudinal characteristics through transition, with wing tilt angles ranging from 0 to 70°, and flap settings ranging from the retracted position to a 60° deflection.

Figure 18 presents typical full span model cyclic pitch control data, in this case, data required with 55° of wing tilt, and 60° of flap deflection at a C_{T_s} of 0.93. This C_{T_s} represents a forward flight path speed of approximately 30 knots. In this plot, the moments have been transferred to a mid c.g. position and are in the slipstream notation. The linearity of the change in pitching moment with cyclic angle and the small variation in effectiveness with angle of attack is characteristic of the other cyclic pitch control data that was obtained.

In general, the cyclic effectiveness decreased at a moderate rate of about 15% from the lowest to the highest shaft angle tested, as illustrated by the example data presented in Figure 19. An important point indicated by the data, is that no noticeable decrease in effectiveness occurred as a result of wing stall. The noted decrease in effectiveness with shaft angle is largely a ramification of the slipstream notation system. All 1/12th scale test runs were performed with a constant propeller RPM and tunnel speed or q, the result being that propeller thrust and slipstream q (q_s) increased with the propeller shaft angle, α_p. Therefore, a hub pitching moment that was found to be virtually independent of shaft angle in propeller notation will apeear to decreace when transcribed to the slipstream notation. Part of the decrease can be identified with the small percentage change in lift accompanying cyclic pitch inputs.

Figure 20 presents a comparison in slipstream coefficients of the pitching moment capability per degree of cyclic obtained on the full span model with those measured on the 1/12th scale isolated propeller model at directly comparable conditions of 5000 RPM and 12° of blade angle. The data presented, is for shaft angles corresponding to essentially constant descent angles over the thrust coefficient range. As indicated, higher shaft angles, which are within 5% of the respective wing tilt angles in this presentation, are required at the larger thrust

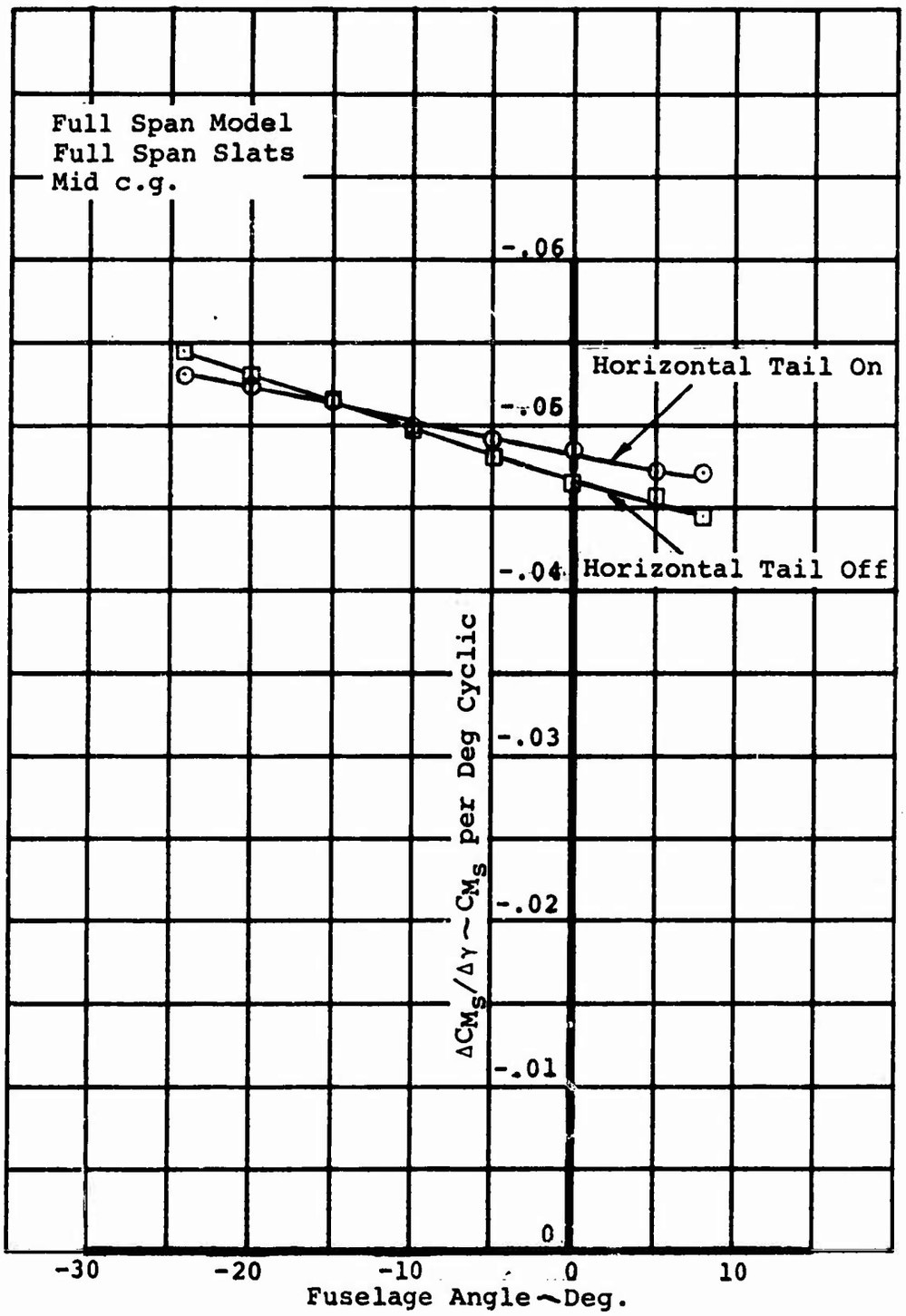

Figure 19. VARIATION OF CYCLIC PITCH EFFECTIVENESS WITH FUSELAGE ANGLE
45° WING TILT/60° FLAPS/NOM C_{T_S} =.81

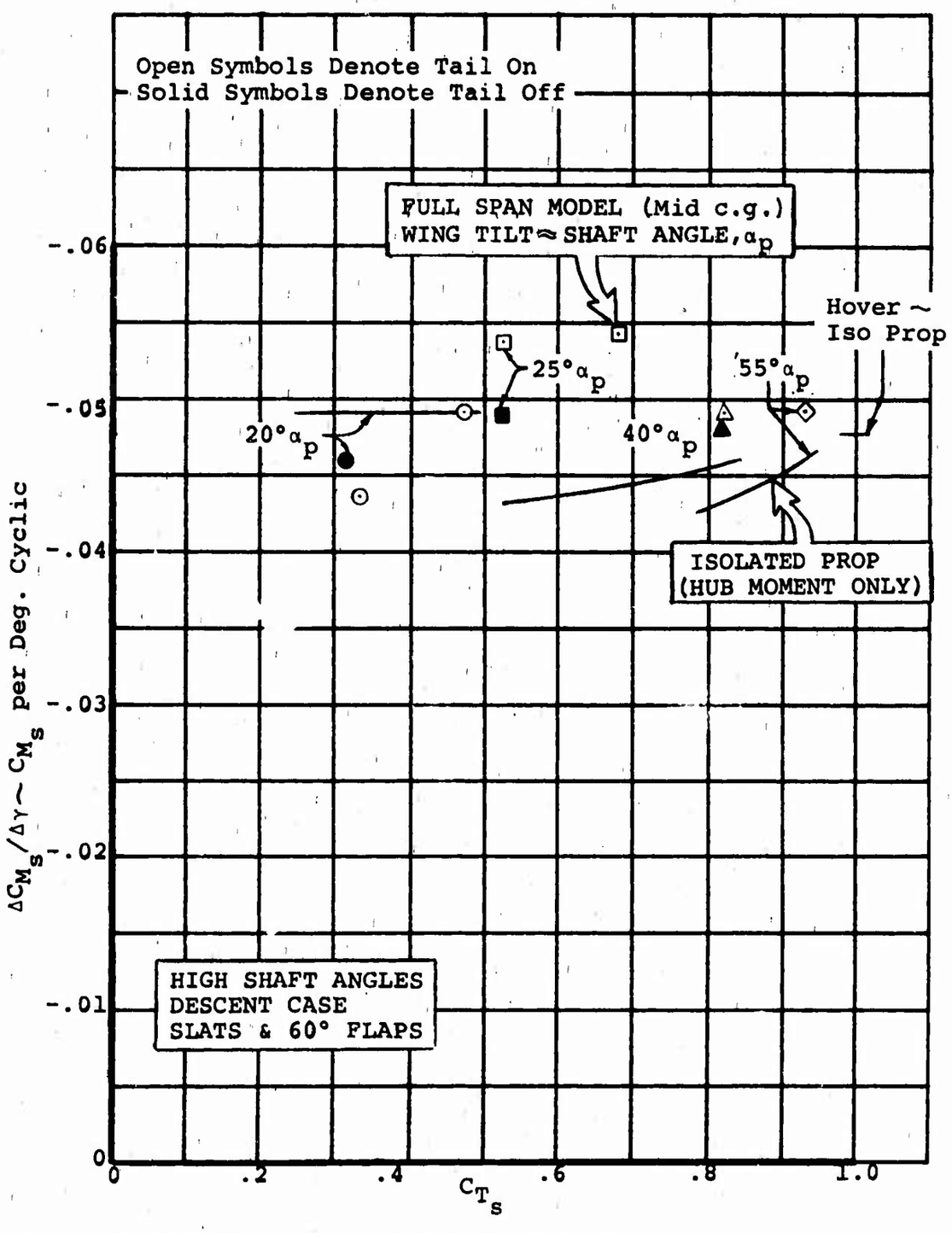

Figure 20. COMPARISON OF CYCLIC PITCH EFFECTIVENESS IN TRANSITION 1/12th SCALE FULL SPAN & ISO PROP MODELS

coefficients or lower forward speeds. The descent case was selected for this presentation, since the combination of shaft angle and wing configuration, full span slats deployed and 60° of flap deflection, would potentially have the largest adverse effect on cyclic pitch effectiveness, due to the increased basic hub pitching moment and possible flow distortion.

Except for the lowest thrust coefficient condition tested (0.32 C_{T_S}), the cyclic pitch effectiveness measured about a mid c.g. of the full span model was larger than that recorded at the hub of the isolated prop model. Some of the increase in cyclic effectiveness recorded on the full span model at the higher C_{T_S} values, undoubtedly reflects the favorable change in prop normal force with cyclic pitch inputs previously observed in the hover mode. See Figure 8. When this is taken into consideration, it is not clear that the wing and flaps actually exert a favorable influence on the cyclic effectiveness as the data in Figure 20 would seemingly indicate. Conversely, any adverse influence of the wing and flaps on the cyclic effectiveness in the C_{T_S} regime where the cyclic requirements are largest (higher C_{T_S} values) must be of a small magnitude.

Figure 20 shows full span model data for both horizontal tail-on and tail-off cases. This data indicates that the horizontal tail has only a small effect, if any in actuality, on the cyclic propeller pitching capability.

SECTION IV

LOW SPEED DESCENT CAPABILITY

1. EFFECT OF CYCLIC PITCH ON DESCENT PERFORMANCE

One of the critical design items for a tilt wing aircraft is the low speed descent capability. Boeing-Vertol has been using as a buffet free design goal, a minimum descent rate of 800 fpm up to a flight speed of 42 knots and a descent angle of 12° at higher speeds. The leading edge slat design and positioning (higher slat angles behind an upturning propeller) plus large chord double slotted flaps with a movable fore flap were developed during the 1969 Boeing-Vertol wind tunnel test program of a four prop tilt wing aircraft, as a means of meeting this descent rate goal.

In the same test program, the placement of the propeller hub ℄'s with respect to the wing leading edge was investigated with regard to maximizing descent performance. In general, the more forward a propeller is located ahead of the wing, the lower the thrust centerline must be with respect to the wing chord plane. These tests, which substantiated previous two-propeller tilt wing test data, indicated, for example, that with a propeller located 35% of the basic wing chord (c) ahead of the wing leading edge, it is necessary to lower the thrust-line by approximately 15% c below the wing chord plane. The lower thrustline provides a more complete immersion of the wing/flap system in the propeller slipstream up to high wing tilt angles. When the propellers are overlapped, the thrustline of the forward-most propeller should be positioned considerably below that of the aft-most propeller for maximum descent capability. Full scale design studies of propeller/transmission/engine placement resulted in some restrictions (from ground clearance, for example) to the amount that the thrust-lines could be lowered. As a consequence, the inboard and outboard prop hub ℄'s of the full span model were respectively located 22%c and 18%c below the wing chord plane for corresponding distances of 58%c and 42%c ahead of the wing leading edge.

Wing fences to contain or prevent separated flow from spreading were also evaluated in the 1969 test program. With overlapped propellers, two fences per wing half are required, one located at the side of the fuselage to contain separated flow on the wing section extending over the top of the fuselage, and the second located on the wing immediately outboard of the

first, to contain any stall emanating from the gap between the propeller tip and fuselage, and the area behind the propeller tip. This fence configuration was incorporated on the 1/12th scale full span model.

Another configuration element investigated during the 1969 test program was the rotation direction of the inboard propeller. Data obtained on models with both overlapped and non-overlapped propellers showed that an inboard propeller rotation of turning down between the nacelles resulted in more descent capability than an opposite rotation direction. The opposite inboard propeller direction of turning up between nacelles precipitated an earlier stall on the wing and thus incrementally decreased the descent performance. Earlier tests (1968) clearly established the superiority of an outboard propeller rotation direction of turning down between the nacelles. This data base was used to select the rotation direction of both propellers turning down between nacelles for the full span model tests.

A final item considered for the full span model tests was the azimuth angle at which the cyclic angular inputs were to be applied. For pure monocyclic pitch with a rigid propeller/hub system, the input of cyclic should occur at the 6 and 12 o'clock azimuth positions (zero lead or lag angle). Test results reported by Canadair indicated a lower loss in descent capability due to nose down cyclic, when cyclic was applied with 22° of azimuth lead angle. This result was checked during the 1/12th scale semispan model test with the propeller rotation direction of both propellers turning down between nacelles. As reported in Section 6.6 of Reference 1, the opposite result was obtained. A net azimuth lead angle of 30° reduced the overall descent performance with 4° of nose down cyclic. Consequently, the cyclic phase angle for the full span model tests was maintained within a small range that varied from a minimum lead angle of 0° to a maximum lead angle of 15°. With the rigidity of the model's propeller/cyclic hub system established during the 1/12th scale isolated prop test (See Section 6.7 of Reference 2), this phase angle range assured that cyclic inputs would be applied close to the 6 and 12 o'clock azimuth positions.

The results of the low speed descent testing on the full span model with the flaps deflected 60° and cyclic pitch applied are presented in Figure 21. Descent rate at buffet onset is shown as a function of flight path velocity for an aircraft with a 73 lb/ft^2 wing loading. In developing this

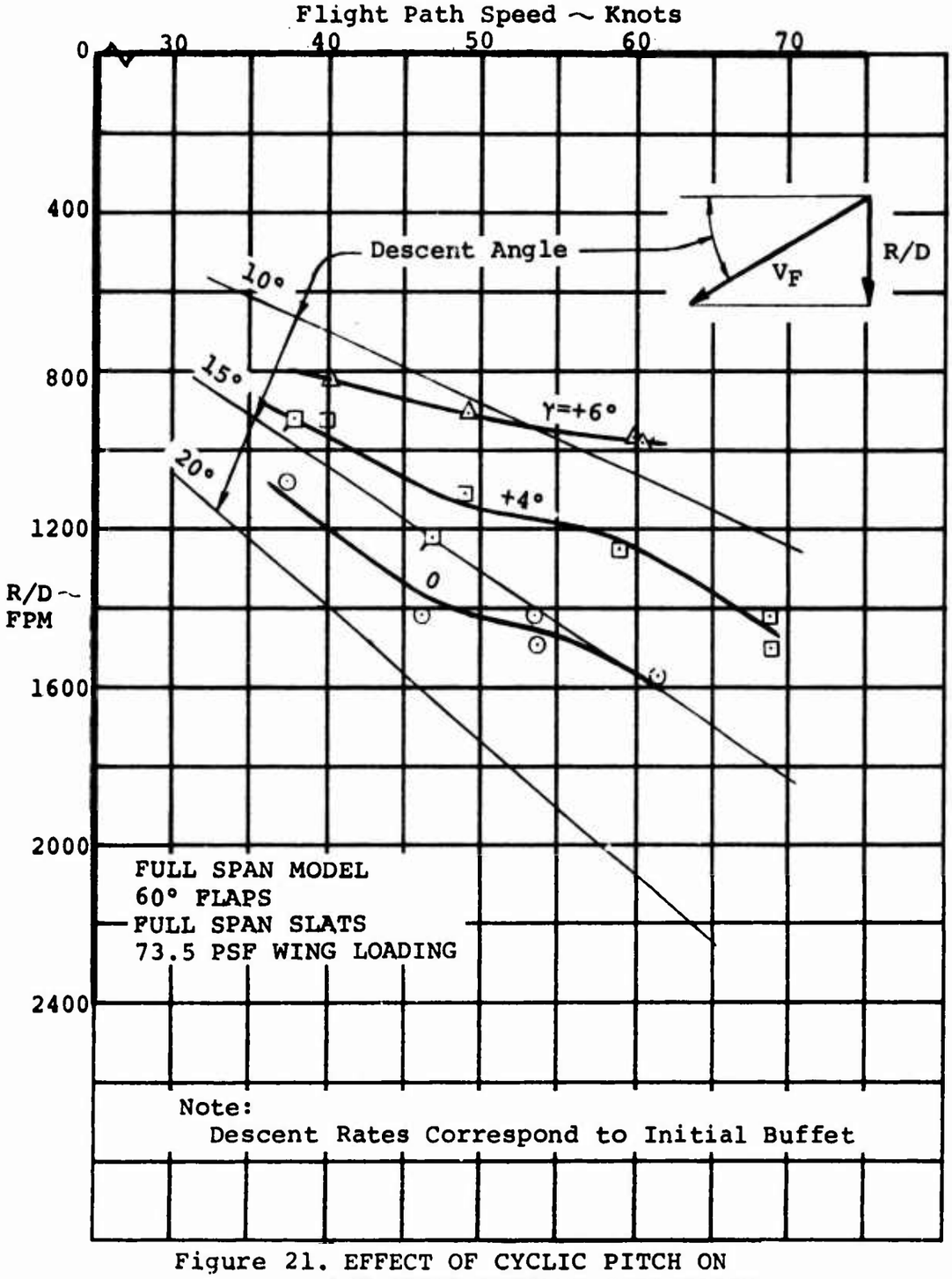

Figure 21. EFFECT OF CYCLIC PITCH ON LOW SPEED DESCENT CAPABILITY

plot, the key element was the interpretation used in determining the buffet onset angle for each of the wing tilt test runs (with zero fuselage angle). The interpretation used is in agreement with the work that Ling-Temco-Vought performed in correlating XC-142 flight test data with wing tunnel data.

Descent capability was determined by establishing the wing incidence angle at which initial stall or separation occurred on the wing outboard of the fences. Inboard areas where stall was tolerated comprise the wing center section over the fuselage and the region between the fences - sections over which freestream q or less than full slipstream q prevail and where roll disturbances are minimal.

In selecting the buffet onset angle, tuft photographs and observer written comments were studied in conjunction with corresponding force polars presented in terms of L/qb^2 vs X/qb^2 rather than the slipstream notation C_{L_s} vs C_{X_s}. With polars in the L/qb^2 vs X/qb^2 format, initial stall coincides with a definite break in the curve at thrust coefficients up to 0.65 C_{T_s} or speeds greater than 55 knots. At lower speeds, the stall build-up is gradual and at a wing angle 10° beyond that selected for buffet onset, the flow remains attached on 75% of the wing.

Examples of buffet onset selection are illustrated by the tuft photos shown in Figure 22. On this model with an average wing thickness of 18% t/c, initial stall occurred at the wing trailing edge over the full C_{T_s} range. The initial stall in these examples is unsymmetrical in that some wing tip stall, along with less inboard stall, was present on the left wing; however, this unsymmetrical situation is not unusual in full span model testing.

Previous Boeing-Vertol tilt wing testing has shown that positive cyclic angles (nose down pitching moment) reduce descent capability and negative cyclic improves it. In line with these results, only positive cyclic angles were evaluated in the subject test program. Figure 21 shows that the loss in descent rate due to positive cyclic averages 100 fpm per degree of cyclic at 62 knots where cyclic is being phased out and 50 fpm per degree of cyclic at a flight speed of 38 knots. This reduction in the loss rate at low speeds is consistent with the hover yaw control testing (discussed later) that shows positive

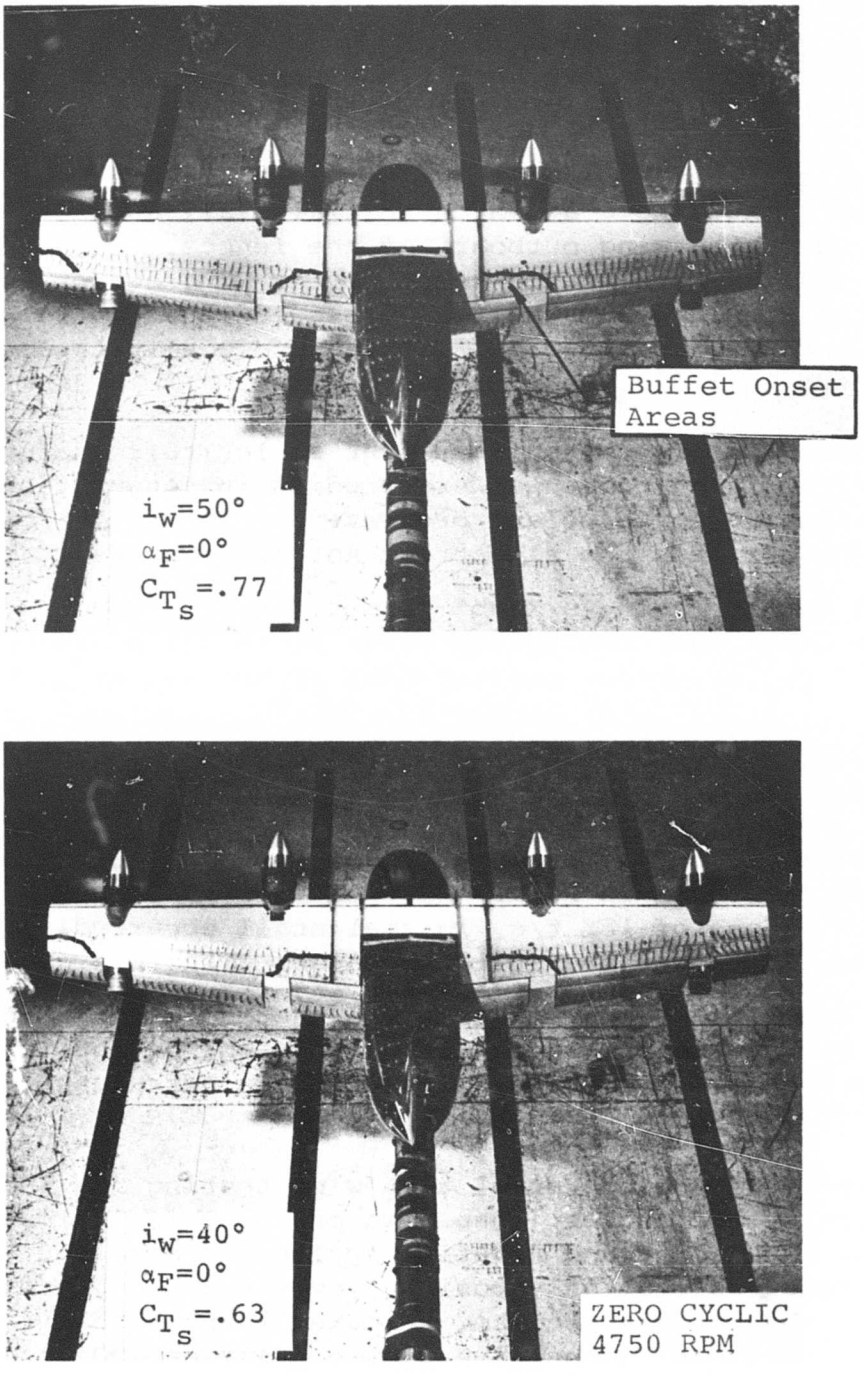

Figure 22. EXAMPLES OF
BUFFET ONSET SELECTION

cyclic to be beneficial and negative cyclic to have the reverse role.

A large portion of the loss in descent performance with positive cyclic has been associated with a reduction in the slipstream turning effectiveness. Evidence of this is included in Figure 23, which presents the buffet onset angles corresponding to the descent data plotted in Figure 21. Buffet onset angles are shown as wing angles of attack at initial stall and as the calculated effective wing angles of attack defined as the angle between the wing chord and the resultant velocity vector at the wing. At 0.77 C_{T_S} (40 knots) the 4° decrease in wing buffet onset angle resulting from the application of 6° of positive cyclic represents only 175 fpm out of the total 500 fpm loss in descent performance. The remainder of the loss, 325 fpm, reflects the reduction in turning effectiveness.

Cyclic pitch testing with the 1/12th scale three-way cyclic hubs was limited to a propeller speed in the order of 5000 RPM (a new design using four blades per the proposed full scale aircraft would permit higher speeds). This model operating condition produced an average slipstream q of 17.5 psf at the combinations of tunnel q and wing incidence angle representative of the descent regime, which in turn resulted in a test Reynolds number per foot of less than 750,000. Of concern during this descent testing was whether the large departure of the disc loading and Reynolds number from full scale values could materially influence a full scale assessment of the measured descent capability. As a consequence of this potential problem, zero cyclic runs with a set of collective hubs capable of operating at a higher speed were performed. The collective hub operating speed of 6800 RPM increased the slipstream q to 38.5 psf, a value close to full scale design, and correspondingly increased the test Reynolds number to 1.2×10^6 per foot, a value considered normal for most low speed wind tunnel testing. A representative Reynolds number for a full scale tilt wing aircraft would be about 15×10^7 based on a mean aerodynamic chord of 12.4 ft.

Figure 24 provides a direct comparison of the measured descent rates with the two different sets of hubs. Since both prop/hub sets were geometrically similar, any difference in descent performance could be attributed to disc loading and Reynolds number effects. The data plotted in Figure 24 shows a maximum difference in the measured descent capability of 100

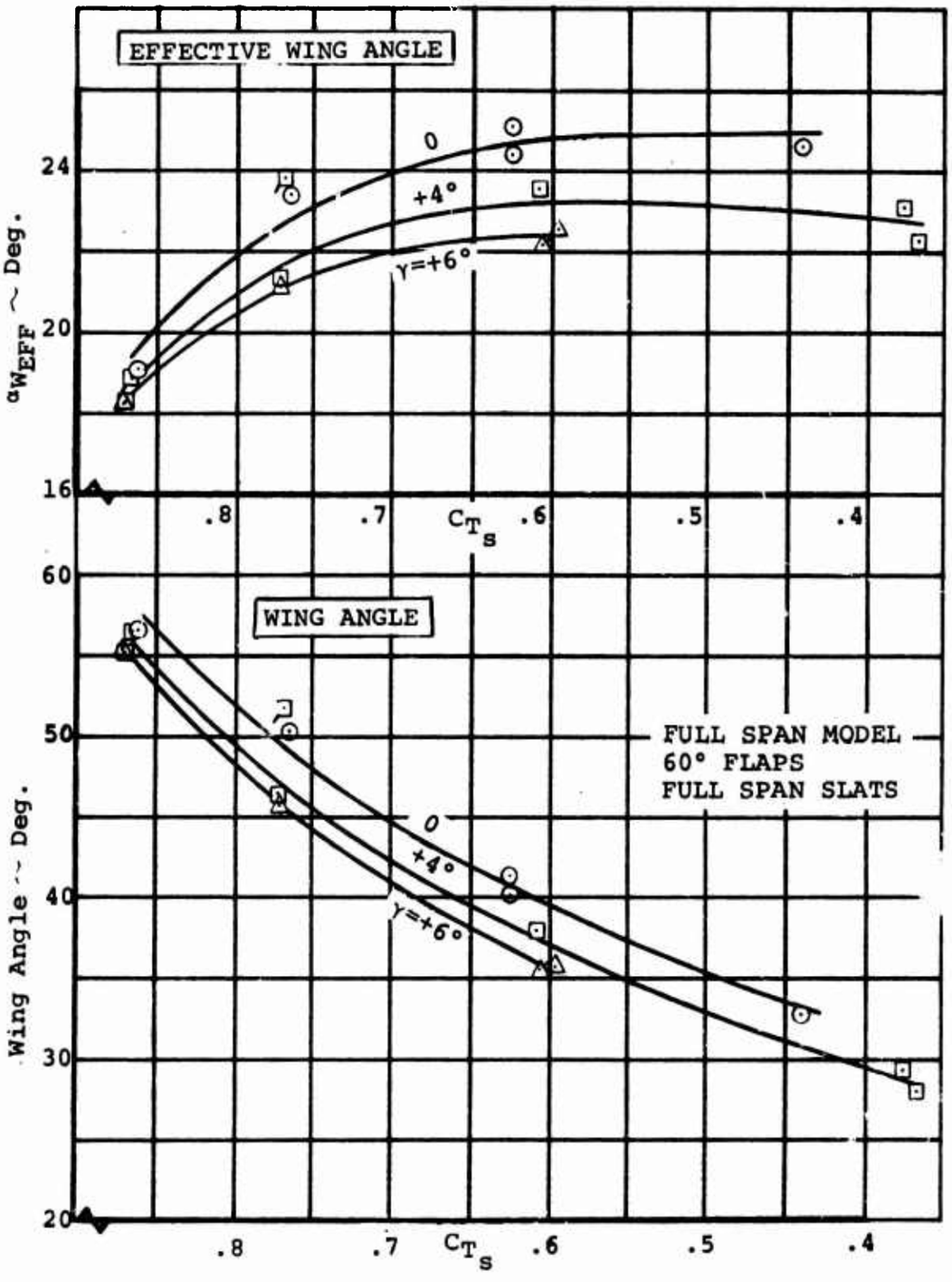

Figure 23. EFFECT OF CYCLIC PITCH ON BUFFET ONSET ANGLE

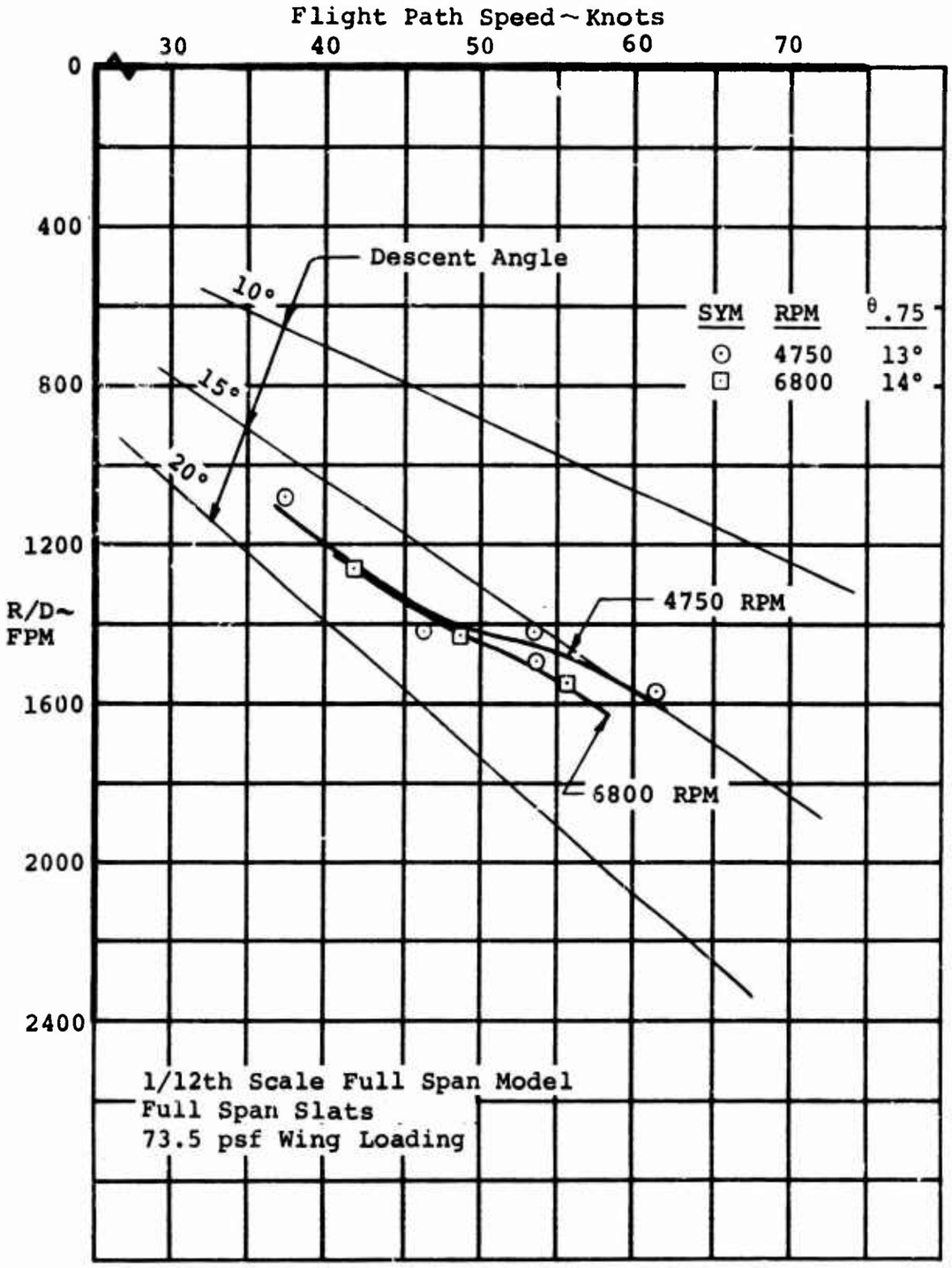

Figure 24. EFFECT OF RPM ON DESCENT CAPABILITY ZERO CYCLIC/60° FLAPS

fpm between the two sets of data, a number that is within data interpretation considerations. Comparative buffet angles presented in Figure 25 substantiate this result with no significant difference being exhibited between the 4750 RPM and 6800 RPM data.

2. DESCENT PERFORMANCE WITH COUPLED CYCLIC PITCH AND LEADING EDGE BOUNDARY LAYER CONTROL

During the development of the subject test program, wind tunnel data was available from Boeing-Vertol tilt wing tests that indicated a loss in low speed descent capability of approximately 100 fpm per degree of positive cyclic input. This data was obtained on models with cyclic pitch propellers having a total activity factor of 273 compared to the projected total activity factor of about 500 for the then current tilt wing designs. At this time, it was not known whether the larger activity factor propeller would increase the loss in descent capability with positive cyclic, and thus result in a less than desired descent corridor. The test of a semispan model with leading edge boundary layer control was included as a part of the overall test program for the purpose of investigating the possibility of using leading edge BLC to offset the degradation of descent capability with cyclic pitch. Work was concurrently taking place establishing descent rate goals based on possible descent requirements plus constraints, and in developing an aircraft configuration that would minimize the effect of cyclic pitch on descent performance.

The data presented in this section (Figures 26 and 27) shows that the semispan model test achieved its intent; however, the use of leading edge BLC is not required as a result of the descent rates acquired on the full span model with cyclic pitch applied (Figure 21). Figure 26 illustrates the low speed descent capability measured by coupling full span leading edge BLC with cyclic pitch inputs and compares this to the zero cyclic case with no blowing. The model configuration used for this example was double slotted flaps deflected 60^{o}, full span slats extended, and a propeller rotation direction of both propellers turning down between nacelles. Both the design of the flaps and slats were similar to that used for the full span model. One of the results obtained in this test was that the use of leading edge BLC did not alter the previously measured 100 fpm loss in descent capability per degree of positive cyclic. Thus, Figure 26 indicates that leading edge blowing

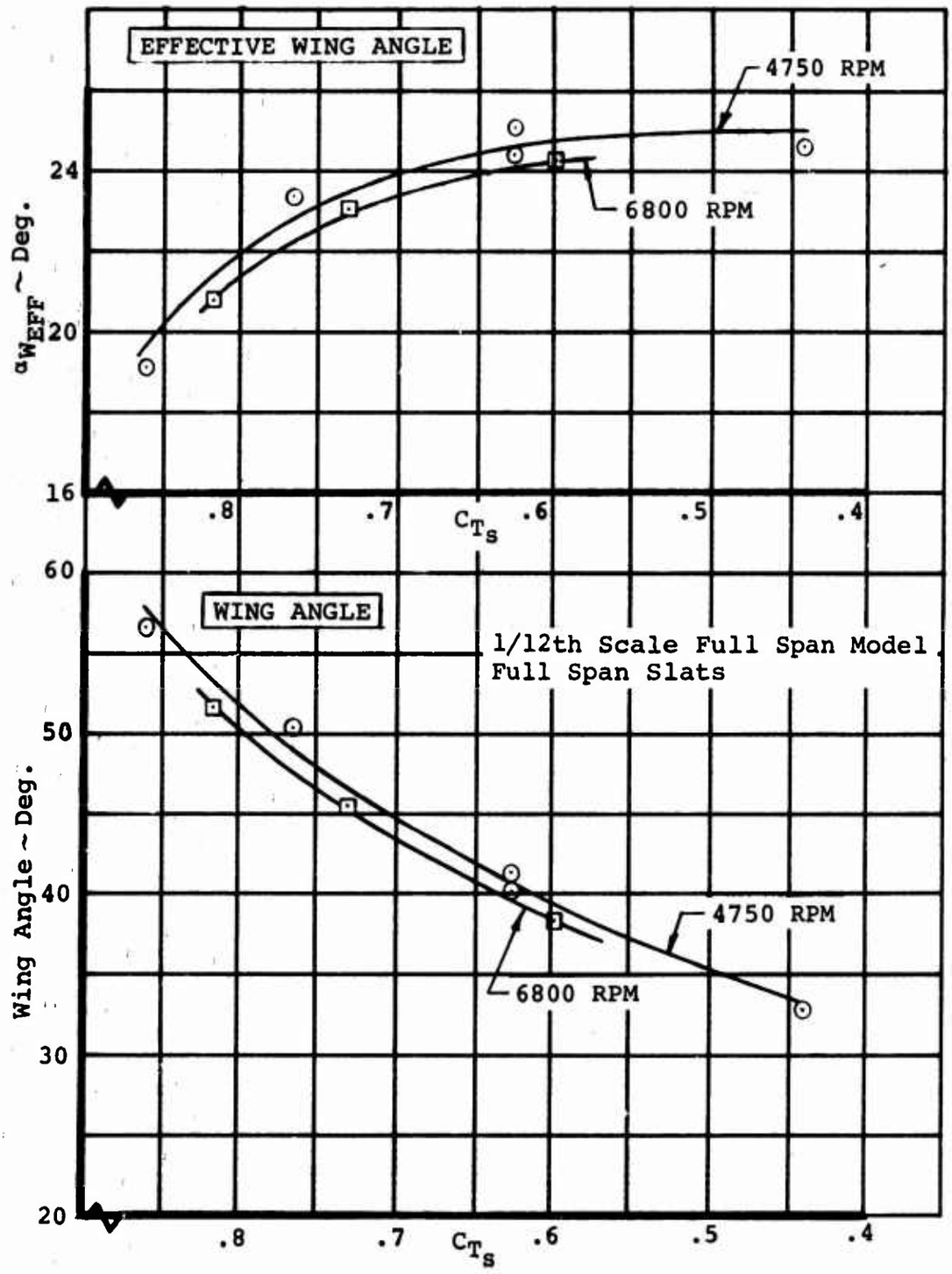

Figure 25. EFFECT OF RPM ON BUFFET ONSET ANGLE
ZERO CYCLIC/60° FLAPS

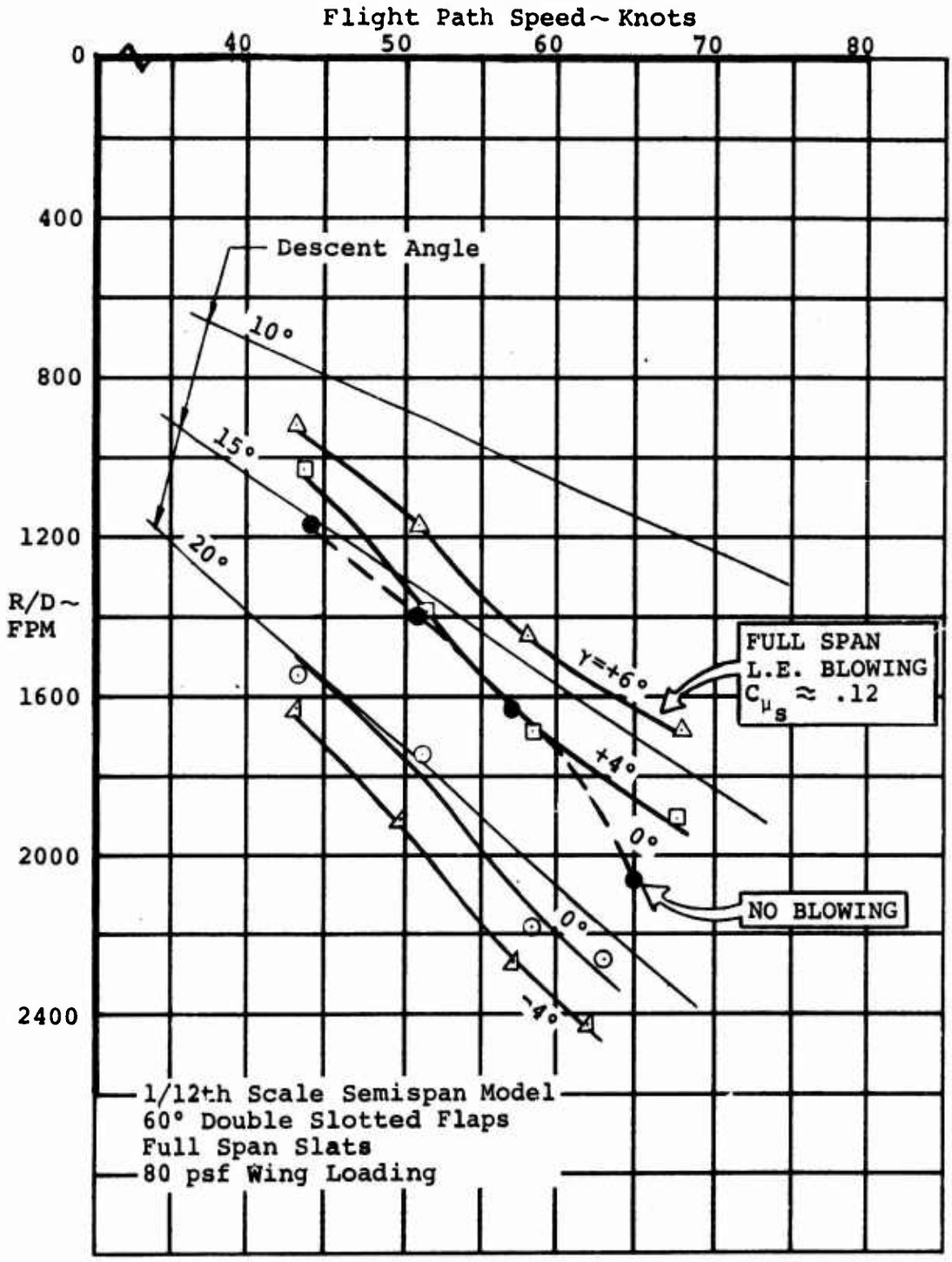

Figure 26. DESCENT CAPABILITY WITH COUPLED CYCLIC PITCH AND L.E. BLOWING

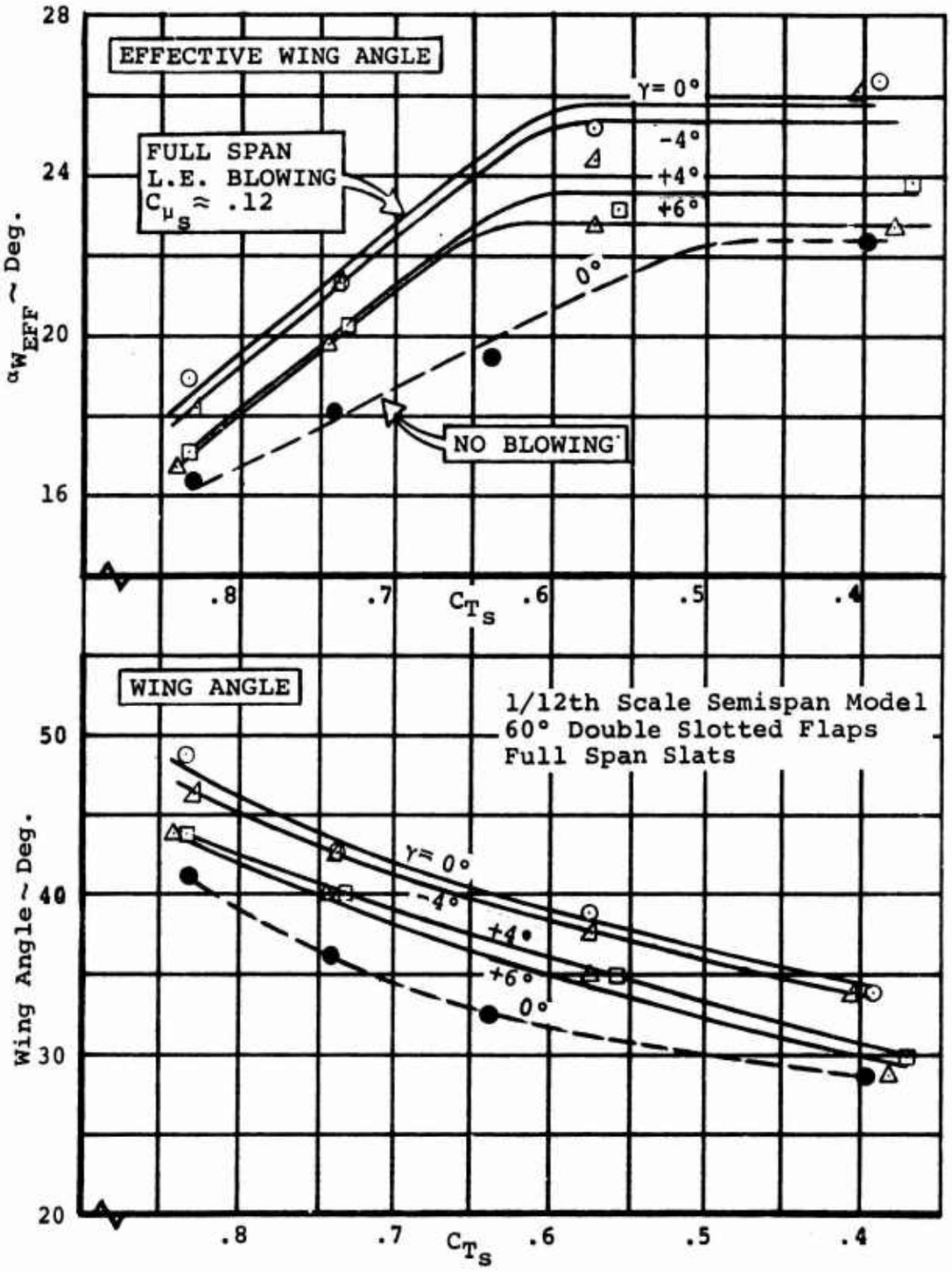

Figure 27. BUFFET ONSET ANGLES WITH COUPLED CYCLIC-PITCH AND L.E. BLOWING

will basically offset the loss in descent rate associated with 4° of positive cyclic. Figure 27, which presents the corresponding buffet onset angles, shows the improvement in stall angle with leading BLC that produced the increase in descent capability.

The data shown in Figures 26 and 27 was obtained with a blowing coefficient (C_{μ_s}) of approximately 0.12. This coefficient is defined in this case with the slipstream q as the reference dynamic pressure and the blown area of the wing as the reference area. The following equation was used to calculate C_{μ_s} values:

$$C_{\mu_s} = \frac{\omega V_j}{32.2 q_s S_E}$$

where ω = mass flow rate, lb/sec

V_j= jet velocity, ft/sec

q_s= slipstream q, lb/sec^2

S_E= blown wing area, ft^2

The high value of C_{μ_s} is not representative of a minimum C_{μ_s} for flow attachment; instead it reflects the minimum C_{μ_s} that could be achieved on the model with a choked slot nozzle. Available power from the electric motors along with the attendant low tunnel q and a minimum slot gap of .005" for accuracy, were the limiting items.

SECTION V

EFFECT OF CYCLIC PITCH ON AIRCRAFT STABILITY

1. LONGITUDINAL STABILITY WITHOUT CYCLIC PITCH INPUTS

Longitudinal stability/control characteristics of the full span four prop tilt wing model were investigated throughout the transition flight regime with and without the horizontal tail (positioned high on the vertical fin). The location of the unswept horizontal tail plus its area of 0.312 times the wing area, resulted in a tail volume of 1.33. This tail incorporated a taper ratio of 0.61 and an aspect ratio of 4.65.

Fuselage pitch runs were performed at a constant RPM (except the zero thrust runs) for selected combinations of wing tilt angle and flap angle that were representative of typical combinations required in transition. Data was taken at wing incidence settings ranging from zero to 70° and flap angles ranging from zero to 60° with the full span slats extended. The slipstream thrust coefficient for these runs varied from zero for the zero wing tilt angle case to 0.96 for the 70° wing tilt angle case.

Moments obtained during the longitudinal stability runs were transferred to a representative mid-center of gravity that moves up and back as the wing tilt angle increases. Positions of the c.g. for the various wing tilt angles were calculated by utilizing the scaled wing-down longitudinal and vertical locations of the fixed mass c.g. and rotating mass c.g. for a representative transport-type four prop tilt wing aircraft with a V-mode gross weight of 87,000 lb., plus the wing pivot location of the model. The movement of the aircraft c.g. with wing tilt angle that was used, is illustrated in Figure 28.

Figures 29 and 30 present the (horizontal) tail-off and tail-on stability for the wing tilt angle/flap angle combinations evaluated. The stability data is plotted in the slipstream derivative form $C_{M_{S_\alpha}}$ as a function of the slipstream thrust coefficient. Slopes shown in these two figures were extracted from the basic stability plots (C_{M_S} vs α_F, fuselage angle of attack) using the linear portion of the curves. The C_{T_S} value designated for each data point is the average value over the measured slope.

Tail-off data presented in Figure 29 shows a decrease in level of instability with increasing C_{T_S} that is in accord with the decreasing freestream q acting on the unstable fuselage and the decreasing lift curve slope in slipstream notation. The

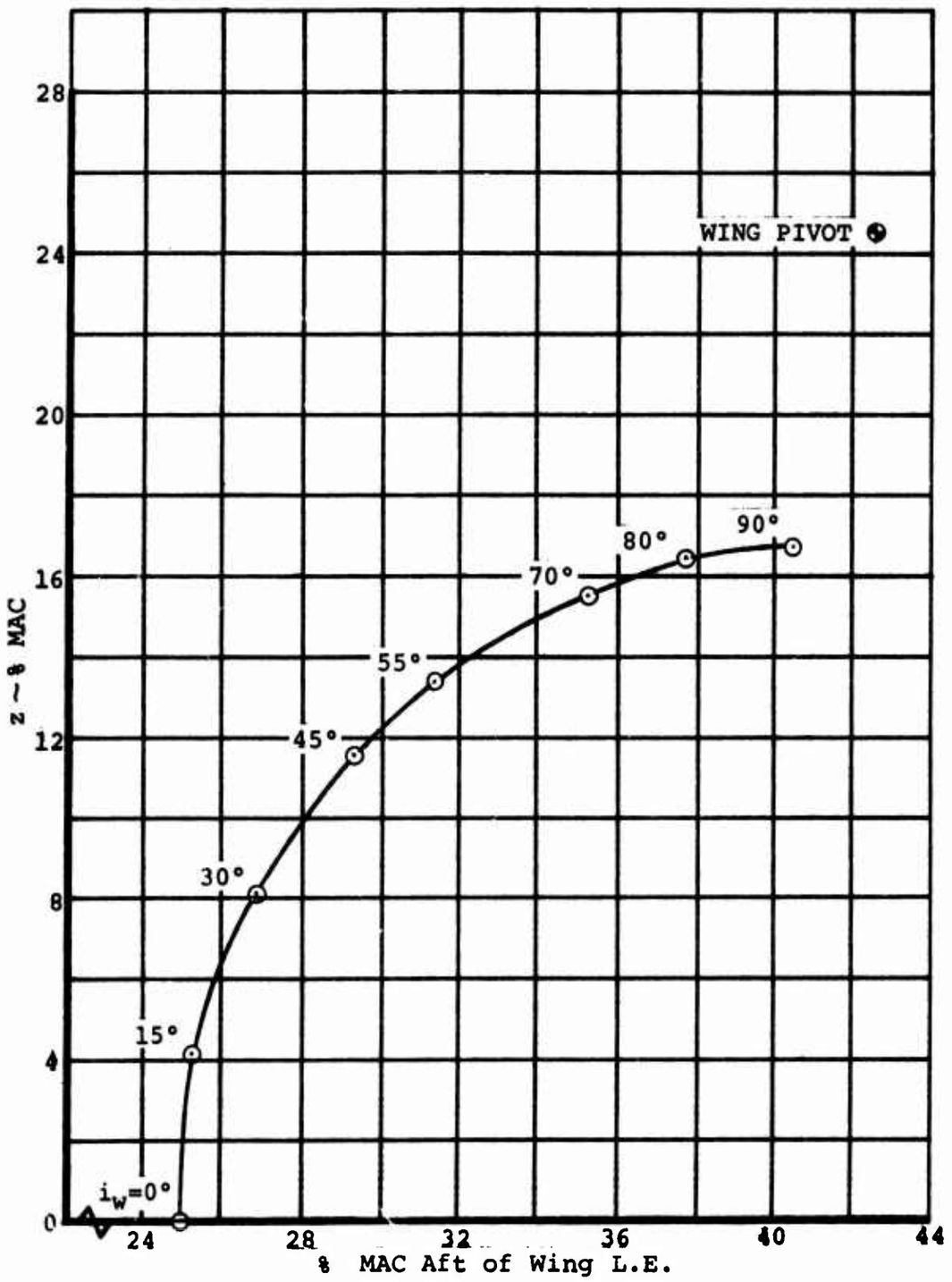

Figure 28. MOVEMENT OF A/C CENTER OF GRAVITY WITH WING TILT

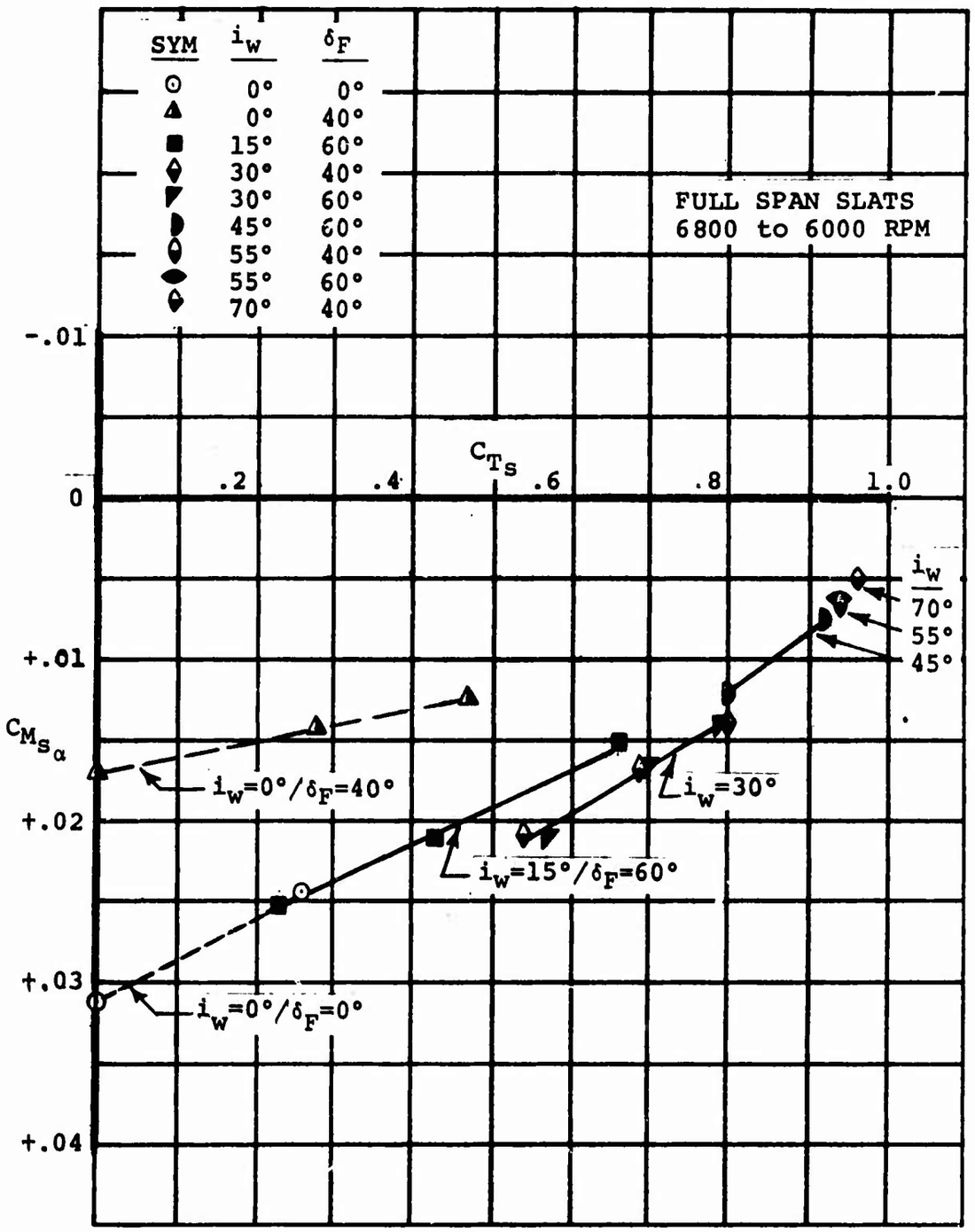

Figure 29. TAIL-OFF LONGITUDINAL INSTABILITY
MID c.g./ZERO CYCLIC

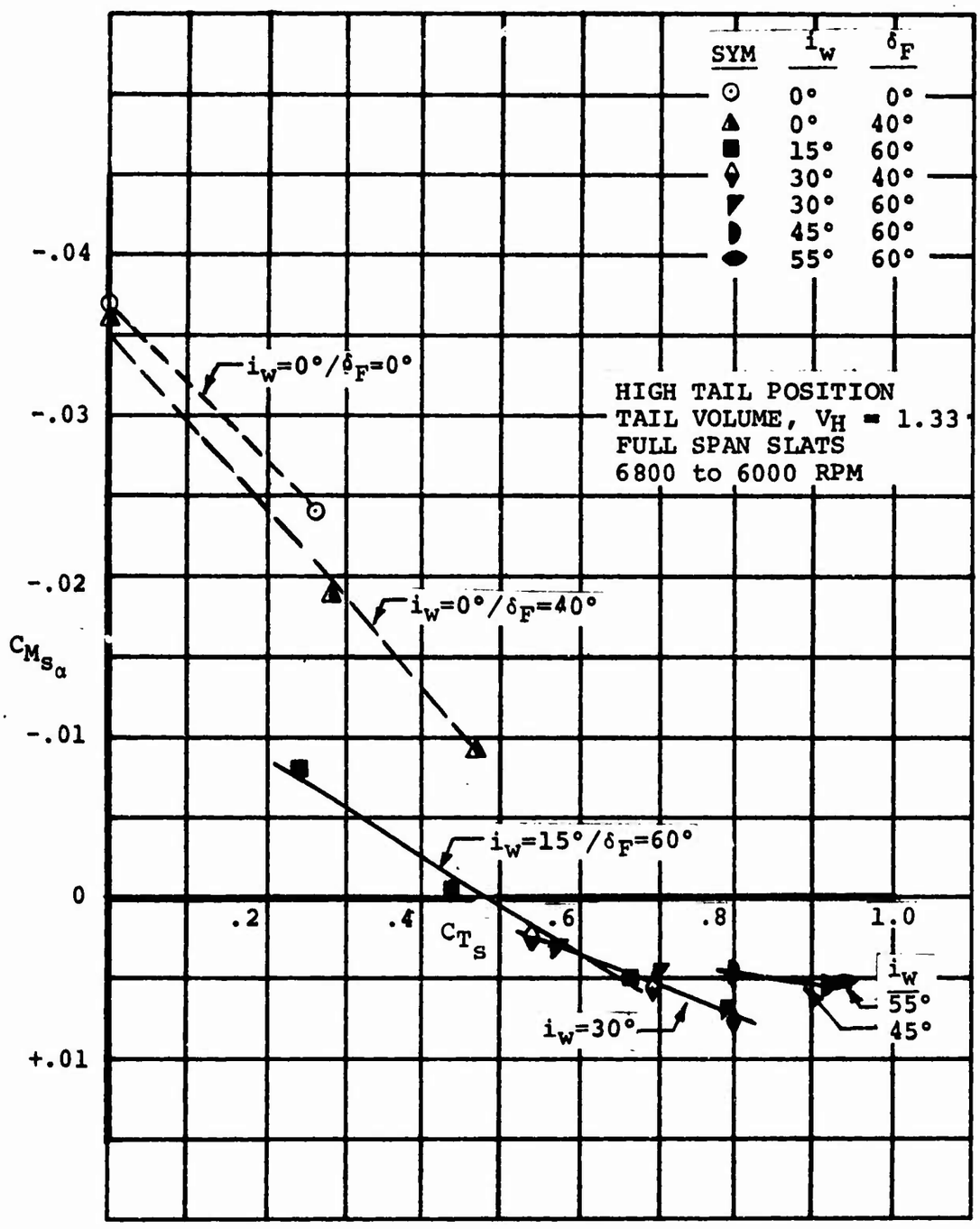

Figure 30. TAIL-ON LONGITUDINAL STABILITY
MID c.g./ZERO CYCLIC

relatively high tail-off instability for the wing down/flaps up case is sharply reduced by deflecting the flaps to 40°. This condition reflects the aftward movement in center-of-pressure associated with the flap Fowler action. Deflecting the flaps to a higher angle (60°) did not result in a further reduction of the tail-off instability per the evaluation made with both 30° and 55° of wing tilt angle.

Tilting the wing up 15° from the wing down position produced a substantial increase in the tail-off instability, a characteristic partially induced by the increased propeller forces and moments. An additional 15° of wing tilt (30° wing tilt angle) produced another increment in tail-off instability. Wing tilt angles higher than 30° (45°, 55°, and 70° were tested) resulted in progressive reductions in the tail-off instability. This situation reflects the aftward movement of the aerodynamic center with respect to the c.g.

The reduction in tail-on stability with C_{T_s} as depicted in Figure 30 for the wing down cases is indicative of the decrease in q acting upon the tail (primarily freestream q) and the increase in downwash gradient with C_{T_s} shown in Figure 31. This downwash gradient plot was developed from data obtained from series of runs with various stabilizer angular settings.

Considering the effect of flap deflection on stability, it is seen in Figure 30 that with the wing down, deflection of the flaps to 40° has a destabilizing effect tail-on whereas the same action decreased the tail-off instability. The reason for this is primarily a loss in the tail's contribution to stability due to an increase in the downwash gradient (Figure 31), i.e. the horizontal tail's contribution to stability varies directly with the function $(1-d\varepsilon/d\alpha_F)$. As in the tail-off case, additional flap extension to 60° from the 40° setting did not change the stability characteristics per the 15° wing tilt data shown in Figure 30.

The initial 15° of wing tilt had a substantial tail-on destabilizing effect resulting in the aircraft being unstable at C_{T_s} values larger than 0.47. This adverse change in stability accompanying the initial 15° of wing tilt was previously noted for the tail-off case by the increase in instability shown in Figure 29. The inference is that the increased propeller forces and moments were primary contributors to the stability change. Increasing the wing tilt angle to 30° did

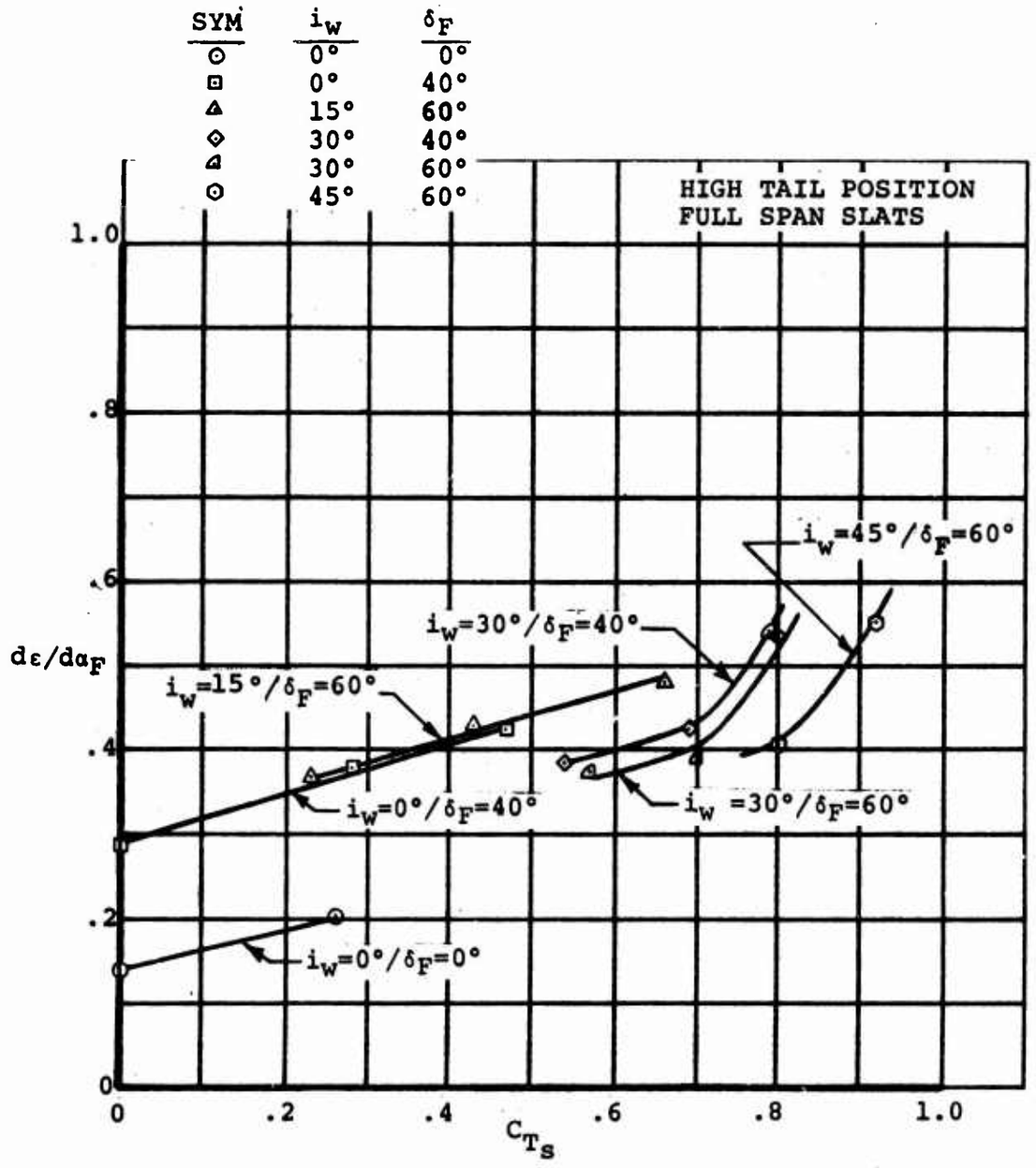

Figure 31. DOWNWASH GRADIENT, $d\varepsilon/d\alpha_F$

not cause a further reduction in tail-on stability even though a destabilizing effect was noted tail-off, i.e., the downwash gradient decreased. The downwash gradient effect was also evident to some extent at the higher wing tilt angles evaluated (45° and 55°). As shown in Figure 30, the net effect is an essentially constant $C_{M_{S_\alpha}}$ value of approximately +.005 from a C_{T_S} of 0.65 to 0.96 with wing tilt angles of 30° to 55° for the mid c.g. case.

The downwash gradient acting on the high horizontal tail is low (0.2 $d\varepsilon/d\alpha_F$ or less) with the aircraft in the clean configuration as indicated in Figure 31. With the flaps deflected the gradient increases with C_{T_S} from a value of 0.3 at zero thrust coefficient to 0.5 at a C_{T_S} of approximately 0.7. Wing tilt angle can be noted to have only a moderate influence on $d\varepsilon/d\alpha_F$.

This completes the presentation of the aircraft's longitudinal characteristics through transition. In the following paragraphs the influence of cyclic pitch inputs on the aircraft stability will be examined.

2. LONGITUDINAL STABILITY WITH CYCLIC PITCH INPUTS

The effect of cyclic pitch on longitudinal stability was evaluated both horizontal tail on and off with 60° of flap at selected combinations of wing tilt angle and slipstream thrust coefficient through transition. Horizontal tail geometry and location were identical to that used for the non-cyclic testing. The data plotted in Figure 32, in the same derivative form $C_{M_{S_\alpha}}$, has been transferred to the representative mid c.g. depicted in Figure 28. It was noted previously that the mid c.g. positions for the various wing tilt angles were calculated using the model wing pivot location of 42.6% MAC aft of the wing leading edge and 11.7% MAC below the wing chord plane.

Figure 32 presents two sets of data for the zero cyclic case. The data denoted by solid and dashed lines was transscribed from the information presented in Figures 29 and 30. This zero cyclic data was obtained at a higher propeller RPM than the cyclic data shown in Figure 32, which was acquired at the cyclic hub operating speed of 5000 RPM. The object of the dual set of data was to ascertain the quality of the information acquired at a lower disc loading and Reynolds number than achieved with an RPM range from 6800 to 6000. The effect on

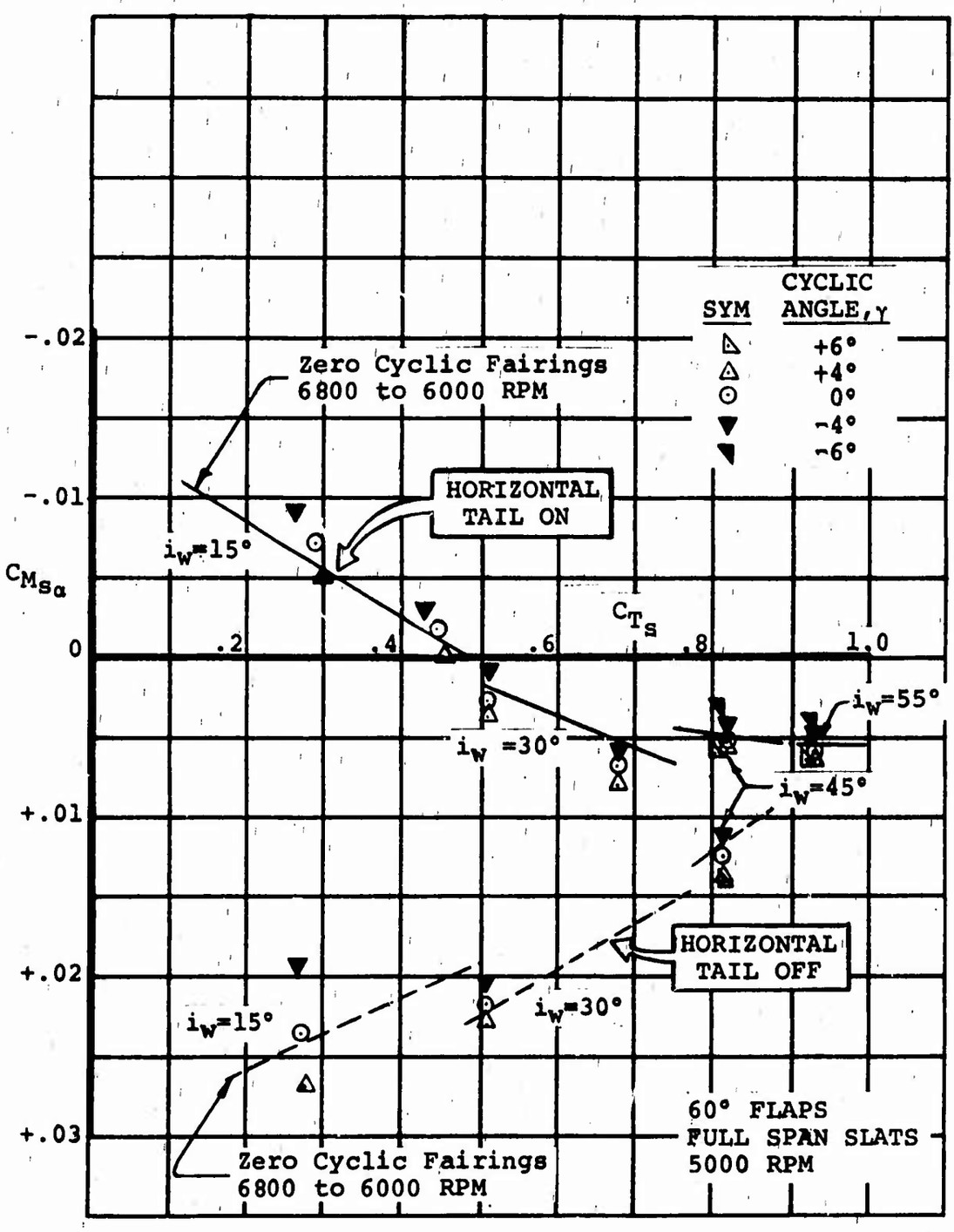

Figure 32. EFFECT OF CYCLIC PITCH ON LONGITUDINAL STABILITY

stability measurements can be noted to be small.

Figure 32 shows that the application of cyclic pitch does not have a large effect on longitudinal stability. The measured changes in stability due to cyclic diminish with increasing thrust coefficient or decreasing flight speed. Positive cyclic angles can be seen to increase the tail-off instability, whereas negative cyclic angles reduce the tail-off instability. Since the same incremental effects due to cyclic were recorded both tail-on and tail-off (except for the 0.28 C_{T_S} condition), the changes in stability probably reflect the combined influence of (1) cyclic pitch on propeller hub moment and normal force (when interpreted in the slipstream notation) plus (2) the change in aircraft lift curve slope with cyclic. Data presented in Section 6.4.2 of Reference 4 shows that the lift curve slope, a parameter that directly influences C_{M_α}, is increased with negative cyclic inputs and decreased with positive cyclic.

Of concern during the longitudinal stability testing was whether the thrustline offset occurring with the application of cyclic pitch would modify the downwash gradient and thus produce substantial changes to tail-on stability, especially at the lower range of thrust coefficients where the horizontal tail is most effective for stability and control. As a simplified explanation, monocyclic produces a pitching moment by offsetting the propeller thrust vector from the normal propeller hub $\mathcal{C}$. The resultant change in q at the tail plane (from effectively raising or lowering the thrustline) would change stability in the opposite direction from the change due to downwash gradient and tend to provide, for example, increased tail-on stability with positive cyclic angles. Apparently the high tail positioning reduces any influence of cyclic pitch on the downwash gradient and q at the tail to a minimum. The only noticeable influence occurred at the lowest thrust coefficient tested with 15° of wing tilt. At this condition of 0.28 C_{T_S}, the incremental change in stability from a tail-off to a tail-on condition increased with positive cyclic and decreased with negative cyclic. This indicates that the q change at the tail due to cyclic was the predominate effect (not downwash gradient) in altering the tail's contribution to stability.

3. LATERAL/DIRECTIONAL STABILITY WITHOUT CYCLIC PITCH INPUTS

In this test program, the lateral/directional stability characteristics of the full span four prop tilt wing model were investigated through the transition flight regime with and without a vertical tail. This tail utilized a 0.52 taper ratio, 1.27 aspect ratio, an area 0.213 times the wing area, and a quarter-chord sweep of 40°. The positioning of the tail on the fuselage resulted in a tail volume of 0.083. For this investigation, the horizontal tail was mounted on the fin in its high position and the stabilizer was set at an angle representative for the wing tilt position.

The yaw runs of this testing were performed at a constant propeller RPM with selected combinations of wing tilt angle and flap angle that corresponded to typical combinations required through transition. All yaw data was acquired with zero fuselage angle, an angle that is representative of the normal body attitude in transitional flight. Moments obtained during the test runs were transferred to the same mid c.g. locations used for the longitudintal stability and control analysis. These moments are shown in the presentation as body axis moments.

The empennage-on lateral/directional stability characteristics are summarized in Figure 33. This plot presents the slipstream yawing moment, rolling moment, and side force derivatives (with respect to the sideslip angle, β) as a function of the slipstream thrust coefficient. All slopes plotted in Figure 33 were read over a yaw angle range that did not exceed $\pm 8°$ and the C_{T_s} values were those prevailing at zero yaw angle.

The first item of interest in Figure 33 is the unstable directional characteristic measured with the wing down and retracted flaps. This situation has been identified to be a direct result of a low effectiveness of the vertical tail. The loss in tail effectiveness was caused by the interaction of the flow emanating from the wing/body juncture on the flow around the root section of the vertical tail. Lowering the flaps to 40° produced a stable aircraft directionally by improving the vertical tail effectiveness as shown in Figure 34. Apparently, lowering the flaps increased the vertical tail effectiveness by deflecting the adverse wing/body juncture flow below the base of the fin. A redesign of the wing/body intersection and vertical tail/fuselage junction could rectify the deficiency.

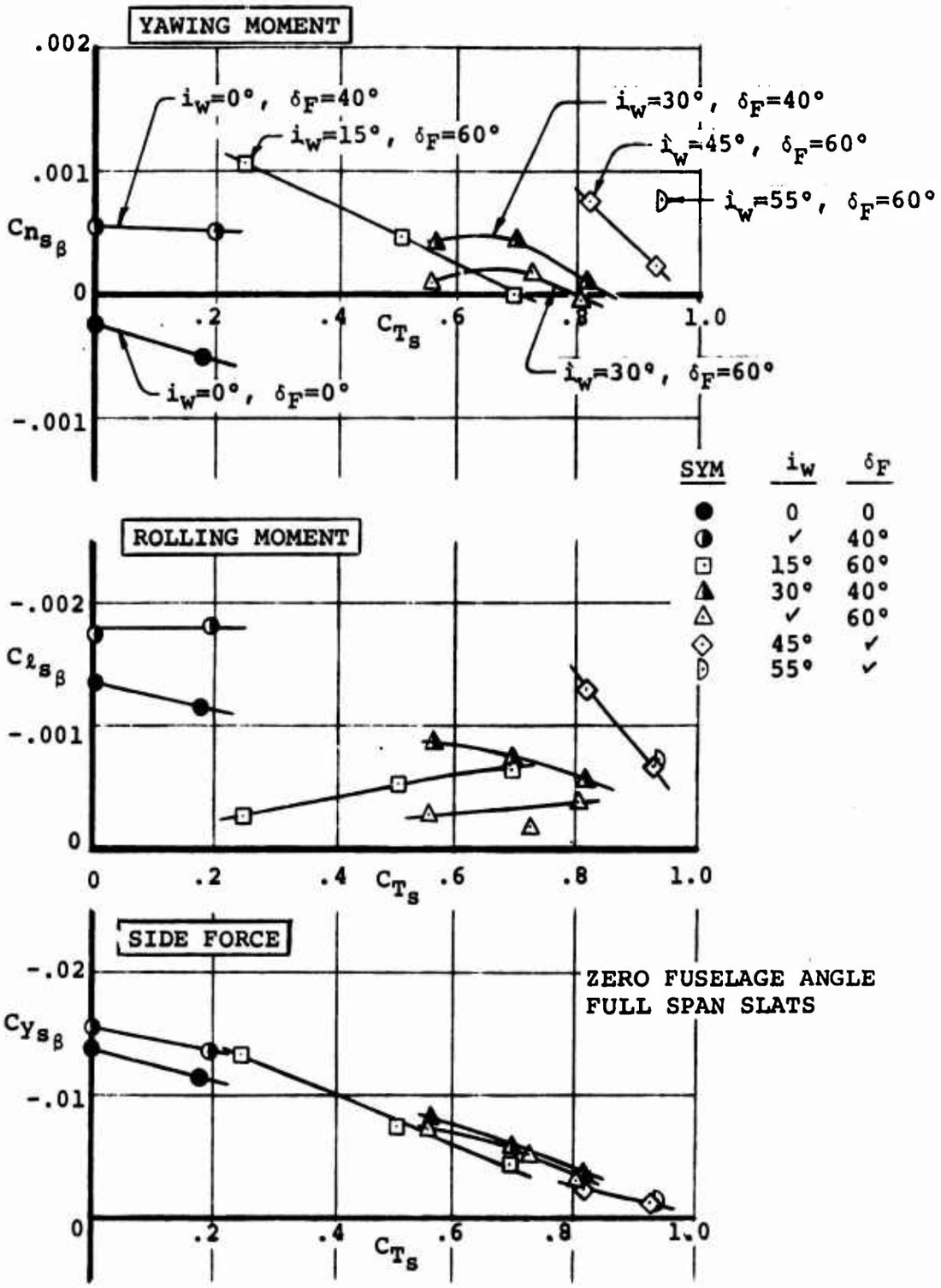

Figure 33. LATERAL/DIRECTIONAL STABILITY
EMPENNAGE ON/ZERO CYCLIC

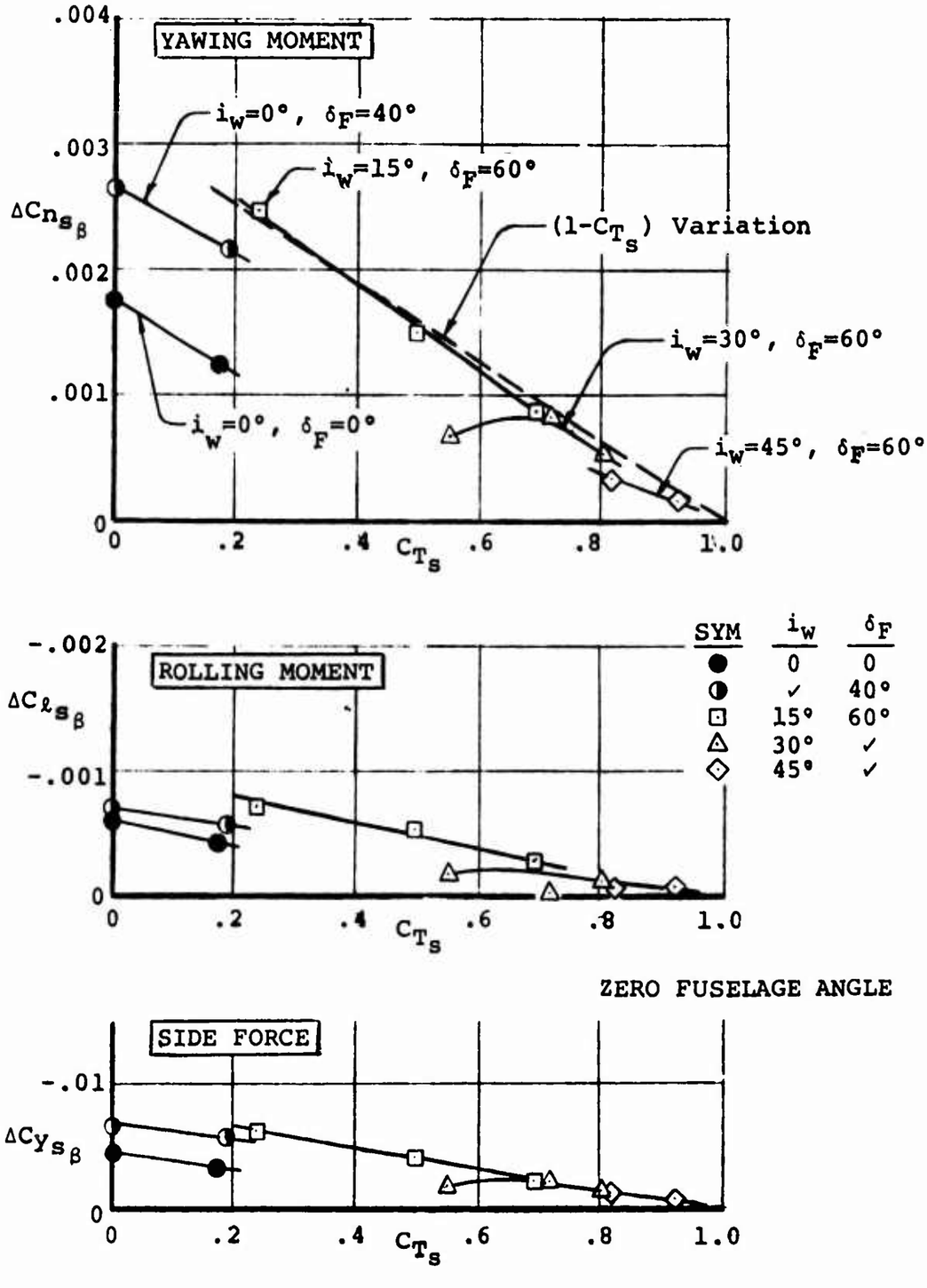

Figure 34. VERTICAL TAIL EFFECTIVENESS

The extended full span slats, however, could have aggravated the condition.

A positive dihedral effect (negative sign on C_{ℓ_β} in Figure 33) was exhibited by the model at the same wing down, flaps up and low C_{T_S} condition. Deflecting the flaps to 40° increased the dihedral effect. It is surmised that the major portion of this increase was caused by a modification in the wing/body interference effects.

A substantial reduction in the measured $C_{\ell_{S_\beta}}$ occurred at 0.2 C_{T_S} when the flap deflection was increased by 20° and the wing was tilted to 15°. A combination of two factors could have produced this effect: the large constant percent chord flaps have a swept forward hinge line, and the slipstream lift coefficient was increased by an increment of 2.15. The subsequent change in dihedral effect with increasing C_{T_S} follows the reduction in C_{L_S} with C_{T_S}.

At 0.2 C_{T_S}, the increase in directional stability accompanying the 15° of wing tilt and additional 20° of flap deflection largely reflects the increase in vertical tail effectiveness illustrated in Figure 34. The subsequent decrease in directional stability and fin effectiveness with increasing thrust coefficient generally follows the linear reduction in freestream q or $(1-C_{T_S})$ function. Except for the special case of 0.55 C_{T_S} where wing stall was present, the vertical tail effectiveness with 30° of wing tilt angle showed no significant departure from the $(1-C_{T_S})$ variation. Some "blanketing" at the base of the fin occurred at 0.8 C_{T_S} when the wing was tilted to 45°.

A substantial change in yaw stability occurred when the wing was tilted up from 30° to 45° at 0.82 C_{T_S}, a thrust coefficient at which the vertical tail is relatively ineffective. This increase in yaw stability was noted in previous tilt wing testing and is attributed to a redistribution of the longitudinal pressures on the fuselage. During tuft studies, the character of the flow aft of the wing was observed to markedly change at combinations of a high C_{T_S} value and wing tilt angles in the order of 45°. The corresponding side force picture, wherein no change in side force was recorded when the wing was raised to 45° from 30°, is consistent with this reasoning. In this case, the increase in the destabilizing propeller side force and propeller yawing moment is offset somewhat by the

respective shortening of the moment arm between the propeller hub and c.g., and by the lessening of the propeller yawing moment acting about the aircraft yaw axis.

Tilting the wing from 30° to 45° at 0.82 C_{T_S} also increased the dihedral effect. It is a reasonable conclusion that this increase primarily resulted from the change in spanwise lift distributions on the inboard portion of the upwind and downwind wings along with the increase in propeller forces and moments acting about the aircraft roll axis. Wing tilt increases the propeller forces and moments, plus vertically raises the vectors reacting about the aircraft rolling axis.

4. LATERAL/DIRECTIONAL STABILITY WITH CYCLIC PITCH INPUTS

Following the investigation of basic lateral/directional stability characteristics, the effect of cyclic pitch on lateral/directional stability was examined at the same points in transition and with the same wing tilt/flap configurations used in the longitudinal investigation. In Figure 35, the data acquired with the empennage on and at zero fuselage angle is again presented in the slipstream derivative format. The zero cyclic fairings shown in Figure 35 are those previously shown in Figure 33.

Both positive and negative cyclic pitch angles are seen to have only a minor effect on the directional stability ($C_{n_{s_\beta}}$) and dihedral effect ($C_{\ell_{s_\beta}}$) at all conditions tested. Positive cyclic angles tend to decrease both the yaw stability and dihedral effect, and negative angles tend to increase them. Thus, the cyclic pitch effects are in the same direction as established for the longitudinal mode, indicating again the influence of cyclic pitch on the propeller forces and moments.

Some data scatter is present in Figure 35; for example, the yaw stability measured with 15° of wing tilt and zero cyclic does not line up exactly with the comparable yaw stability data acquired with both positive and negative cyclic pitch inputs. This situation is understandable when it is realized that in powered model testing, back-to-back runs for accuracy purposes are not always feasible because the length of a test series can extend over a couple of days.

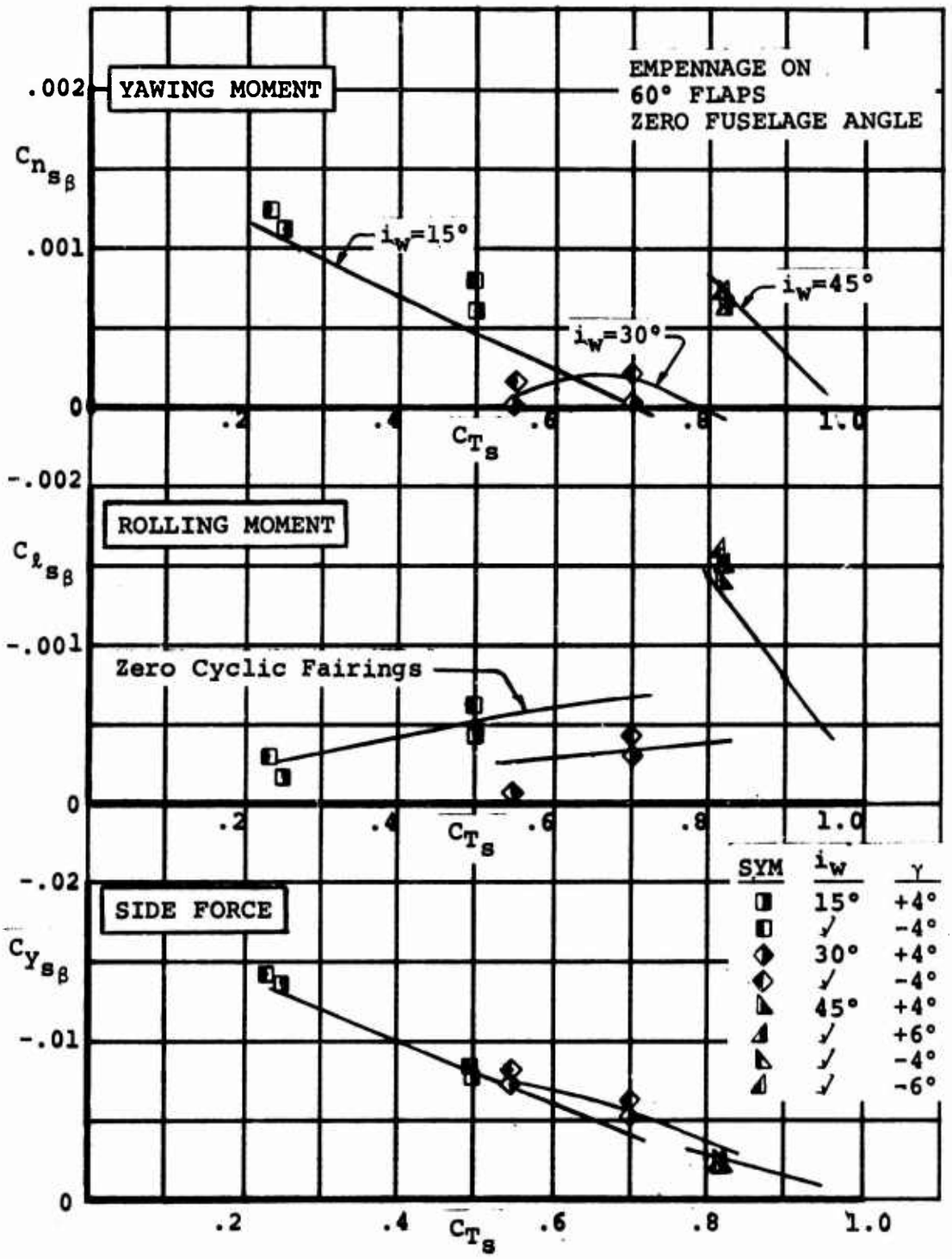

Figure 35. EFFECT OF CYCLIC PITCH ON LATERAL/DIRECTIONAL STABILITY

SECTION VI

EFFECT OF CYCLIC PITCH ON AIRCRAFT SURFACE CONTROL POWER

1. HOVER YAW CONTROL AND THE EFFECT OF CYCLIC

On the full span model tested, hover yaw control was provided by differential control deflections; that is, the double slotted flaps are deflected down on one wing, and the spoilers are deflected up on the opposite wing. An evaluation was also made of an up flap in combination with an up spoiler on the same wing.

The hover mode yaw control testing was accomplished with the leading edge slats retracted, a wing tilt angle of 90°, and a propeller rotation direction of both props turning down between the nacelles. Data, acquired over a range of model ground heights that represented moving from an out-of-ground effect condition to in-ground effect conditions, was obtained with the 29 ft. long test section walls and ceiling removed, which opened a hover test area that measured 50 ft. from the solid test section floor to the top of the 67 ft. diameter plenum chamber.

Figure 36 presents the hover yaw control available with flaps deflected down 60° on the right wing plus spoilers deflected up 60° on the opposite wing, along with a comparison of the control power that would have been available if the individual contributions shown for the flaps and spoilers were directly additive. The yaw data depicted in Figure 36 is a non-dimensional form, Y.M./ℓT, that represents the ratio of the measured yawing moment divided by a representative moment arm (distance from the body centerline to midway between the nacelles) times the total propeller thrust. This information, plotted against the ground height ratio h/D (which is the ratio of the height of an outboard propeller above the ground plane to propeller diameter) shows a 30% reduction in hover yaw control power as the model descended from an out-of-ground effect condition to a 2ft. wheel height. The reduction is associated with a loss in flap turning effectiveness in-ground effect.

Shown in Figure 36 is data acquired at two different propeller speeds: 6800 RPM with the collective hubs, and 5000 RPM with the cyclic hubs. The respective out-of-ground effect hover disc loadings were 33.4 lb/ft^2 with a blade angle setting of 14° on the collective hubs, and 16.7 lb/ft^2 with 12.5° of blade angle on the cyclic hubs. A direct comparison of the effect of disc loading is available with the double slotted flaps deflected 60° on the right wing and a clean left wing. It is reasonable to conclude that the decrease in Reynolds number associated with the reduction in disc loading resulted in

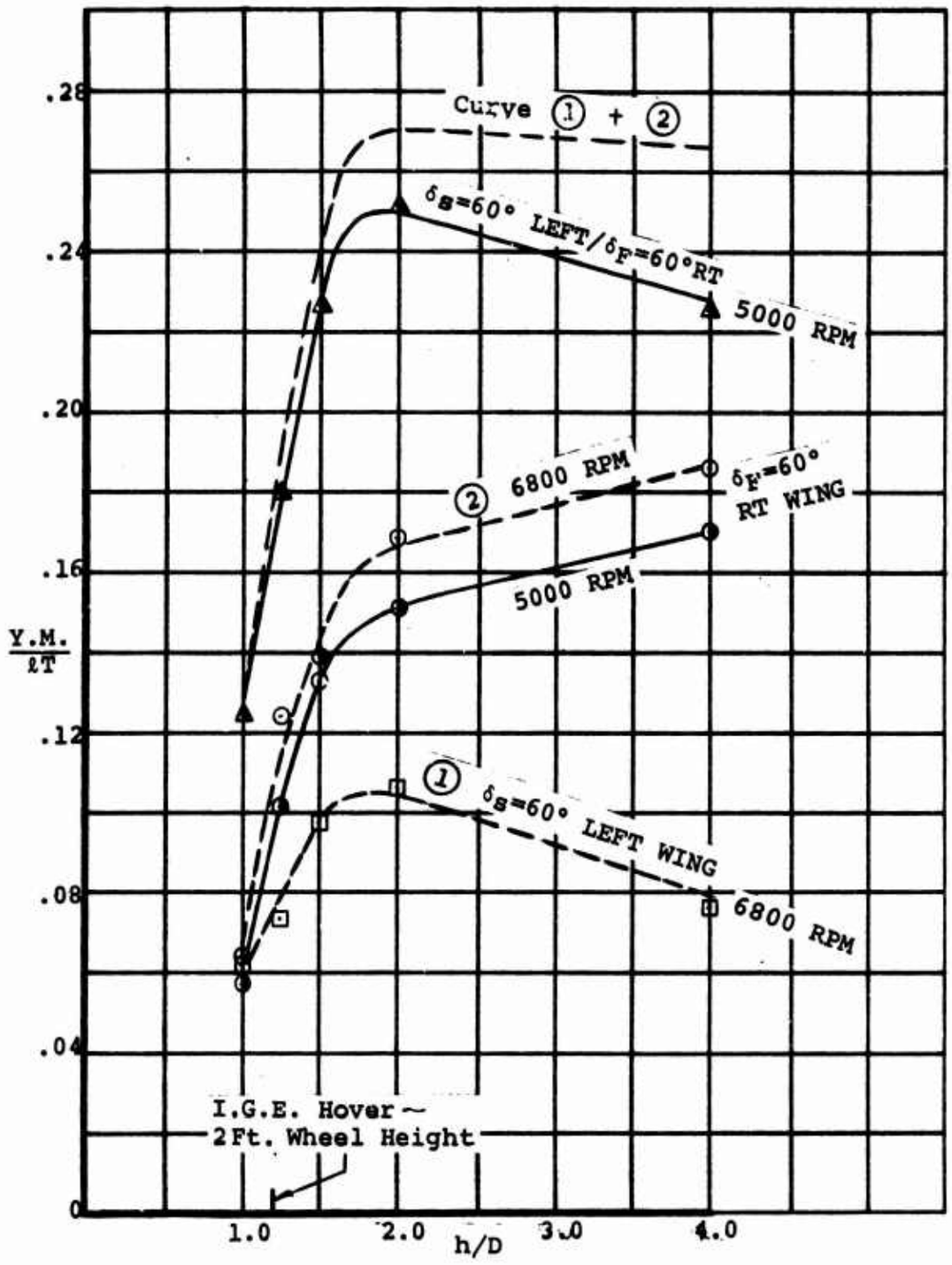

Figure 36. HOVER YAW CONTROL BUILDUP WITH FLAPS (RT WING) AND SPOILERS (LEFT WING)

a lower flap turning effectiveness and,consequently, incrementally decreased the measured yawing moment capability.

Further, it would be anticipated that Reynolds number would not influence spoiler turning effectiveness to the degree that it affected flap turning effectiveness. Thus, it appears that some loss in yaw control power occurred when down flaps on the right wing were tested in combination with up spoilers on the left wing. This condition of the individual contributions of down flaps and up spoilers not being directly additive was observed in previous tilt wing hover yaw control testing, and is attributed to the occurrence of transverse flow from one side of the aircraft to the opposite side.

An apparent anomaly exists in Figure 36 wherein the measured yawing moment capability decreased or increased between ground height values (h/D) of 2.0 and 4.0. Since an out-of-ground effect condition should exist at h/D's greater than 2.0, it would be expected that the measured yawing moment would not change (definitely not decrease) between values of h/D of 2.0 and 4.0. Visual observations were performed with the aid of tufts to investigate the possibility of a flow recirculation in the test area that could alter the measured yawing moment. Particular attention was directed towards detecting changes with ground height. No noticeable flow activity was discernible; however, some amount of flow recirculation could have been present that required anemometers for detection. Model dynamic problems is another source of the anomaly. These dynamic problems, which resulted from the frequency response characteristics of the model structure, fuselage balance, and 25 ft. long sting, required a 10 sec. data sampling period to minimize data scatter during the hover yaw control testing.

In Figure 37 the yawing moment capability is plotted against the hover download generated by various deflections of the wing control surfaces used for hover yaw control. The plotted points were obtained by averaging the data acquired over ground height ratios between 2.0 and 4.0. At these O.G.E. conditions, download is a maximum. This figure, which presents data for the individual contributions of spoilers (20.4% chord) and flaps (39% chord retracted) with the opposite wing clean, and for combined flap and spoiler configurations, shows that the hover download is essentially a direct function of the yawing moment developed.

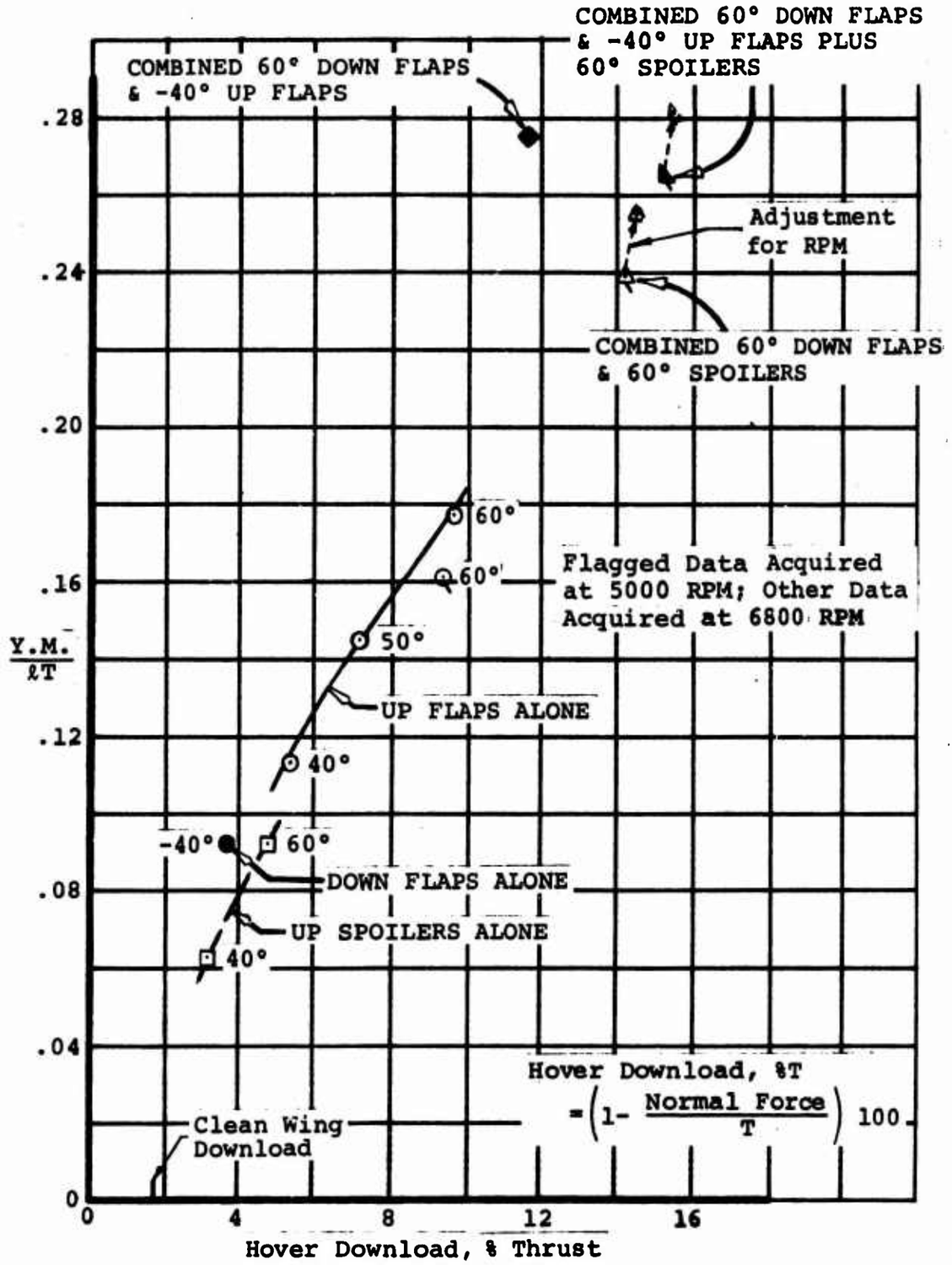

Figure 37. HOVER DOWNLOAD AS A FUNCTION OF YAW CONTROL CAPABILITY/O.G.E. CONDITION

Three of the data points plotted in Figure 37 (flagged symbols) were acquired at 5000 RPM (cyclic hubs) during the Phase II test (Reference 4) of the full span model. The other data points were obtained at 6800 RPM (collective hubs) during the Phase I test (Reference 3). Note that the 5000 RPM data with combined flaps and spoilers has been adjusted upward per the RPM differences measured during these two tests with 60° of flaps alone. The incremental difference in yawing moment due to the RPM change is illustrated in Figure 36. A detailed examination of the data from the tests indicated that the propeller thrust data from the Phase II test could have been 2.5% high in magnitude compared to the Phase I data. This percentage was established by individually examining the nacelle balance calibrations for the two separate tests. Since the hover download measurement is almost a direct function of the accuracy of the thrust data, a possibility exists that the hover download shown for the 5000 RPM data in Figure 37 is up to 2% high with respect to the 6800 RPM data. The hover download equation expressed on Figure 37 illustrates this point in that if the thrust measured from the nacelle balances is low in magnitude, the calculated download will be high in magnitude (normal force was measured from the fuselage balance).

With this in mind it appears that the yaw control configuration of 60° down flaps on one wing and 40° up flaps on the opposite wing is the most favorable configuration with respect to maximum yawing moment capability and minimum download considerations. This argument, however, does not take into account the loss in yaw control power that occurs as the aircraft descends into ground effect. When this factor is included in the selection, the combined down flap/up spoiler configuration is superior due to a higher yaw control power at the 2 ft. wheel height (20% better). Testing established that the spoiler retained its turning effectiveness better than a flap when the model was in close proximity to the ground. This configuration comparison is illustrated in Figure 38.

Figure 38 also shows that the incremental improvement in yawing moment capability obtained out-of-ground effect, with an up flap used in conjunction with the up spoiler, diminished to zero in ground effect. As a consequence, an up-moving flap does not appear to have sufficient effectiveness to warrant its use as a yaw control device in hover when a spoiler is already being considered for a roll/yaw control in transitional flight.

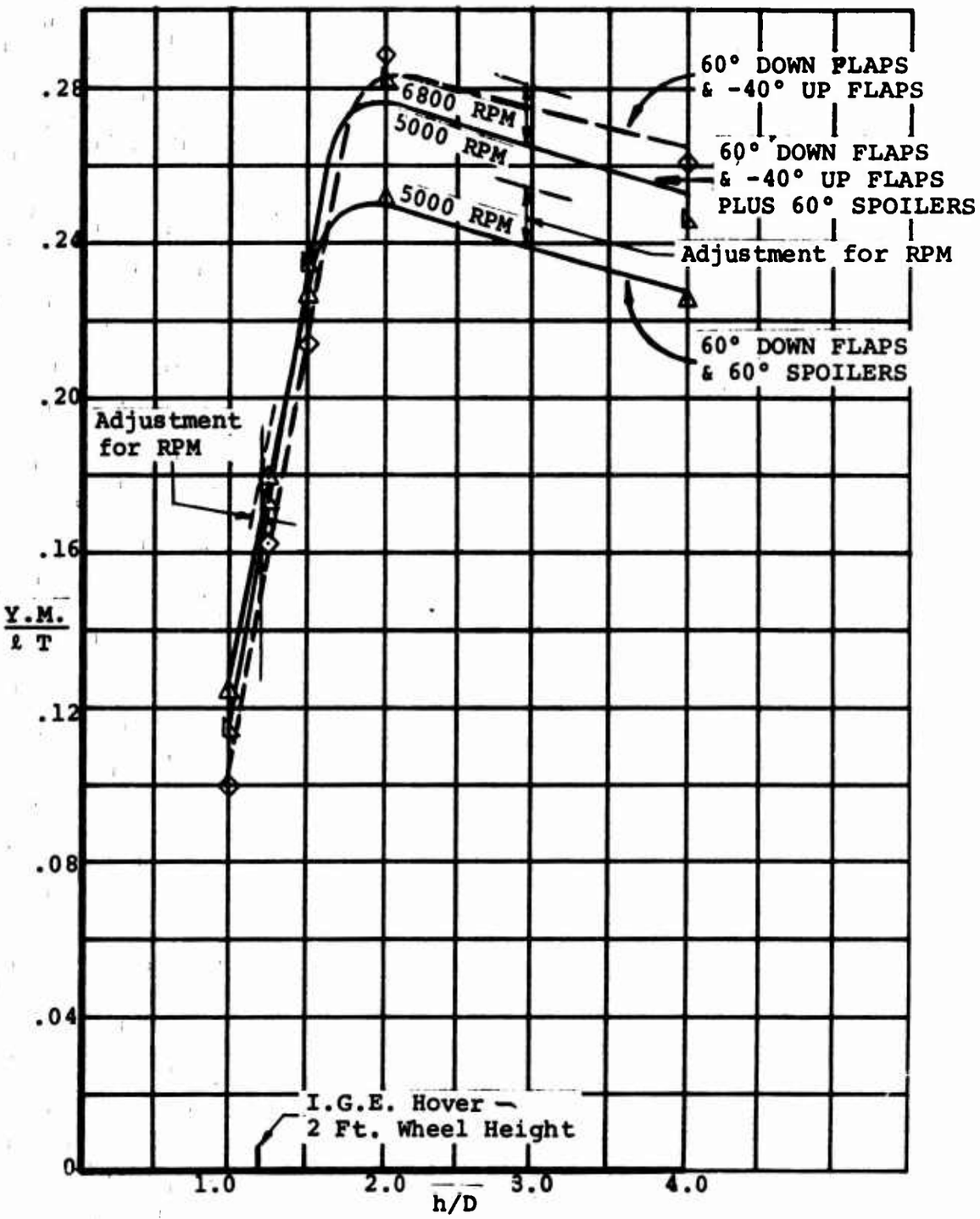

Figure 38. HOVER YAW CONTROL WITH COMBINED FLAPS AND SPOILERS

As a final point of interest, the necessary value of the non-dimensional parameter Y.M./ℓT is 0.293 for a representative tilt wing transport-type aircraft hovering at its design "V" gross weight of 87,000 lb. and meeting a 0.5 radian/sec^2 yaw angular acceleration level[2]. The hover yaw control configuration of combined down flaps and up spoilers that was tested produced a moment that is within 14% of this goal per the O.G.E. data presented in Figure 38.

An evaluation of the effect of cyclic pitch control inputs on hover yaw control power was performed with a differential yaw control configuration of 60° down flaps on one wing and 60° up spoilers on the opposite wing. Model configuration details such as retracted slats, 90° wing tilt, and propeller rotation direction were identical to that used for the basic hover yaw control testing.

From the data presented in Figure 39, it can be seen that positive cyclic (nose down pitching moment) increases the yaw control power while negative cyclic (nose up moment) produces an opposite effect. This variation is a result of the location of the propeller centerlines (both inboard and outboard) below the wing chord plane in combination with the shift in the center of pressure at the propeller disc due to cyclic pitch action. Positive cyclic shifts the center of pressure closer to the wing chord plane thus increasing the dynamic pressure acting over the wing. Negative cyclic has an opposite effect — a shift in the center of pressure further away from the wing.

The increase in hover yaw control effectiveness with a positive cyclic angle and decrease with a negative angle provided the reasoning for the comment made in the discussion on the effect of cyclic pitch on low speed descent performance.

---

[2] The value of 0.293 was developed from the following equation and values:

$$\frac{Y.M.}{\ell T} = \frac{\ddot{\Psi} I_{zz}}{\ell T}$$

$\ddot{\Psi}$ = 0.5 radian/sec^2, yaw angular acceleration
I_{zz} = 1.66(10^6) slug ft^2, yaw moment of inertia
ℓ = 32.53 ft (full scale aircraft)
T = 87,000 lb. (assuming T/W = 1.0)

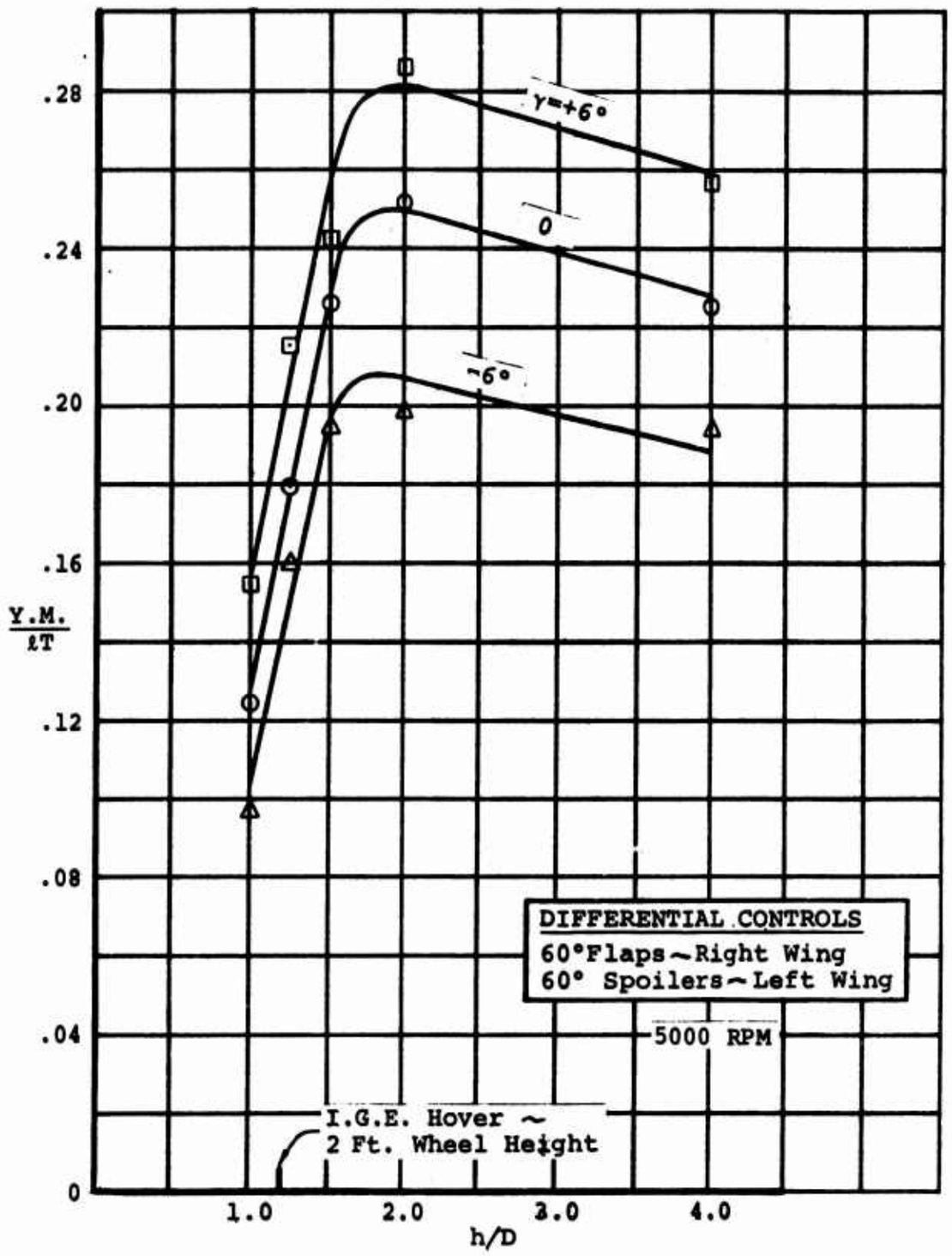

Figure 39. EFFECT OF CYCLIC PITCH ON HOVER YAW CONTROL

This comment (See Page 39) anticipates that at forward speeds in the 30 knot range, positive cyclic would reverse its role of degrading descent capability. As shown in Figure 21, the degradation in descent performance with a positive cyclic input decreased in magnitude with a decrease in forward speed. Since slipstream flow deflection is produced with trailing edge flaps in both the descent condition and hover yaw control condition, it should be expected that changes in capability due to cyclic pitch inputs would vary smoothly from descent flight to hover.

2. EFFECT OF CYCLIC PITCH ON ROLL/YAW CONTROL IN TRANSITION

Wing surface controls, when used as a yaw control in hover with the wing tilted about 90°, becomes a combined roll and yaw control in transition where tilt angles can vary from about 45° at 0.81 C_{T_s} to 15° at 0.25 C_{T_s}. Roll and yaw control available for a configuration consisting of 20° differential flaps and 40° spoilers was evaluated in pitch sweeps at three selected wing tilt/thrust coefficient combinations with a nominal 40° flap deflection. The data plotted in Figure 40 in slipstream form shows the buildup in roll control and phasing out of the yaw control as the wing is tilted down. This is illustrated in the figure by the dashed line representing a constant propeller shaft angle. The variation of rolling moment with fuselage angle is similar to the variation of slipstream lift coefficient with fuselage angle.

Figure 40 also shows the changes associated with cross-coupling cyclic pitch control and the roll/yaw control. Both positive and negative pitch inputs of 4° magnitude are noted to have only a small effect on the control effectiveness.

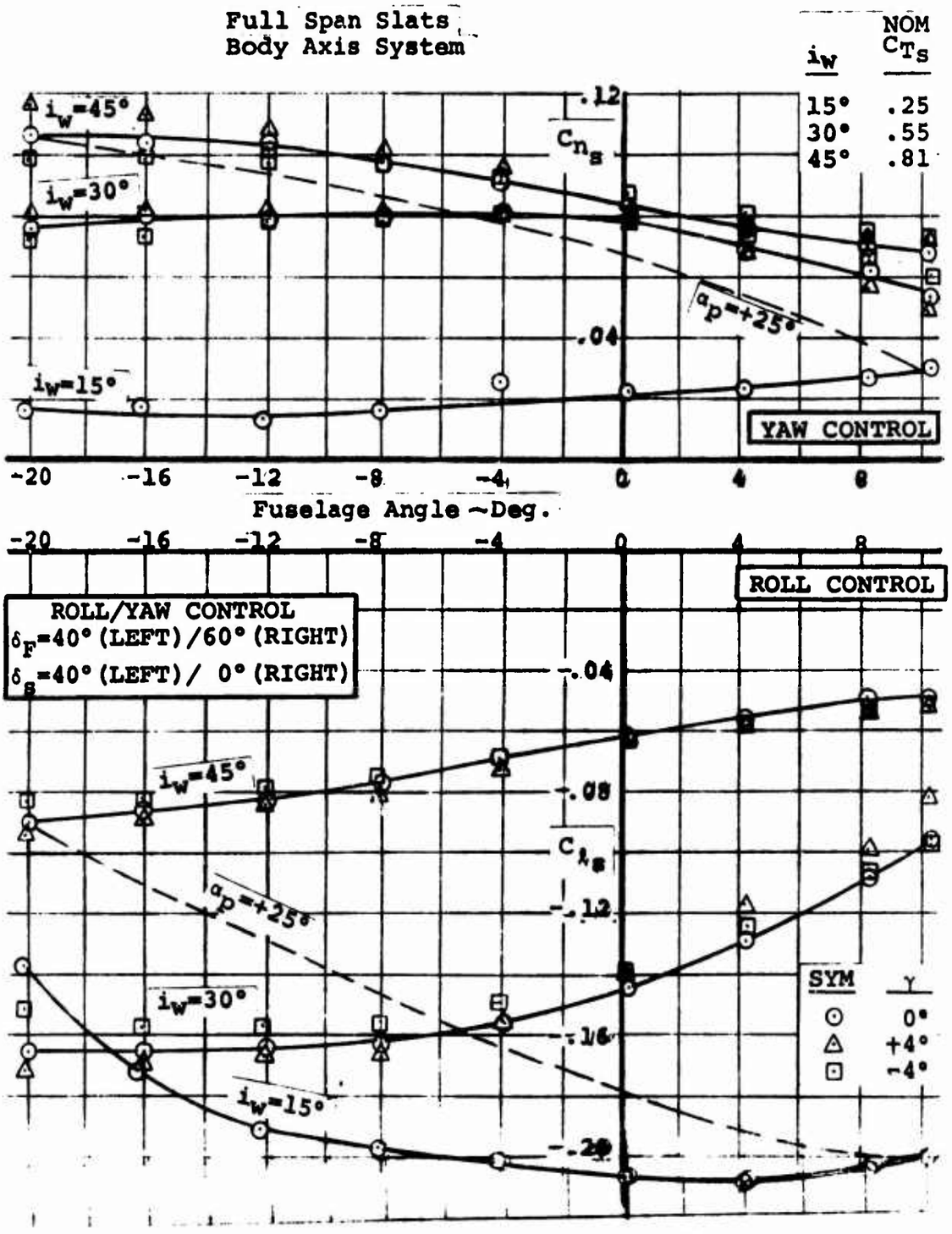

Figure 40. EFFECT OF CYCLIC PITCH ON ROLL/YAW CONTROL

3. HORIZONTAL TAIL EFFECTIVENESS AND THE EFFECT OF CYCLIC

The effectiveness of the horizontal tail in producing pitching moment about a mid c.g. is presented in Figure 41 in terms of $\Delta C_{M_S}/\Delta\Delta$ or the increment of slipstream pitching moment per degree of stabilizer angle. Values are shown for the various combinations of wing tilt angle/flap angle/thrust coefficient evaluated during the longitudinal stability and control investigation in transitional flight with the tail in the high position. This testing was performed with a series of stabilizer angular settings that increased with wing tilt.

As would be expected, the stabilizer effectiveness decreases with increasing C_{T_S} (decreasing aircraft speed). The decrease is seen to be a function of $(1-C_{T_S})$ as denoted in Figure 41. Thus, it can be concluded that the horizontal tail is essentially outside the influence of the propeller slipstream and is acted upon primarily by freestream q. Wing tilt is seen to decrease stabilizer effectiveness to some extent. The reduction is a function of tilt angle magnitude.

Also noted in Figure 41 is the value of $\Delta C_{M_S}/\Delta\Delta$ predicted from DATCOM[3] for the props off (zero C_{T_S}) condition assuming a unity ratio of q at the tail to freestream (or tunnel) q. The maximum value of $\Delta C_{M_S}/\Delta\Delta$ measured on the model is 0.86 of the predicted value.

The effect of cyclic pitch control on stabilizer control power was independently evaluated at selected points in transition. Results presented in Figure 42 are compared with the stabilizer effectiveness curves of Figure 41 as established from the more extensive investigation with zero cyclic and a high propeller RPM. The reduction in propeller speed to 5000 RPM for cyclic pitch operation, which decreased the slipstream q by almost 50%, did not have a significant effect on the measured tail control effectiveness in the linear range over which the data was interpreted.

---

[3]USAF Stability and Control DATCOM, October 1960, Revised August 1968, Page 4.1.3.2-2.

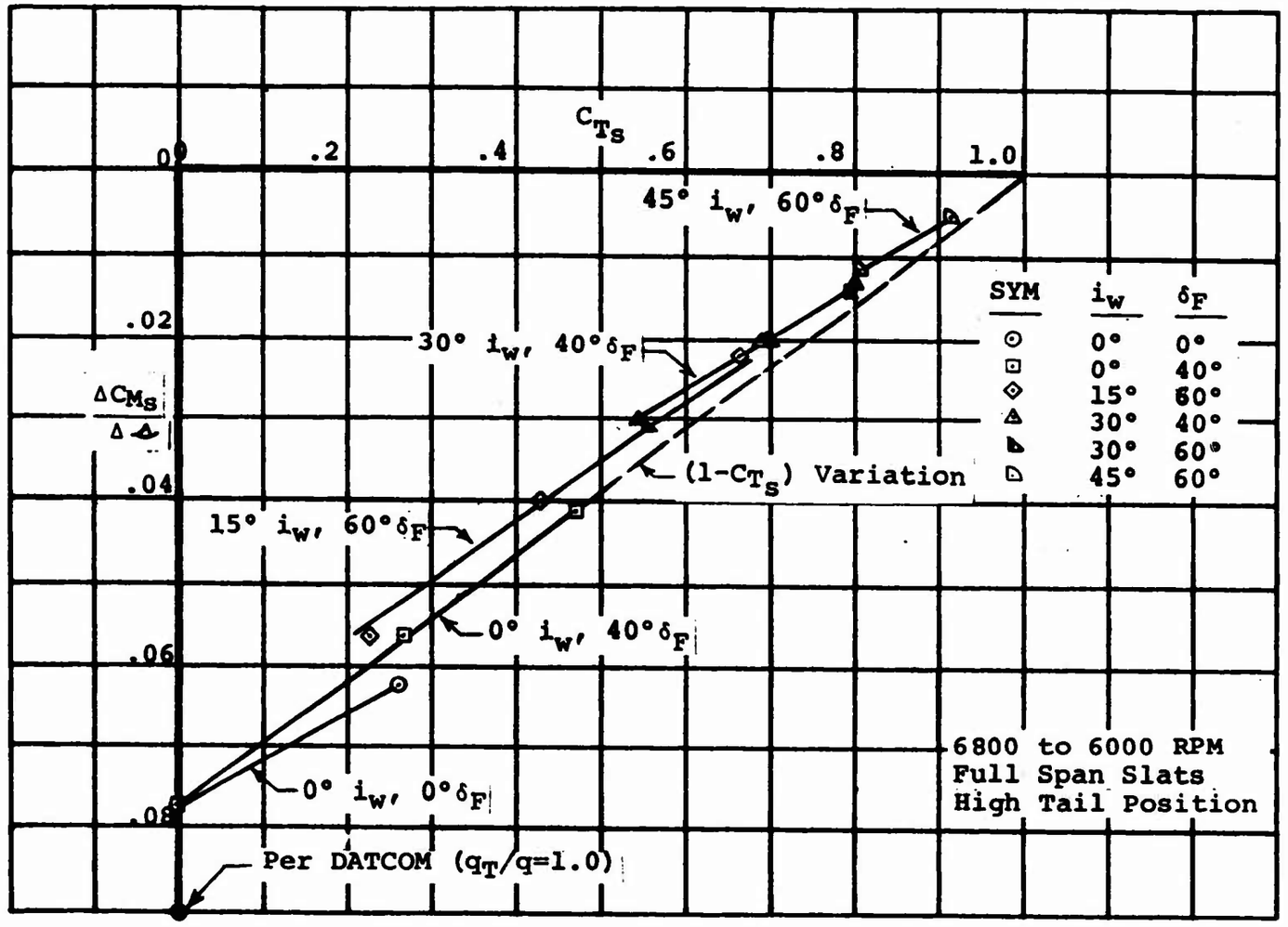

Figure 41. HORIZONTAL TAIL EFFECTIVENESS

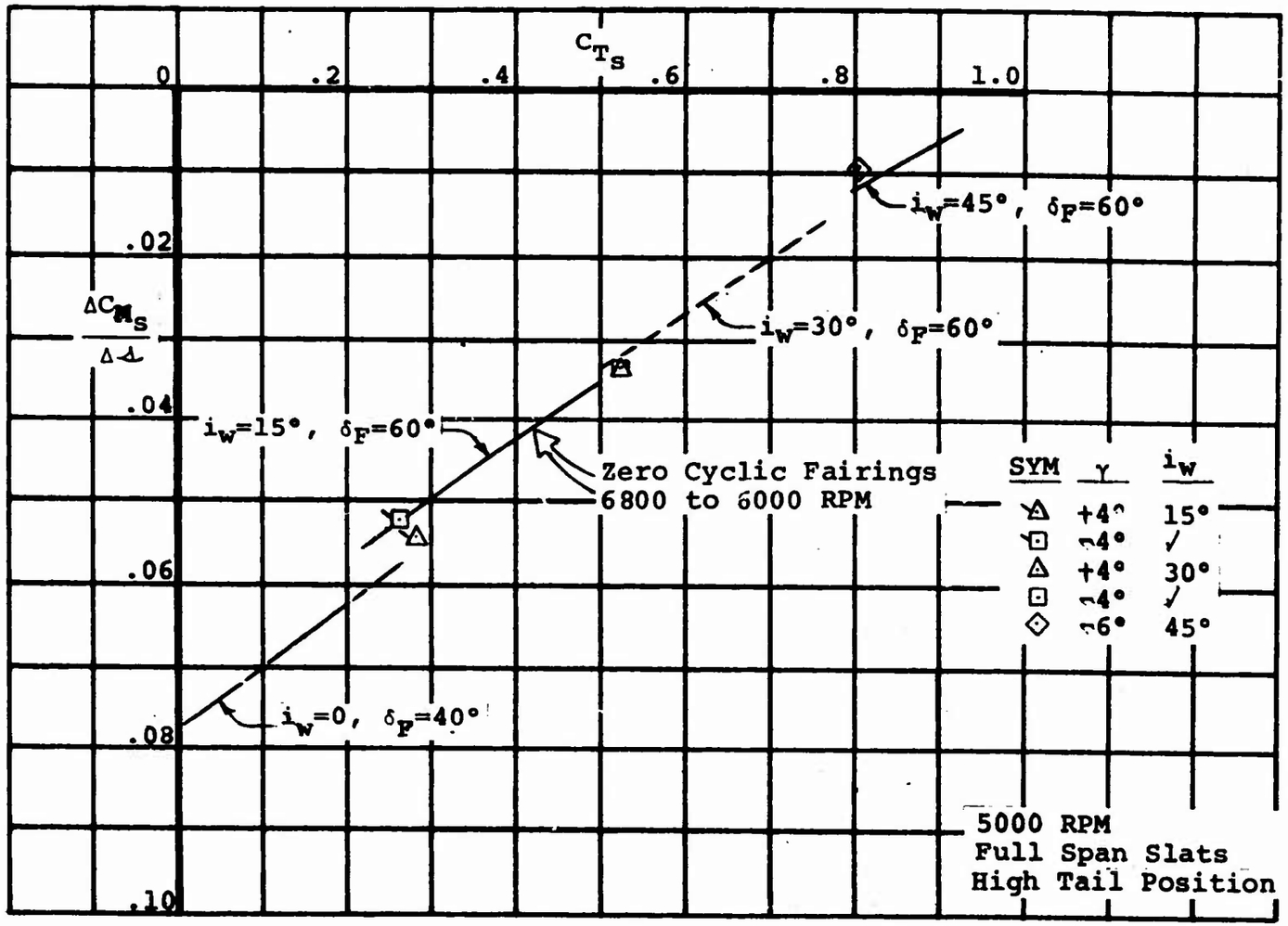

Figure 42. EFFECT OF CYCLIC PITCH ON HORIZONTAL TAIL EFFECTIVENESS

Figure 42 shows that the application of cyclic pitch has only a small influence at most on the basic tail effectiveness in transition with the only noticeable effect occurring at 0.28 C_{T_S} with 15° of wing tilt. Positive cyclic can be noted to increase the tail effectiveness. This result is reasonable since positive cyclic effectively raises the thrustline and thus should increase the q acting on the tail. Tilting the wing to a higher angle will lower the slipstream wake with respect to the tail chord plane and should diminish the effect. It can be inferred that cyclic pitch would have a larger effect on stabilizer effectiveness if the horizontal tail was located in a lower position.

SECTION VII

CYCLIC PITCH EFFECTIVENESS WITH COUPLED AIRCRAFT SURFACE CONTROLS

The previous section of the report illustrated the effect of cyclic pitch inputs on yaw control power in hover from the flaps and spoilers, on the roll/yaw control in transition from the same control surfaces, and lastly, on the horizontal tail effectiveness in transition. This report section presents the opposing effect of the aircraft surface controls on the cyclic pitch effectiveness.

Figure 43 shows the moment produced on the full span model by the application of cyclic pitch with the hover yaw controls deflected, and compares this data with the cyclic moment produced with the wing in a clean configuration. This latter curve was previously presented in Figure 7. The moment data of Figure 43, shown for an out-of-ground effect hover condition with the moments referred to the wing pivot, is depicted in a non-dimensional form, M/DT, a form used in Figure 7. Deflecting the right wing flaps down by 60° and the left wing spoilers up by 60° is seen to displace the clean wing pitching moment curve, but not alter the cyclic pitching moment capability.

Cyclic pitch effectiveness with a coupled roll/yaw control configuration of 20° of differential flaps and 40° of spoilers is shown in Figure 44 as an increment in slipstream pitching moment per degree of cyclic. Two typical conditions in transition are compared with corresponding tail-on data obtained during the cyclic pitch effectiveness runs with a full 60° of flap deflection. The decrease in incremental cyclic pitching moment capability with fuselage angle of attack was mentioned earlier in the report (See Page 32) as being largely a result of the constant RPM method of testing, wherein slipstream q increased as the model was pitched.

Figure 44 indicates that at the 45° wing tilt/0.81 C_{T_S} condition, coupled roll/yaw control produced a change in cyclic pitch effectiveness that varied from -2% to +10%. At the 30° wing tilt/0.55 C_{T_S} condition the change varied between -3% and -7%. This total variation, though moderate in magnitude, does not appear to be consistent in its change in sign from a negative to a positive effect. A logical explanation is that the overall effect of the application of roll/yaw

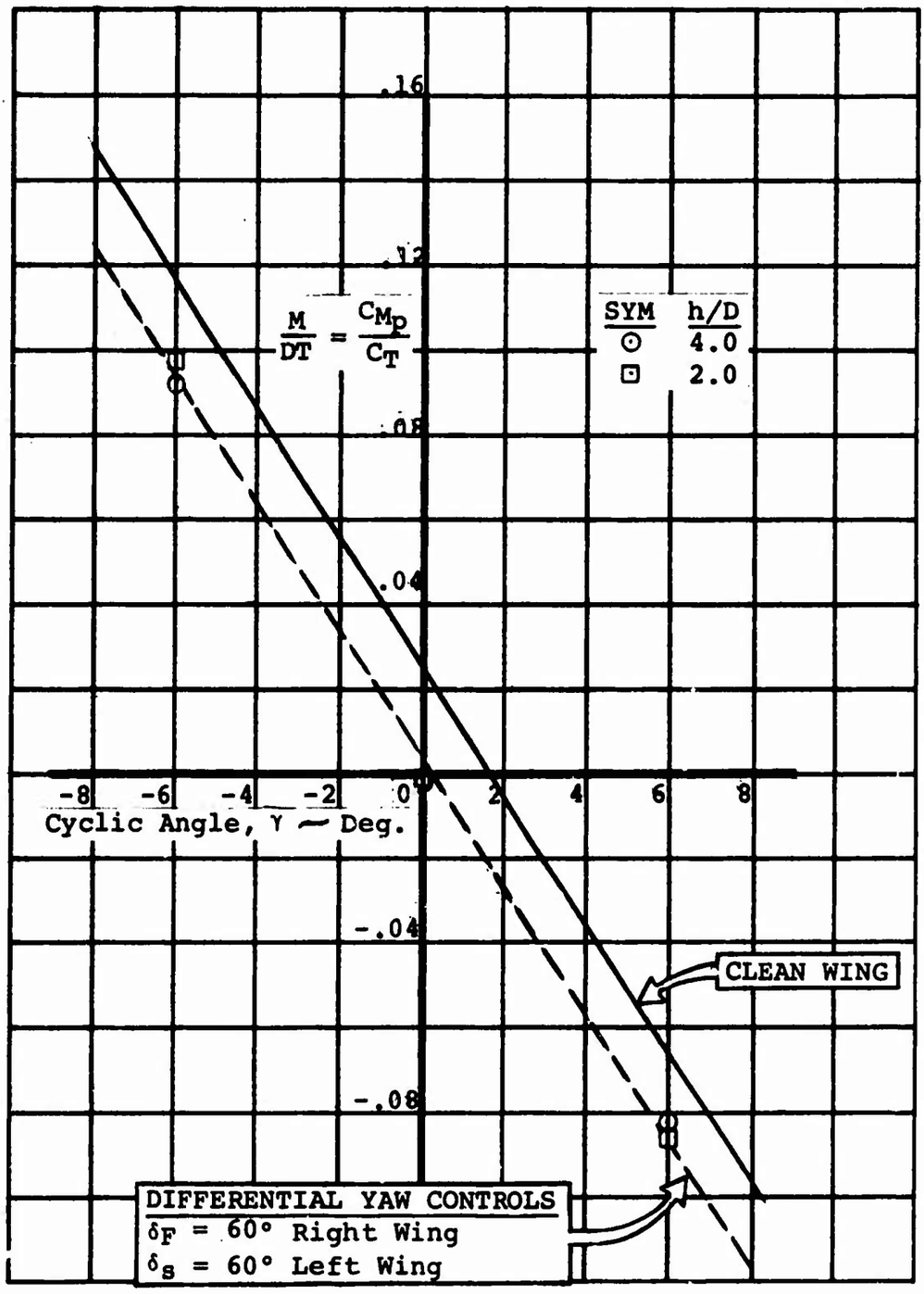

Figure 43. CYCLIC PITCH CONTROL WITH COUPLED HOVER YAW CONTROL

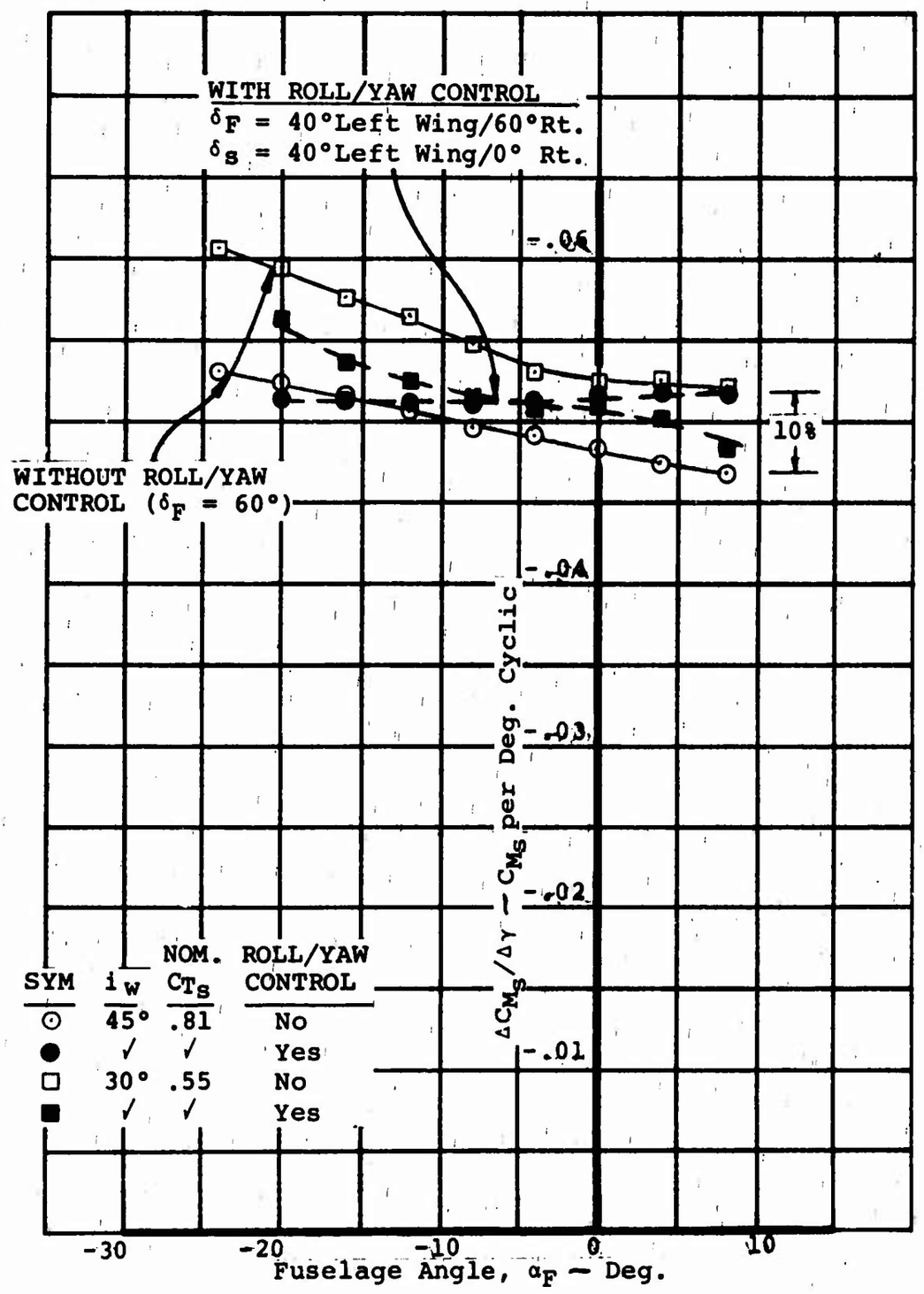

Figure 44. CYCLIC PITCH EFFECTIVENESS IN TRANSITION WITH COUPLED ROLL/YAW CONTROL

controls on cyclic pitching capability is small, and that the results shown in Figure 44 merely reflect a normal amount of data scatter that occurs when tests extend over a period of several weeks and back-to-back run comparisons are not always possible. One source of error was the accuracy of the cyclic angular settings.

Cyclic pitch effectiveness, $\Delta C_{M_S}/\Delta\gamma$, shown in Figure 44 was established by first cross-plotting aircraft pitching moment against cyclic angle (at a constant fuselage angle) from the applicable test runs and then measuring the slopes. The accuracy of these slope measurements are a direct function of the accuracy of the cyclic angular settings. For three of the four combinations presented in Figure 44 (wing tilt angle/ C_{T_S} combinations) data was available from runs with three different cyclic angles (+4°, -4°, and 0°). During the full span model tests, it was established that the cyclic angles could be consistently set within 0.4° using the cyclic hub blade angle fixture. With three data points available for establishing each slope, a maximum slope error of 10% to 13% could be involved. Since each blade of the four propellers was individually set, the probability for experiencing this maximum slope error is low. On the other hand, the percentage of error was increased for the comparison shown in Figure 44 by using data from runs that were not back-to-back. The runs without roll/yaw control were conducted earlier in the Phase II test program than the runs with roll/yaw control (See Section 5.2 of Reference 4). As a consequence, the resetting of the cyclic angles for the coupled roll/yaw control runs introduced an error. The total possible slope error between directly comparative runs shown in Figure 44 then becomes double the previously noted 10% to 13%, assuming that the setting error was in the opposite direction for the runs to be compared, i.e., a +4.4° cyclic setting compared to a +3.6° cyclic setting. Again, the probability of experiencing this large error was highly improbable due to the compensating effect of individually setting each of the 12 propeller blades. In summary, it is reasonable to assume from the percentages discussed that an error of 5% to 10% could have existed for the cyclic pitch effectiveness comparsion of Figure 44.

The influence of the horizontal stabilizer on cyclic pitch effectiveness was previously illustrated by the comparative data presented in Figures 19 and 20. It is readily apparent that any influence is small in magnitude.

SECTION VIII

IN-GROUND EFFECT EVALUATION WITH CYCLIC PITCH

An in-ground effect (I.G.E.) evaluation of cyclic pitch effects in both the longitudinal and lateral/directional modes was performed with the full span model utilizing the Boeing-Vertol moving belt ground plane. This investigation was conducted with the aircraft level and a scaled ground height representing the aircraft with the wheels 3 feet off the ground (The h/D per the definition on Page 64 will vary with the change in wing tilt angle). Slats were extended and the flaps were deflected 40° for the longitudinal testing and 60° for the lateral/directional testing. The 40° flap setting corresponds to a compromise between a lower deflection for takeoff with a wing tilt angle in the order of 20° and a higher deflection for landing approach. The selection of a typical landing flap angle of 60° for the lateral/directional testing was based on an analysis which indicated that the directional characteristics were most critical for the landing condition. A similar analysis of the longitudinal characteristics was inconclusive as to whether the takeoff or landing condition was most critical for a tilt wing aircraft employing cyclic pitch control. This analysis result was the basis for the selection of an average flap setting during the longitudinal testing.

The desire to obtain in-ground effect information at a low wheel height precluded performing the longitudinal mode runs with the standard fuselage angle pitch sweeps and constant wing tilt angles. This restriction resulted from the clearance problem between the long straight sting and the moving ground plane. Wing tilt sweeps with a level fuselage and tail removed, that were made in place of the fuselage sweeps, do not allow a direct data comparison to show the influence of ground effect on the aircraft longitudinal stability. An examination of the in-ground effect longitudinal data presented in Section 6.7.2 of Reference 4 does show, however, that the effect of cyclic pitch inputs on the variation of pitching moment with wing tilt angle to be small. A positive cyclic pitch angle of +4° increases the tail-off pitching moment slope by a small percentage (about 6%) and a negative cyclic angle of -4° decreases it by a small percentage over the C_{T_S} range evaluated with representative wing tilt angles. This indication of the effect of cyclic pitch on longitudinal

stability is in the same direction with respect to angularity of cyclic inputs and is of the same small magnitude as shown in Figure 32 for the out-of-ground effect tail-off case. Thus, it can be inferred that cyclic pitch control action in-ground effect has the same influence on longitudinal stability as recorded out-of-ground effect.

Figure 45 compares the cyclic pitch control capability (in terms of slipstream pitching moment per degree of cyclic) as measured in-ground effect with that measured out-of-ground effect. Even though the flap angles are different for the two sets of data, 40° flaps for the I.G.E. data and 60° flaps for the O.G.E. data, this configuration change should not be of a magnitude that would materially alter the comparison. It would not be expected for a flap angle change from 60° to 40° to measurably alter the cyclic pitch effectiveness when the differences in cyclic effectiveness shown in Figure 20 for a more extreme configuration change (isolated prop model to the full span model with slats extended and 60° of flaps) were not of a major magnitude. The variation of cyclic pitch effectiveness in-ground effect, namely, the small increase with C_{T_S} at a constant shaft angle (α_p) and the small decrease as the shaft angle is increased, are the same trends exhibited by the 1/12 scale isolated propeller data presented in Figure 20. Figure 45 shows that moving from an out-of-ground effect flight condition to a flight condition with the wheels 3 feet off the ground results in some reduction in the cyclic pitch effectiveness, but only by an average of 6%.

The results of the in-ground effect lateral/directional stability investigation with empennage on are presented in Figure 46 as slipstream stability derivatives. Also shown in this figure is the comparable out-of-ground data (dashed lines) obtained with zero cyclic angles.

With 15° of wing tilt and zero cyclic the primary influence of ground effect was to incrementally reduce the directional stability over the 0.29 to 0.69 C_{T_S} range evaluated. It is not discernible whether the decrease in directional stability is primarily caused by an increase in the basic tail-off instabilitity or a loss in vertical tail effectiveness since only tail-on data was acquired. Increasing the wing tilt angle to 30° exhibited the same trend up to a C_{T_S} of 0.76, which corresponds to a full-scale speed of approximately 45 knots. In this test range, the effect of a positive cyclic input is similar to the result recorded out-of-ground effect in that

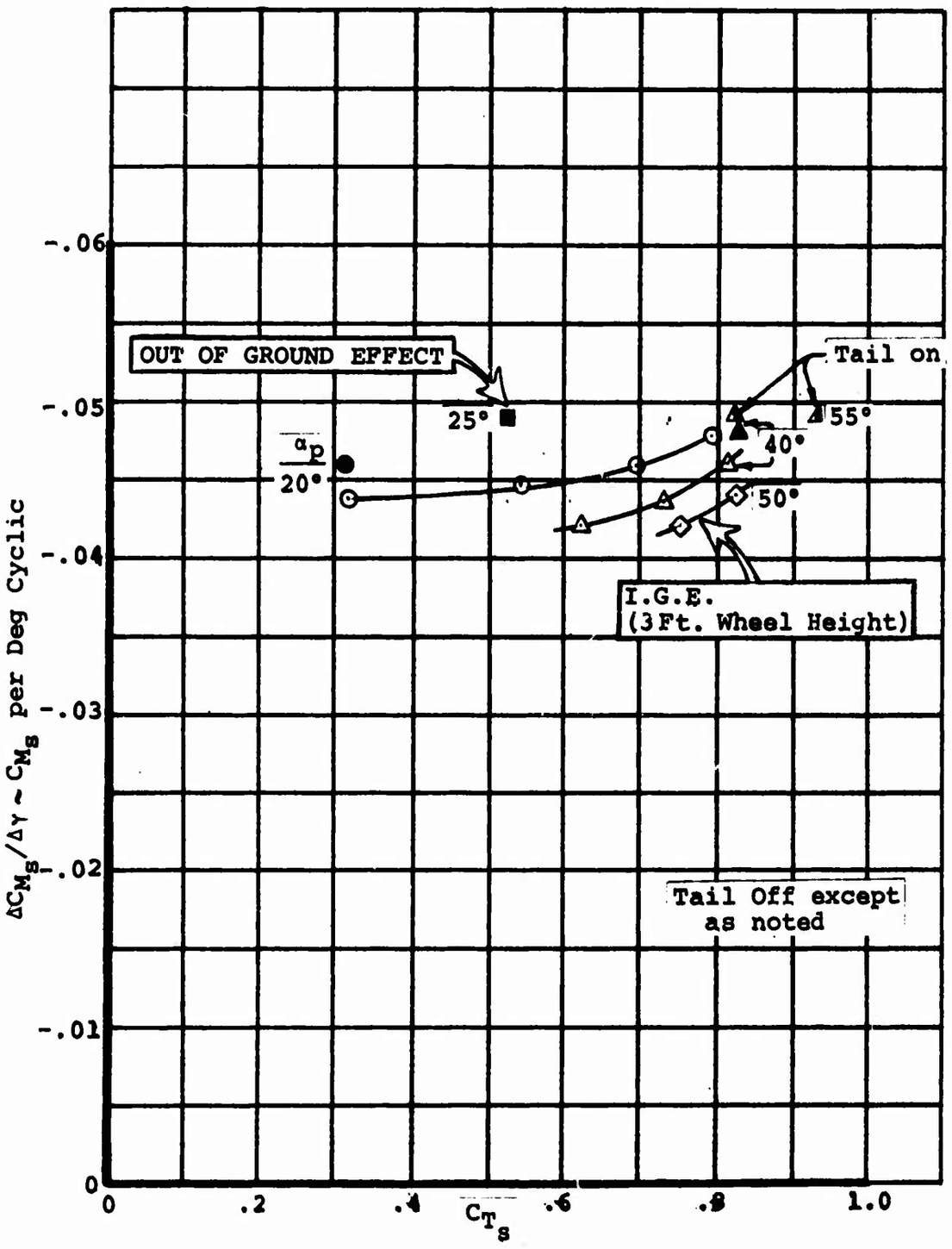

Figure 45. INFLUENCE OF GROUND EFFECT ON CYCLIC PITCH EFFECTIVENESS

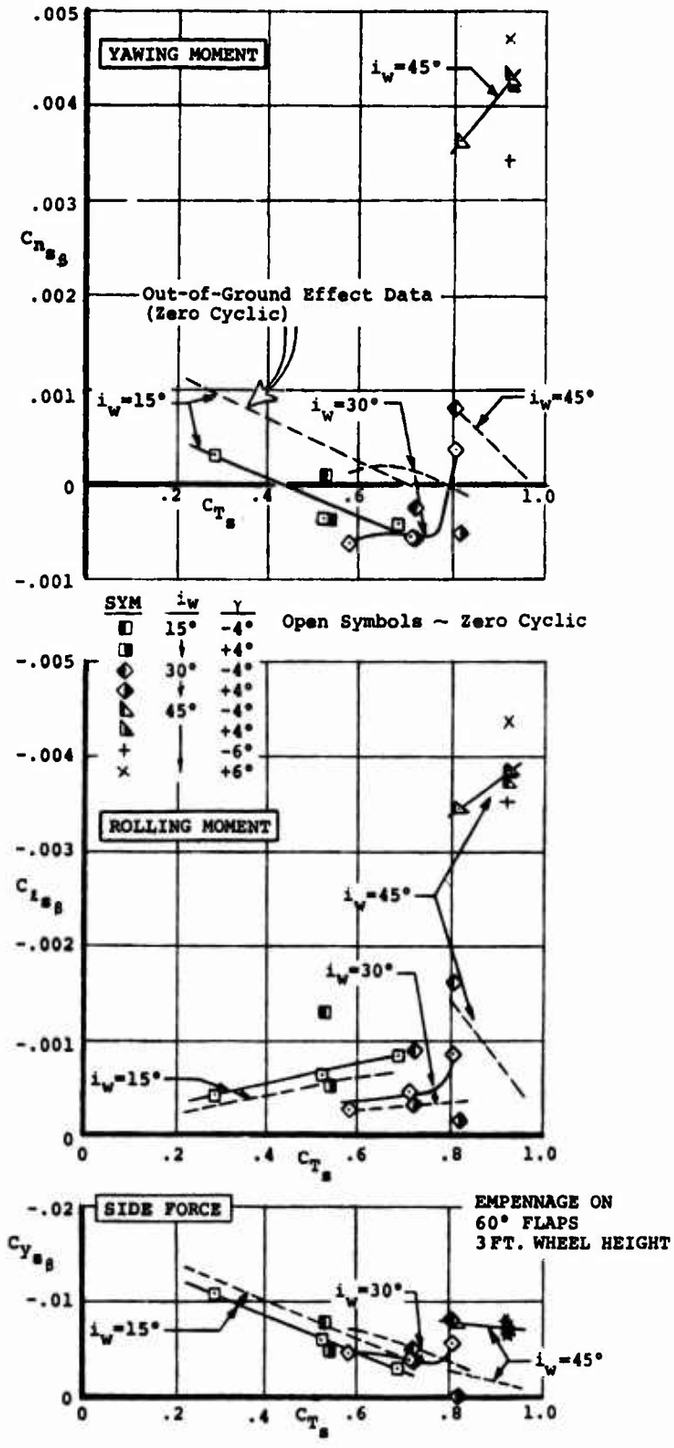

Figure 46. EFFECT OF CYCLIC PITCH ON LATERAL/DIRECTIONAL STABILITY IN GROUND EFFECT

the changes in lateral/directional stability are small. Negative cyclic has a more pronounced influence in-ground effect, increasing both the directional stability and dihedral effect by larger increments than for the out-of-ground effect case.

A condition was encountered at 0.8 C_{T_S} that is identified as ground recirculation. Ground recirculation is an aerodynamic flow condition that occurs when the air that normally passes between the wing and the ground can no longer negotiate this path. The diverted flow recirculates in front of the wing as the aircraft moves along the ground. At the 0.8 C_{T_S} test point an increase in directional stability, dihedral effect, and side force were measured with zero cyclic pitch. The values for these derivatives changed as a result of cyclic pitch inputs. A negative cyclic angle increased the derivative values and a positive angle reduced the derivative values to a level consistent with the lower C_{T_S} data. This leads to the conclusion that at this C_{T_S} condition, ground recirculation was in the initial stages of formation. The application of negative cyclic, which effectively increases the propeller shaft angle and thus the angle of attack of the total lifting system, induced a stronger case of ground recirculation. Positive cyclic lowered the effective angle of attack sufficiently to completely relieve the model from ground recirculation. It can be assumed that a lower flap angle would have produced the same result. As a final point, a question exists as to whether the low tunnel q prevailing at this test point (2.7 lb/ft)was a factor in precipitating ground recirculation for this particular condition.

At the high C_{T_S} values of 0.81 to 0.92 investigated with 45° of wing tilt, ground recirculation was well developed as evidenced by the large increase in directional stability and dihedral effect over that recorded out-of-ground effect. The magnitude of these stability changes was probably influenced by the wing configuration: a tapered wing with straight leading edge and swept forward flap hingeline. It would appear from the direction of these forces and moments, nose-right yawing moment, right wing-up rolling moment and left side force, that the up-wind wing and fuselage side tended to "funnel" the air into the wing/body junction and the air on the down-wind wing side was partially diverted spanwise and around the wing tip.

SECTION IX

LEADING EDGE BLC ON THE WING CENTER SECTION

In the semispan tilt wing model test (Reference 1), leading edge boundary layer control (BLC) was applied as a means of increasing the wing stall angle and thus improving the descent performance. Leading edge BLC was installed and investigated over the full wing span and over selected sections of the span. As a part of this investigation, BLC was individually applied to the wing section over the top of the fuselage and the area between the inboard wing fences.

The "unbathed" wing/body center section of a tilt wing aircraft is particulary susceptible to stall. Because of this, considerable configuration work has been performed on delaying stall of this area. Both the full span model and semispan model utilized a full span slat that extended across the wing center section. This center section slat was found to substantially improve the stall angle of this area on the full span model. See Section 2.1 of Reference 1 and Section 2.1 of Reference 3 for a description of the slat geometry used for the models.

Figure 47 illustrates a problem that was observed via tufts as a result of wing center section stall. As the full span model was pitched during the longitudinal stability and control testing, the flow separation that started at the wing center section progressed aft along the fuselage to the vertical tail. Further pitching of the model caused the separated flow region to move up the fin. At some fuselage angle of attack, the horizontal tail (mounted at the top of the fin) entered the wake. The first visual indication of the horizontal tail encountering the wake was a slight buffeting or "flicking" of the tufts, usually at the root section of the tail. Further pitching of the model lowered the tail with respect to the disturbed flow and increased the buffeting or tuft activity. Complete immersion of the tail in the wake was evidenced by total flow separation (stall) on both the top and bottom surfaces of the tail. See Section 6.4, Reference 3 for details.

The results of the stabilizer tuft observations for the majority of the wing tilt angle/flap angle/C_{T_S} combinations tested are presented in Figure 47 as a function of C_{T_S}. For each wing tilt/flap angle combination, a band of fuselage

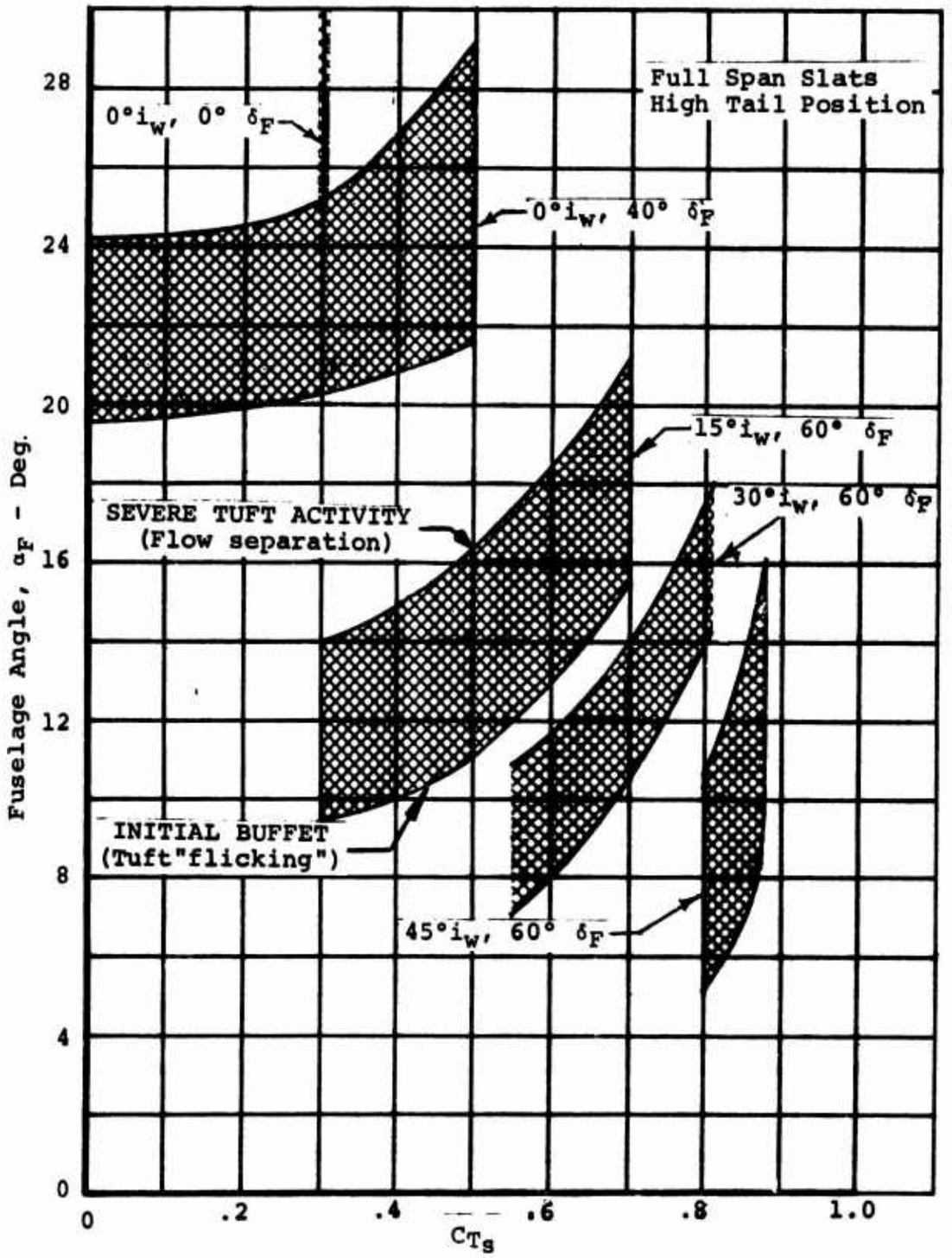

Figure 47. HORIZONTAL TAIL BUFFET TUFT OBSERVATIONS

angles over which tail buffeting was observed is shown. The bottom of the band corresponds to initial buffeting or "tuft flicking" and the top of the band corresponds to heavy buffeting or essentially total flow separation.

From this plot, it can be seen that the fuselage angle at which tail buffeting is encountered increases with increasing C_{T_S} and decreases with wing tilt as would be expected. No tail tuft activity or buffeting was recorded at the 45° wing tilt/0.92 C_{T_S} test condition or at combinations of higher thrust coefficients (0.94 and 0.97 C_{T_S}) and higher wing tilt angles (55° and 70°). At these conditions the character of the flow aft of the tilted wing changed and no separated flow was observed in the vicinity of the vertical tail.

There is a strong possibility of increasing the fuselage angle of attack at which tail buffeting first occurs by application of leading edge BLC to the wing center section region. An indication of the increase in center section stall angle that can be achieved with BLC in conjunction with the slat is presented in Figure 48. This semispan model data, obtained during wing tilt angle sweeps with a propeller rotation of both turning down between nacelles, shows that leading edge blowing improved the stall angle of the wing center section by a constant increment of 18° over the range of slipstream thrust coefficients (C_{T_S}) tested. Leading edge blowing applied to the wing area between the inboard fences increased its local stall angle by an average of 9° over the same C_{T_S} range.

Of special concern when tufts are utilized to interpret the occurrence of stall, as was done for the noted test, is whether the tufts are recording only the flow activity on the surface of the wing and not the character of the flow a small distance above the surface. To resolve this factor, an inverted "V" shaped tuft stalk was mounted on the movable wing/body fairing aft of the tilting wing center section for most of the BLC test (Reference 1). Observations established that separated flow did not exist above the surface when the surface flow was attached, and that stall on and above the surface occurred almost simultaneously.

The data shown in Figure 48 was obtained with a blowing coefficient (C_{μ_S}) of approximately 0.10. As discussed in Section IV.2, this coefficient is defined with the slipstream q as the reference dynamic pressure and the blown area of the

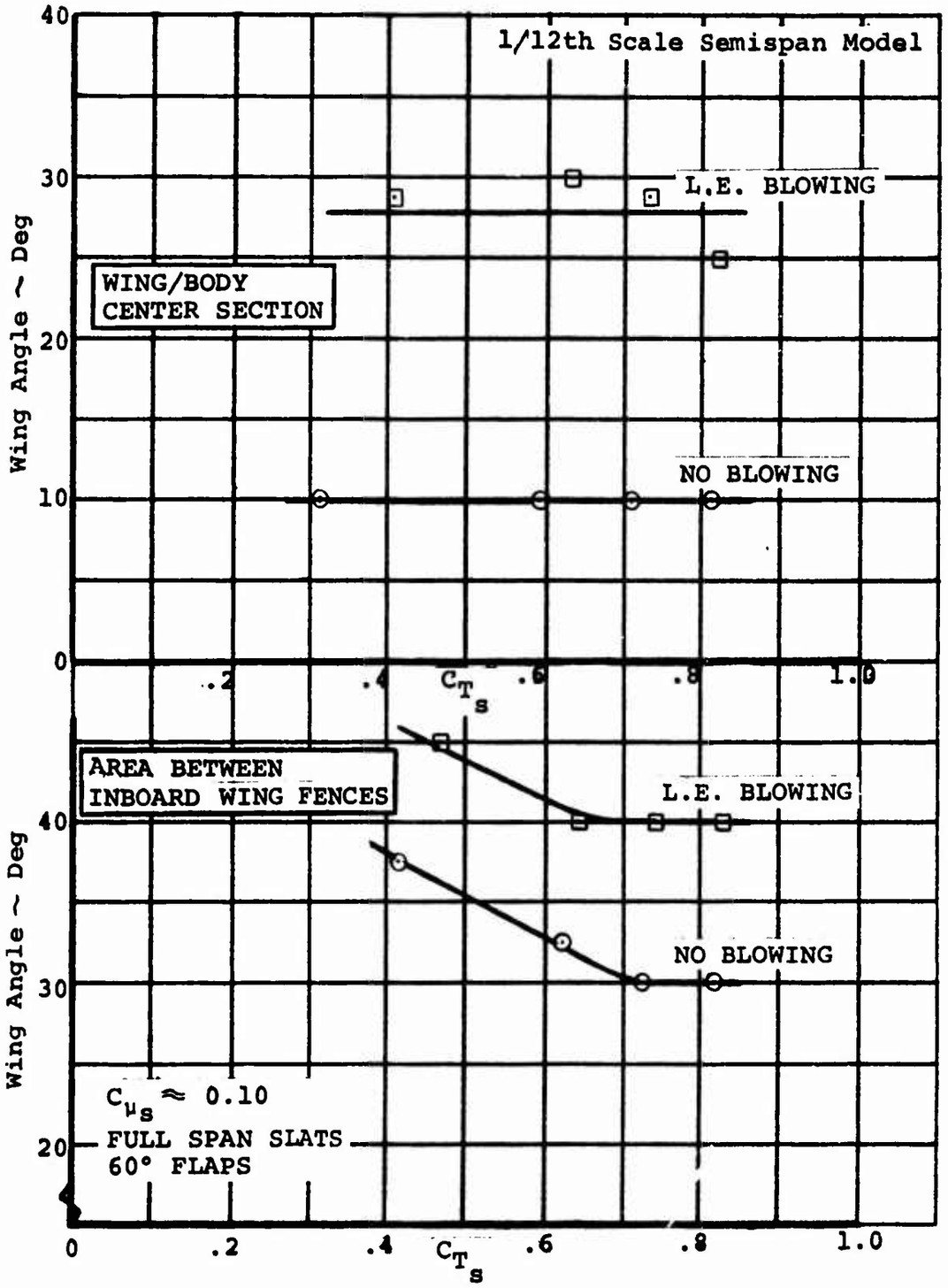

Figure 48. INCREASE IN WING CENTER SECTION STALL ANGLE WITH LEADING EDGE BLOWING

wing as the reference area. Also, the high value of C_{μ_s} is not necessarily representative of a minimum C_{μ_s} for flow attachment and instead reflects the minimum C_{μ_s} that could be achieved on the model with a choked slot nozzle, primarily as a result of model power limitations. Assuming a reasonable blowing coefficient of 0.05, calculations indicate a power requirement of 250 HP to provide leading edge blowing of the wing center section and area between the fences at flight speeds in transition down to 40 knots. This power value is valid for a representative tilt wing aircraft having a "V" gross weight of 87,000 pounds.

An interesting possibility, if leading edge BLC is being studied as a solution to the wing/body center section separation problem, is to consider full span leading edge blowing in lieu of full span slats for achieving the desired level of low speed descent performance. This situation was examined during the semispan tilt wing model test (Reference 1). The results are presented in Figure 49.

The data in this figure compares the descent capability achieved with and without the full span slats when full span leading edge BLC is applied in conjunction with +4° of positive cyclic. During these runs the double slotted flaps were deflected 60° and a propeller rotation direction of both props turning down between the nacelles was maintained. Figure 49 indicates that the removal of the slats will reduce the descent capability by a maximum of 300 fpm.

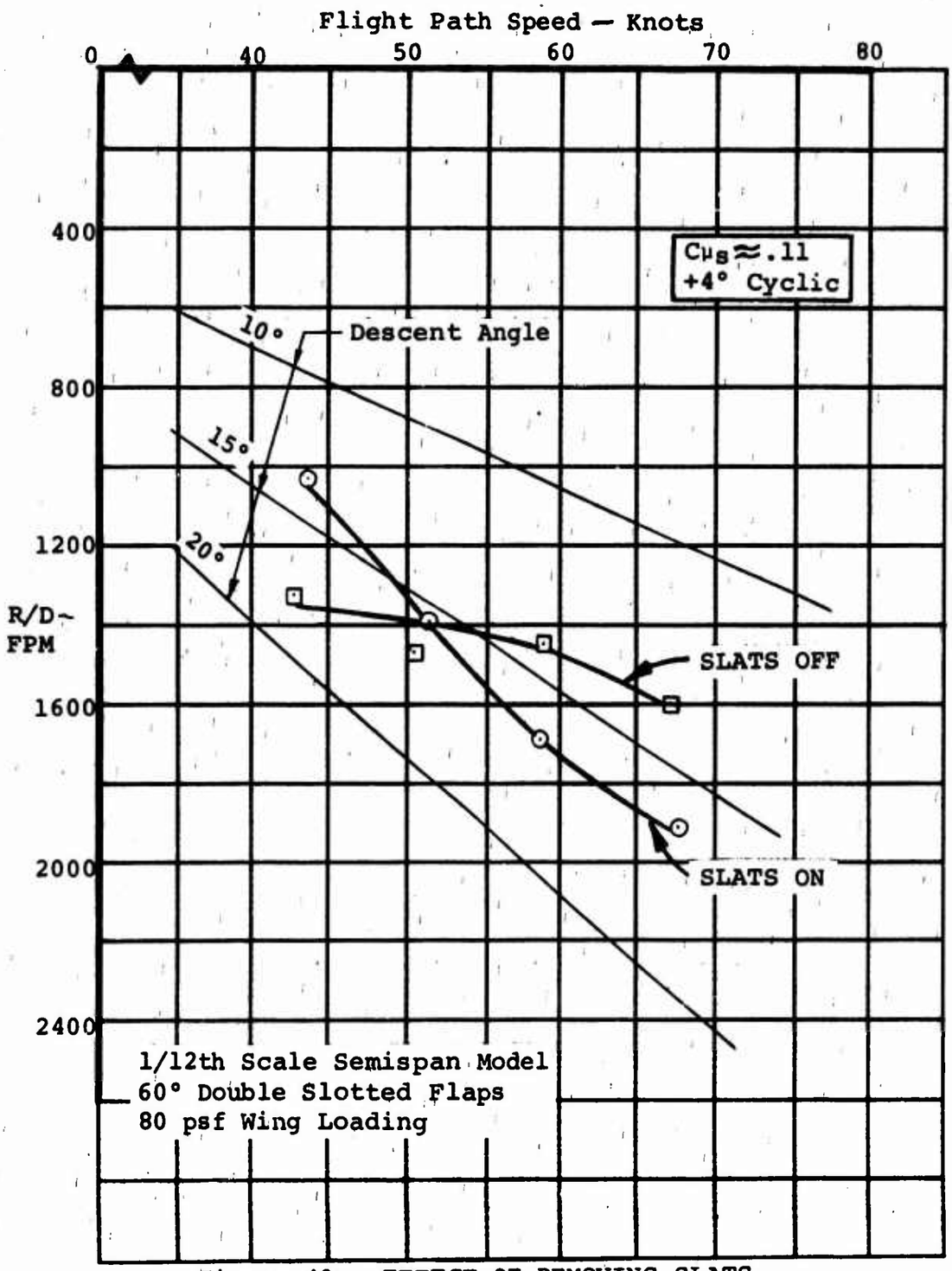

Figure 49. EFFECT OF REMOVING SLATS WITH FULL SPAN L.E. BLOWING

SECTION X

PROPELLER BLADE LOADS IN TRANSITION

The blade loads experienced by a propeller during a typical tilt wing aircraft transition in unaccelerated flight were measured on the 1/3rd scale propeller model (Reference 5). Strain gages were mounted on a blade of this model at the 0.22 radial station to measure flap bending, chord bending and torsion. Additional strain gages were located at the 0.45 radial station for flap and chord bending, and on a control arm to measure pitch link loads.

A sample of the data is presented in Figure 50 for flap bending as measured at the 0.22 radial station. In this example, shaft angle decreases from 68° at 0.98 slipstream thrust coefficient (in the background of the plot) to 11.5° at 0.08 C_{T_S} (in the foreground). Shown at the far left of each cross section is the maximum alternating load (zero to peak) on a logarithmic scale. Progressing to the right are given the first twelve harmonics of the alternating load.

As can be seen by comparing the total load to each individual harmonic content (and keeping in mind the logarithmic scale), the alternating load primarily consists of the first harmonic with some contribution from the second. The harmonics higher than two contribute only a small percentage to the total load. Further, it may be seen that the maximum alternating loads occur at the high shaft angle case, decreasing as the propeller is tilted down until the forward speed build-up begins as transition is completed. Loads arising from cyclic pitch control inputs must be added vectorially to the transition loads. Chord bending, torsion and pitch link loads exhibited similar trends.

The alternating flap bending loads measured at the 0.22 radial station during the typical transition are presented in Figure 51 in another format. The total alternating load and first three harmonics are shown as a function of advance ratio in the lower half of the figure; the schedule used for propeller shaft angle and blade or collective angle during the transition are shown in the top half.

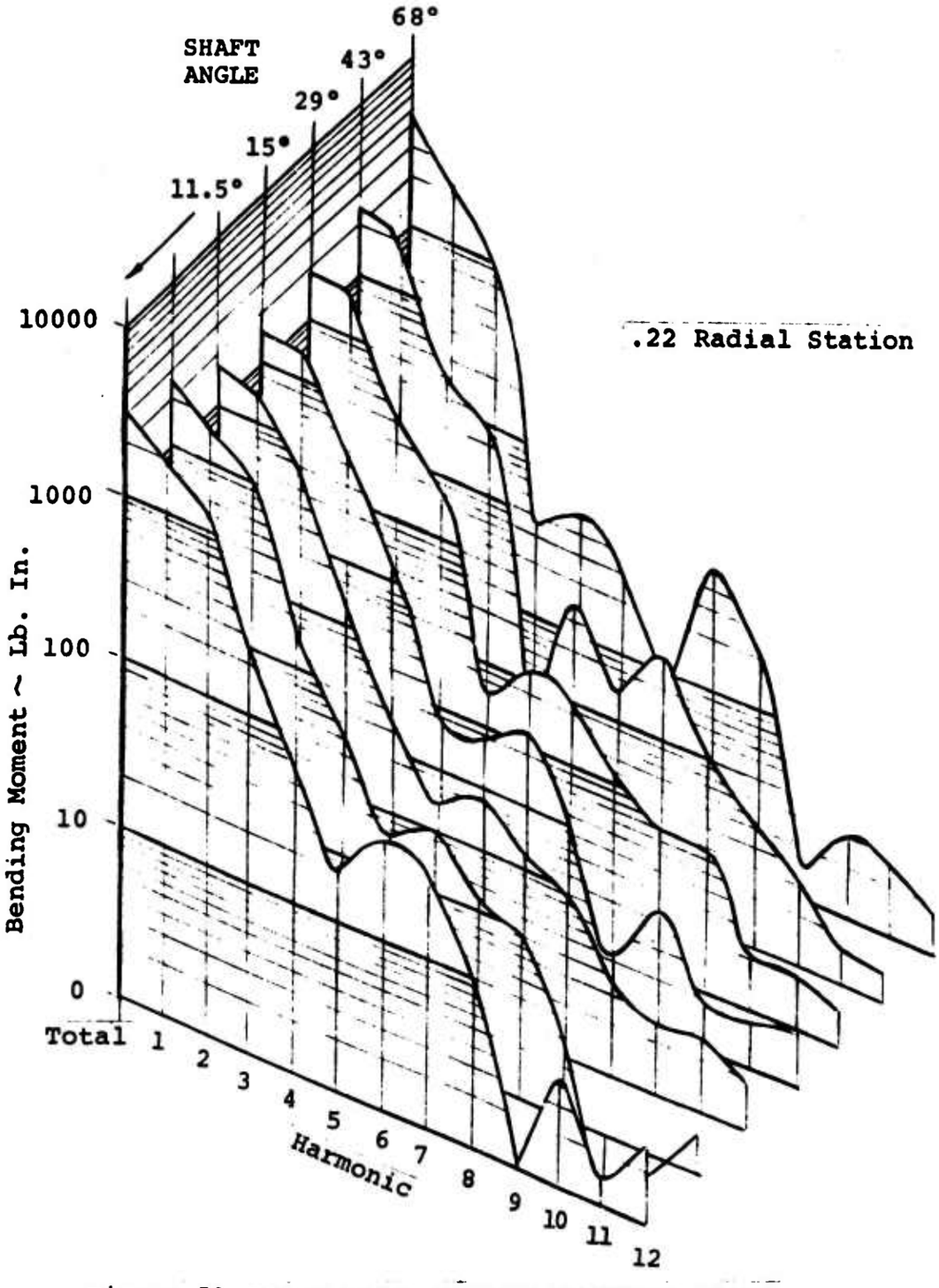

Figure 50. BLADE FLAP BENDING HARMONIC LOADS
THROUGH TRANSITION
1/3RD SCALE PROPELLER MODEL

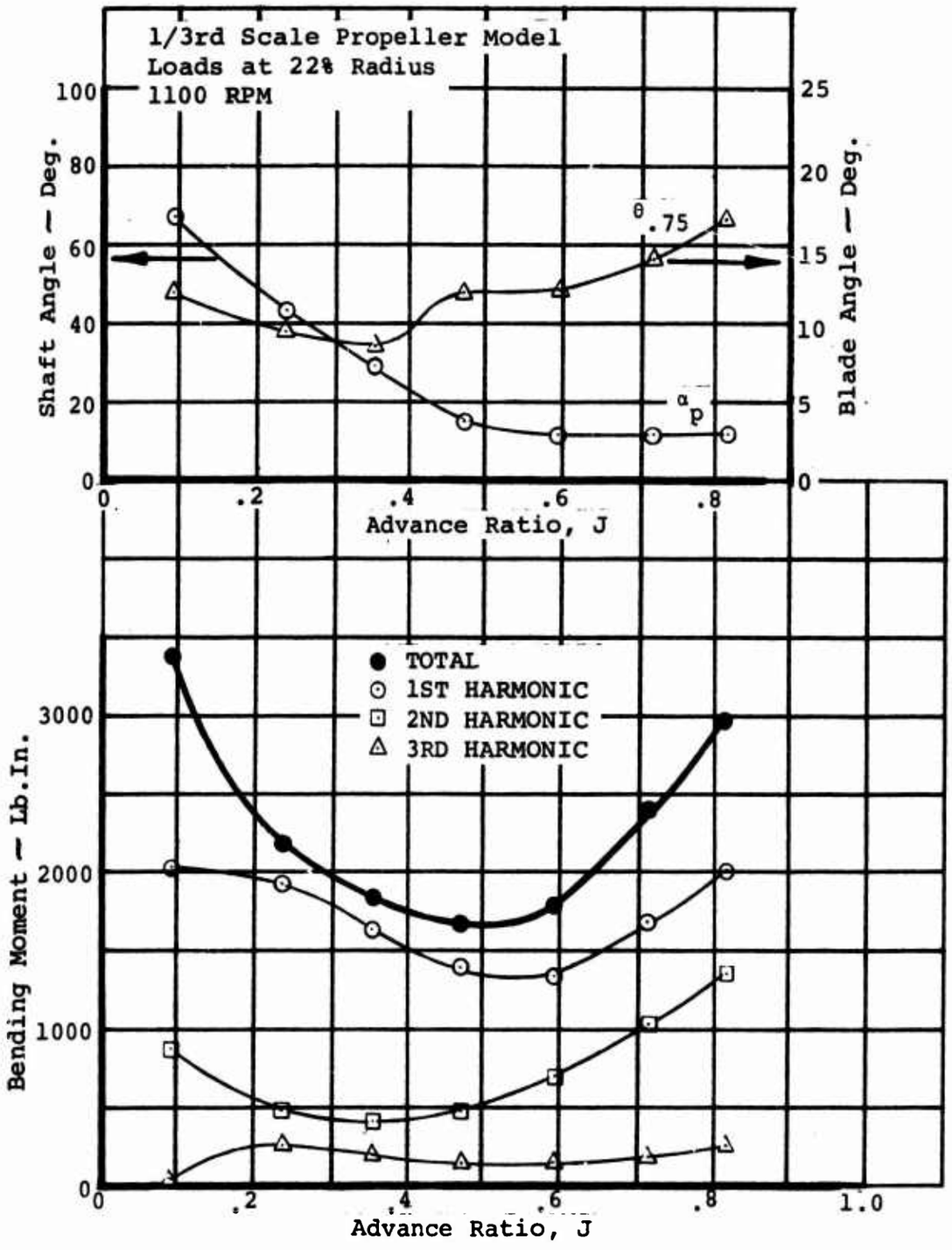

Figure 51. ALTERNATING FLAP BENDING LOADS THROUGH TRANSITION

As J was increased from 0.1 to 0.5 and the propeller was tilted down from 68° to 15°, the total flap bending moment decreased by a factor of two. Above a J of 0.5, the flapping moment increases with speed. The higher harmonics do not contribute significantly to the flap bending during the low J portion of the transition; however, the second harmonic makes an appreciable contribution at advance ratios greater than 0.5.

The variation of the alternating chord bending moment with advance ratio during the transition was similar to that recorded for the flapping moment. Total chord bending moment decreased by a factor of two at 0.5 J and then increased with higher J values.

The higher harmonic content of the alternating blade torsion load was quite small and essentially invariant with advance ratio. A maximum variation of 25% of the moment during the transition was measured, with the highest values occurring at the start of transition and at the high J value. The alternating pitch link load did not vary by a significant amount throughout the transition.

Figure 52 shows the measured alternating flap bending loads resulting from cyclic pitch application in hover. The moments are presented as a total alternating moment and the first three harmonics. The figure shows that the total alternating loads are linear with cyclic angle up to the highest angle tested and that the largest contribution is due to the first harmonic. The higher harmonics contribute little to the total moment and are essentially independent of cyclic angle.

1/3rd Scale Propeller Model

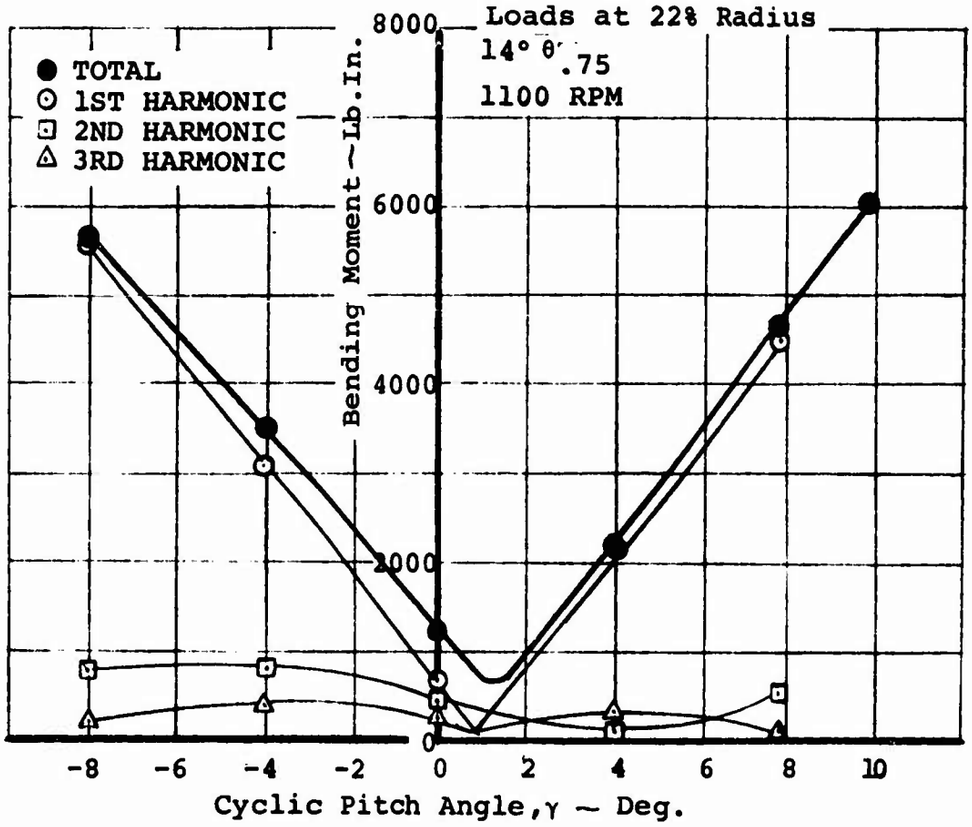

Figure 52. EFFECT OF CYCLIC PITCH ON ALTERNATING FLAP BENDING LOADS IN HOVER

SECTION XI

CONCLUSIONS

The most important conclusions derived from the model wing tunnel test program applicable to the use of cyclic pitch propellers for the low speed longitudinal control system of a V/STOL tilt wing aircraft are:

1. The hub pitching moment, generated by cyclic pitch propellers operating in hover, is linear and matches theory. Test data from the 1/3rd scale propeller model shows that a total cyclic angle of 8.7° is required to trim c.g. travel and provide a pitch control capability of 0.6 radians/sec^2. The angular value applies to a four-propeller tilt wing aircraft hovering at a 87,000 lb. gross weight and 2500/93°F atmospheric conditions.

2. A power increment is associated with cyclic pitch action. The increment varied from a 6% increase in power with 6° of cyclic to a 19.5% increase with 10° of cyclic. These percentages were measured on the 1/3rd scale propeller model operating in hover, the most critical mode powerwise.

3. The cyclic pitch effectiveness (pitching moment per degree of cyclic) was not impaired through installation on a wing with large chord flaps deflected 60° and full span slats extended. In actuality, an increase in aircraft pitching moment occurred as a result of the favorable influence of cyclic pitch on propeller normal force.

4. High wing tilt angles did not significantly alter the basic cyclic pitch control capability. This statement is valid for wing tilt angles up to 63° at 0.93 C_{T_S}, the low speed end of transition, and correspondingly small tilt angles (but past wing stall) at lower thrust coefficients where cyclic pitch control is phased out (0.45 C_{T_S}). Moving from an out-of-ground effect condition to a 3 ft. wheel height reduced the cyclic pitch

effectiveness by a small amount (6%).

5. Positive cyclic angles (nose down pitching moment) reduced the low speed descent capability. The increments measured on the full span model with slats extended and 60° of flaps are as follows: 100 fpm per degree of cyclic at a full-scale speed of 62 knots which decreased to 50 fpm per degree of cyclic at a speed of 38 knots.

6. In the transition regime, cyclic pitch control had only a small influence on the horizontal tail control capability and on the roll/yaw control capability from the wing surface controls (flaps and spoilers). Cyclic pitch did alter the hover yaw control capability from the flaps and spoilers. A positive angle of 6° increased the hover yawing moment by 15% and a negative cyclic angle of 6° decreased it by 17%.

7. The use of cyclic pitch had no marked effect on either longitudinal stability or lateral/directional stability through transitional flight or in-ground effect (3 ft. wheel height). An exception was the increase in directional stability and dihedral effect for an in-ground effect condition with negative cyclic.

8. Leading edge boundary layer control can be used to increase the stall angle of the critical wing center section. The reduction in descent capability due to positive cyclic inputs can be offset with leading edge BLC.

9. The 1/3rd scale propeller test established the feasibility of using Lamiflex bearings for blade retention and angular oscillation requirements.

10. A 1/12th scale model with 2 ft. diameter cyclic pitch propellers is satisfactory for aircraft configuration work. The power increments associated with cyclic pitch action, as measured on a 1/12th scale model, are excessive due to bearing friction from the high model RPM. Caution must be exercised in blade angle settings and in interpreting the power data at cyclic angles above 6° due to Reynolds number effects.

REFERENCES

1. C. Kolesar, G. Kassianides and J. Andrews, Four Prop Tilt-Wing with Leading Edge BLC: Results of Semi-span Wind Tunnel Test, Document D170-10036-1, The Boeing Company, Vertol Division, 1970.

2. C. Kolesar, G. Kassianides, J. Andrews and T. Armstrong, Isolated Cyclic Pitch Propeller: Results of Wind Tunnel Test, Document D170-10037-1, The Boeing Company, Vertol Division, 1970.

3. C. Kolesar, G. Kassianides and J. Andrews, Four Prop Tilt Wing with Cyclic Pitch Propellers: Results of Full Span Wind Tunnel Test/Phase I, Document D170-10038-1, The Boeing Company, Vertol Division, 1970.

4. C. Kolesar, Four Prop Tilt Wing with Cyclic Pitch Propellers: Results of Full Span Wind Tunnel Test/ Phase II, Document D170-10039-1, The Boeing Company, Vertol Division, 1971.

5. E. Widmayer and J. Tomassoni, 1/3rd Scale V/STOL Cyclic Pitch Propeller: Results of Wind Tunnel Test, Document D170-10040-1, The Boeing Company, Vertol Division, 1971.